Rear Wheel Steering:
Applications Beyond the Conventional

By

Jonathan Loyola
Dissertation

Submitted in partial satisfaction of the requirements for the degree of

Doctor of Philosophy

in

Mechanical and Aerospace Engineering

in the

Office of Graduate Studies

of the

University of California

Davis

Approved:

Donald Margolis, Chair

Dean Karnopp

Francis Assadian

Committee in Charge

2022

To Katie and my family.

Contents

List of Figures

List of Tables

Abstract

Rear Wheel Steering:
Applications Beyond the Conventional

Rear-wheel steering as we know it today is an idea that has been around for decades. Almost all literature discusses the technology though the conventional use, where the rear steers opposite the front at low speeds and in phase at high speeds. The work in this dissertation explores additional uses and benefits for using rear-wheel steering (RWS).

The first idea explores decoupling yaw motion and lateral motion in order to allow the vehicle to behave with much more freedom than its front steering only counterpart. The handling characteristics are then controlled by a novel model reference concept, a virtual wheel base.

The second use explores how rear-wheel steering can enhance safety features in the vehicle. Rear-wheel steering is coupled with antilock braking and electronic stability control. These concepts show promising results and improvements to the vehicle.

Acknowledgments

I would like to express my sincere gratitude to my advisor Prof. Donald Margolis for the guidance and support throughout this research. I would also like to express my sincere thanks to Prof. Dean Karnopp. I am indebted to the program they had put together at UC Davis that I was able to take part of. The Hyundai Center of Excellence exposed me to so many different aspects of engineering and vehicle dynamics that I find invaluable to my learning. I tried very hard to absorb all of the advice, intuition, and wisdom they dispensed in meetings over the years. I would also like to express my sincere thanks to Prof. Francis Assadian, who as my Master's advisor, imparted onto me the tools and inspiration to continue onto a doctoral degree.

I would not be able to say into words how much my love and my partner Katie Habash has meant to me during these years. The sacrifice and support she gave unflinchingly for my studies are something I hope I can repay someday. Also, the three amigos Gigi, Henry, and Feli who supported and inspired me.

Finally, nobody is more important to me in the pursuit of this degree than my family. My parents and siblings, and the Habash family, all gave me unconditional support through the years.

Chapter 1

Introduction

1.1 Bicycle Model Review

A bicycle model of a car, also known as a planar model, is one of the first models considered when studying handling dynamics. It is referred to and used in countless works and needs to be understood in order to discuss the literature review. Therefore, a short review is included here.

The bicycle model usually assumes the forward velocity to be constant, and the motion is constrained such that it only allows independent movement in the lateral and yaw directions. Motion is not allowed in the heave, pitch, and roll directions. This is shown in Figure 1.1, where the body-fixed coordinate system uses v_{x0} for the constant forward speed, v_y for the lateral velocity, and ω_z is the yaw rate. This is the starting point for studying the fundamentals of handling dynamics of a vehicle. With the assumption that the vehicle's slip angles at the front and rear (α_f and α_r) are small, the equations of motion can be put in state-space form as shown in Equation 1.1. The parameters used are described in Table 1.1.

The two tires at the front are combined into one tire which has the properties of both put together. This is also done for the rear, resembling a bicycle. Here, the normal forces are ignored, given that in a turn the outside tire is loaded equally and opposite to the

Table 1.1: Description of parameters of the bicycle model.

Description	Symbol	Unit
Distance From C.G. to Front	a	m
Distance From C.G. to Rear	b	m
Total Mass of Vehicle	m	kg
Moment of Inertia of Vehicle	J_z	kg-m^2
Front Cornering Coefficient	C_f	N/rad
Rear Cornering Coefficient	C_r	N/rad

inside tire. This assumption is reasonable for maneuvers that are not considered harsh.[1]

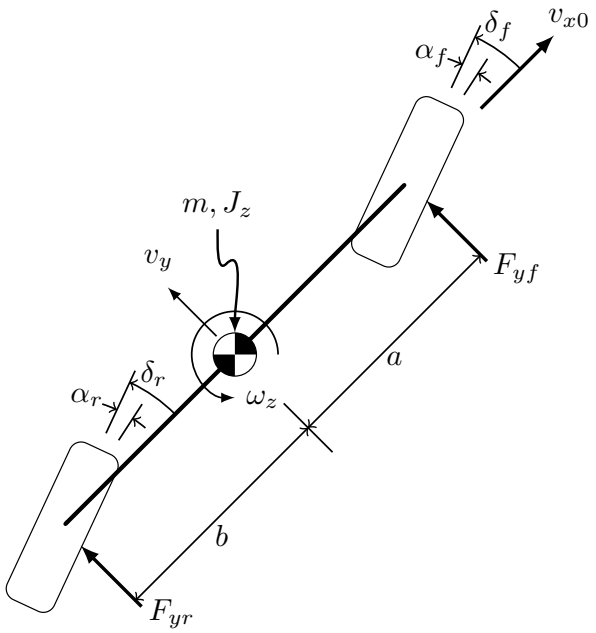

Figure 1.1: Bicycle model of a car.

$$\begin{bmatrix} \dot{v}_y \\ \dot{\omega}_z \end{bmatrix} = \begin{bmatrix} -\frac{C_f+C_r}{mv_{x0}} & -\left(v_{x0}+\frac{aC_f-bC_r}{mv_{x0}}\right) \\ -\frac{aC_f-bC_r}{J_z v_{x0}} & -\frac{a^2C_f+b^2C_r}{J_z v_{x0}} \end{bmatrix} \begin{bmatrix} v_y \\ \omega_z \end{bmatrix} + \begin{bmatrix} \frac{C_f}{m} & \frac{C_r}{m} \\ \frac{aC_f}{J_z} & -\frac{bC_r}{J_z} \end{bmatrix} \begin{bmatrix} \delta_f \\ \delta_r \end{bmatrix} \tag{1.1}$$

Transfer functions relating the inputs to the states are derived as follows:

[1]It should be noted that differences in roll stiffness between the front and rear can alter vehicle behavior, and extreme differences may have an impact in moderate maneuvers.

$$\frac{v_y}{\delta_f} = \frac{\frac{C_f}{m}\left[s - \frac{ma}{J_z}v_{x0} + \frac{b(a+b)C_r}{J_z v_{x0}}\right]}{D} \tag{1.2}$$

$$\frac{v_y}{\delta_r} = \frac{\frac{C_r}{m}\left[s + \frac{mb}{J_z}v_{x0} + \frac{a(a+b)C_f}{J_z v_{x0}}\right]}{D} \tag{1.3}$$

$$\frac{\omega_z}{\delta_f} = \frac{\frac{aC_f}{J_z}\left[s + \frac{(1+\frac{b}{a})C_r}{mv_{x0}}\right]}{D} \tag{1.4}$$

$$\frac{\omega_z}{\delta_r} = -\frac{\frac{bC_r}{J_z}\left[s + \frac{(1+\frac{a}{b})C_f}{mv_{x0}}\right]}{D} \tag{1.5}$$

where

$$D = s^2 + \left[\frac{C_f + C_r}{mv_{x0}} + \frac{a^2C_f + b^2C_r}{J_z v_{x0}}\right]s + \frac{(a+b)^2C_fC_r}{mJ_z v_{x0}^2} + \frac{bC_r - aC_f}{J_z} \tag{1.6}$$

An important signal used to describe the handling of a vehicle is the lateral acceleration, shown in Equation 1.7.

$$a_y = \dot{v}_y + w_z v_{x0} \tag{1.7}$$

The transfer functions are now combined using Equation 1.7, yielding the transfer functions from the inputs to the lateral acceleration as seen below.

$$\frac{a_y}{\delta_f} = \frac{v_y}{\delta_f}s + \frac{w_z}{\delta_f}v_{x0} \tag{1.8}$$

$$\frac{a_y}{\delta_r} = \frac{v_y}{\delta_r}s + \frac{w_z}{\delta_r}v_{x0} \tag{1.9}$$

Substituting in the transfer functions give

$$\frac{a_y}{\delta_f} = \frac{\frac{C_f}{m}\left[s^2 + \frac{b(a+b)C_r}{J_z v_{x0}}s + \frac{(a+b)C_r}{J_z}\right]}{D} \tag{1.10}$$

$$\frac{a_y}{\delta_r} = \frac{\frac{C_r}{m}\left[s^2 + \frac{a(a+b)C_f}{J_z v_{x0}}s - \frac{(a+b)C_f}{J_z}\right]}{D} \tag{1.11}$$

Virtually all the literature studying rear-wheel steering (RWS) use the bicycle model as a starting point for analysis. Many ideas have been developed and explored regarding what would be best for the rear tires to do while a driver directly steers the front tires.

The body side slip (or body slip, float angle) is a signal often considered in various works and is often used in lieu of the lateral velocity. The body slip is simply the angle that the overall velocity of the vehicle is pointing at relative to the longitudinal axis. Due to linearization and small angle approximations in the bicycle model, this output can be simply described as $\beta = v_y/v_{x0}$. Therefore its transfer function is the lateral velocity divided by the forward velocity, which is essentially just the lateral velocity with a different gain.

1.2 A Comment on Terminology

RWS, four-wheel steering (4WS), and all-wheel steering (AWS) are all used to describe the same technology, which is a direct and purposeful articulation of the rear wheels in addition to the front wheels. This direct articulation is distinct from changes of the toe direction due to kinematics of the suspension. This is also distinct from active geometry, where hard points of the vehicle are actively moved in order to make changes to how the kinematics affect the toe direction through kinematic and compliance (K&C) suspension effects. RWS attempts to give the tire angle desired no matter the condition.

Virtually all passenger vehicles use the front wheels as the primary actuation method to affect lateral motion of a passenger vehicle. When a vehicle uses only the front wheels to steer, this is typically referred to as front-wheel steering (FWS) or two-wheel steering (2WS). When the wheels are controlled by an actuator which is electronically controlled, the qualifier active is used.

Which term is used depends on the source. RWS is a more conventional term, while 4WS is often used in academia, and AWS is used in internationally. All of the terms are used in this paper depending on the source being used to describe the technology.

1.3 Background: A Short History of RWS

1.3.1 Early Prototypes

The idea to use the wheels of the rear axle to help steer a ground vehicle has been around since before the creation of the first modern automobile. There has existed steam powered vehicles which implemented this idea, noteably a vehicle built by Amedee Bolee

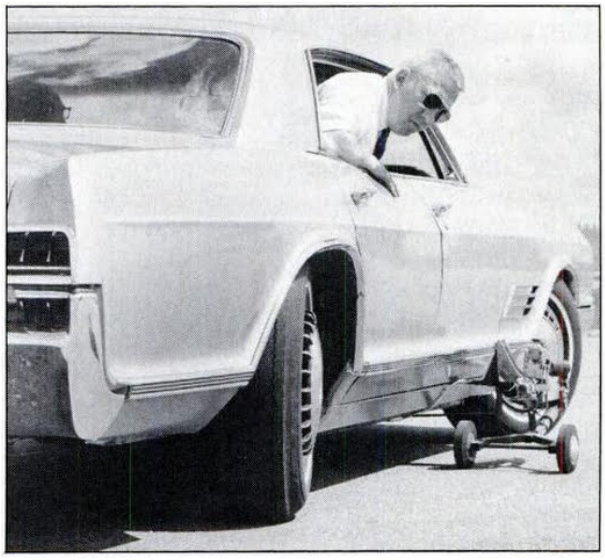

Figure 1.2: General Motors' experimental car in 1968 [1].

in 1876 [1]. RWS (interchangeable with 4WS and AWS) has come and gone in many experimental automobile builds.

In the beginning of the 1900's, the German Colonial Office placed its production order for a reliable vehicle that would withstand long journeys on unmade roads. Daimler-Motoren-Gesellschaft (DMG), delivered the 'Dernburg-Wagen' [2]. Designed by Paul Daimler, the son of the company founder, the vehicle was built in 1907 and featured all-wheel drive and RWS. To keep sand and airborne particulates out of the many joints, Paul Daimler shrouded the vulnerable components with a cylindrical sleeve. This limited the maximum steering angle at the front to just 23 degrees. Therefore, the vehicle was equipped with RWS to achieve a respectable turning circle. The vehicle impressed many for its durability and how well it traversed off-road. A precise log of the vehicle showed that in 1910 the vehicle had traveled 10,000 kilometers. However, after the First World War the 'Dernburg-Wagen' was lost.

Many more vehicle models were built by Daimler and Mercedes for offroad and military which implemented RWS. In 1936, the 170 VL (W139) was built by Mercedes-Benz with permanent all-wheel drive which also featured RWS [3]. This reduced the turning circle from eleven meters to seven meters. Less than 100 of this model along with another model were delivered for the German armed forces. This was a precursor for the Mercedes-Benz

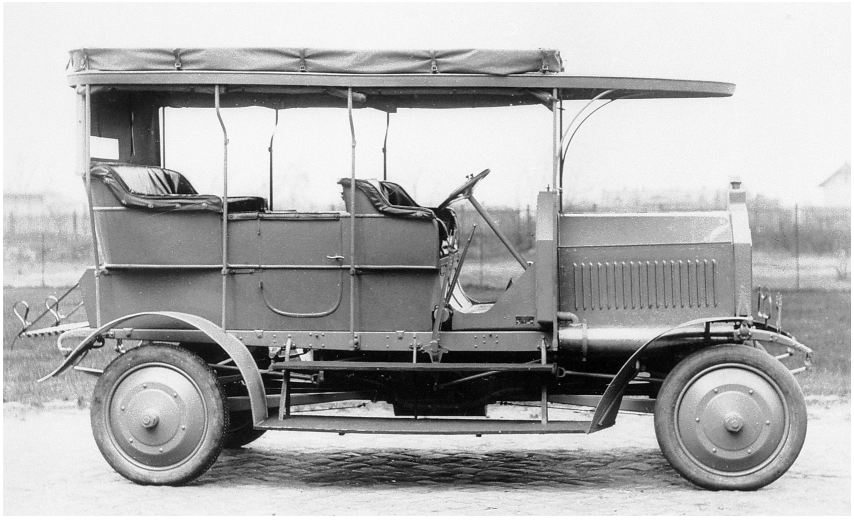

Figure 1.3: 'Dernburg-Wagen,' the worlds first all-wheel drive passenger car which also features RWS [2].

G5 (W 152 series). Built from 1937 to 1941, the Mercedes-Benz G5 had all wheel drive and selectable all-wheel steering [4]. Although the military showed little interest, the company presented the G5 at the London Motor Show in October 1938 as a "colonial and hunting vehicle." The vehicle was used with the German mountain rescue services where it was praised. It had a max speed of 85 km/h, although the operating manual said not to exceed 30 km/h when all-wheel steering was activated. Unfortunately the G5 had little success, where only 378 units were built in total.

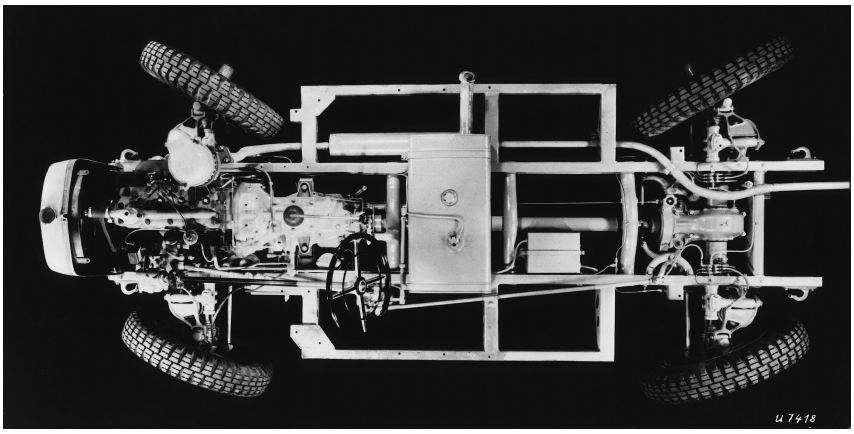

Figure 1.4: The Mercedes-Benz G5 (1937-1941) [4].

The rear wheels were also considered for improving high peformance vehicles. In 1967

Mickey Thompson, a racing automobile builder, entered his Wynn's Spit-Fire Special into the Indy 500. It featured RWS to give his car "much improved high-speed cornering ability [5]." Unfortunately Thompson and his drivers failed to qualify with the vehicle.

Car manufacturers in other countries were also experimenting with RWS. General Motors had an experimental vehicle with the capability in 1968 [1]. In 1977, Honda began thinking about implementing RWS concept, and by 1981, had a test vehicle created by welding together two front ends of an Accord [6]. By 1983, Mazda had the MX-02 concept car which featured RWS while Toyota revealed the FX-1 concept car at the 1983 Tokyo Motor show [7]. The idea has not been implemented in a mass produced vehicle for the regular consumer. Yet, actuating the rear wheels has slowly grown in interest by the manufacturers, primarily the Japanese manufacturers. By the late 1980s, technology had advanced enough to make RWS a hot trend. According to one manufacturer, "We had to wait until computers and actuators became small and cheap enough [8]."

Figure 1.5: Honda's test car in 1981 [6].

1.3.2 The 1985 Tokyo Motor Show

The November 1985 Tokyo Motor show debuted many RWS concept cars. The new RWS systems were to "radically improve handling and stability [8]." Around this time, Mazda, Nissan, Mitsubishi, Toyota, Honda, and Mercedes-Benz have all built four-wheel-steering cars.

Mazda had a newer version of its MX-02 concept, the MX-03, while Nissan revealed its Mid4 concept car [9]. Both concepts use a computer to determine the rear tire angle depending on road speed and other electronic measurements. This was for "road hold" and to "extend cornering potential." The advantages were touted as "faster, more controlled turns and lane changes at high speeds" and "low-speed agility [8]." The Mazda MX-03 concept car had a maximum rear steering angle of six degrees. Mazda's manager of chassis testing and research, Noritaka Yasuda, claimed that the high-speed stability of the vehicle is increased, and "the performance is improved on both wet and dry roads-and on gravel roads [8]."

The Mitsubishi concept car, the MP-90X, accomplishes "zero slip cornering." It used the engine rpm, vehicle speed, and the steering angle of the front to control the rear wheels to give the car "crisp handling and allows a driver to use four-wheel steering's potential to the limit in avoiding obstacles or switching lanes at high speed [8]."

Toyota's RWS system debuted on its FXV concept car. It used direct mechanical linkages to control the rear steering [10]. The system had a maximum of ten degrees of rear-wheel steer. A Toyota exectutive vice president, Kiyoshi Matsumoto, commented that with the new RWS system is " a great boon when you want to negotiate a winding series of bends at high speed. You can do this about 6 mph faster with four-wheel steering [8]." This mechanical system was a simpler concept compared to other manufacturers' approach with computers and electrical sensors. According to Toyota's chief designer Dr. Teruhiko Tamamoto, the RWS system "does take some getting used to [10]."

On August 19, 1985, Nissan introduced a RWS option for its R31 Skyline for the Japanese market [11]. The R31 had the ability to move the rear wheels up to half a degree in response to steering angle and car speed. This analog system was known as high-capacity actively-controlled steering (HICAS), and responded to the lateral acceleration in order to steer the rear wheels. This system used spring-loaded hydraulic actuators to steer when the lateral acceleration surpassed .5g of lateral acceleration. This system resembled more closely to the passive systems of the time used in the Mazda RX-7 (Dynamic Tracking Suspension System) and the Porsche 928 (Weissach Axle) to change the rear toe when

cornering to provide stability. In addition to the R31, Nissan also had a concept car. Nissan's CUE-X concept had the capability to steer the rear wheels up to seven degrees to aid in low-speed maneuverability using an eight-bit computer. Nissan engineers said that half a degree of RWS was suitable for the current generation of cars, but may be increased in the future "as drivers get used to it [8]."

Herbert Shuldiner of Popular Science had the opportunity to test some of the Japanese auto maker's experimental vehicles [8]. Shuldiner's test of a prototype Mazda at high speeds revealed that with a sharp jerk of the steering wheel, the vehicle with RWS deactivated (in 2WS mode) fishtailed and was a struggle to keep stable, while when the system was activated and the steering wheel was jerked again, the vehicle remained "perfectly stable and completely under control." According to Shulinder, "There was no question in my mind that when four-wheel steering was used, the car was more controllable and handled more crisply."

Shulinder also tested the production Skyline at Nissan's Tochigi proving grounds. Nissan claimed that its HICAS gives the impression to the driver that its using racing tires when equipped with street tires. The price for the option on the Skyline was about $500 extra, while Mazda's system was expected to add on about $700. Shulinder finishes his article by positing that once a driver tries the new system, they'll never want to drive without it.

1.3.3 From Concept to Consumer: The Prelude and the 626

The first commercial car in America to offer RWS was the 1988 Honda Prelude Si (released in 1987 for the Japanese Market) and was the result of a ten year study by Honda [6]. The 1988 Mazda 626 was also released later in the same year. Although they use the the same overall engineering principle to control the rear wheels, the implementation was different. The idea was to have the front and rear wheels turn opposite of each other in low speeds to help maneuverability, such as in parking. At high speeds, the wheels would turn together to assist in a quicker and more stable lane changes. This is shown in Figure 1.6 and is described by some engineers as Contra-Phase and Same Phase, respectively.

The response time in high-speed lane changes for 2WS vehicle is dependent on a

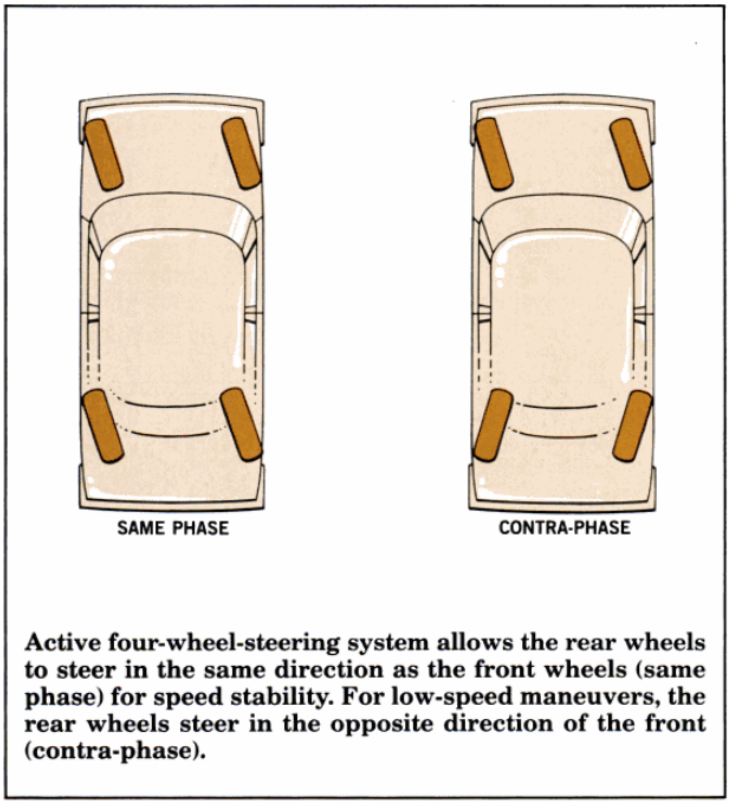

Figure 1.6: The different phase modes the RWS system takes [8].

number of design parameters. The 2WS car needs to yaw before the rear wheels generate forces. The speed at which this happens depends on the car itself which can make this slow and sloppy, or quick and crisp like in a sports cars. When the vehicle has the ability to steer the rear wheels, these rear wheels now have the ability to generate lateral forces much faster and to decouple its dependency on vehicle parameters.

The Mazda 626 used a computer, mechanical gearbox, and hydraulic cylinder to steer the rear wheels. With this advanced system at the time, the 626 steered the rear wheels based on the steering wheel and the forward velocity. Mazda engineers claim that it can closely approximate the ideal relationship between road speed and rear steering [12]. As shown in Figure 1.7(a), when the velocity of the vehicle reaches 22 mph, the steering ratio from front to back is zero, meaning that the rear wheels are not steered at all. At speeds above 22 mph, the rear wheels steer in phase with the front wheels. At speeds below, the rear wheels steer in opposite (contra) phase with the front.

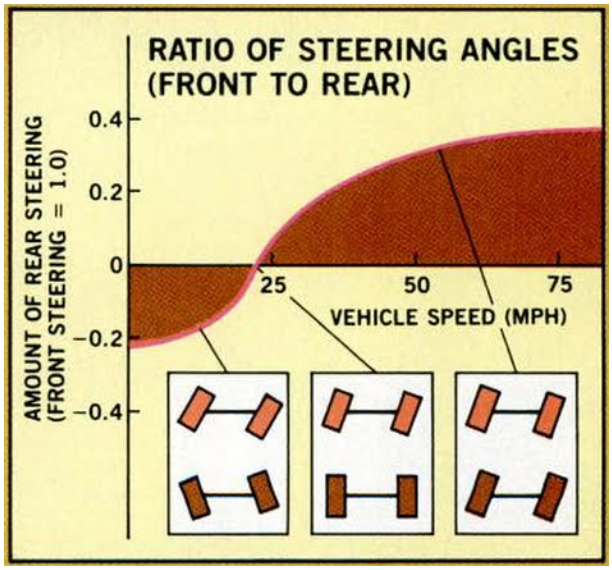

(a) Mazda 626

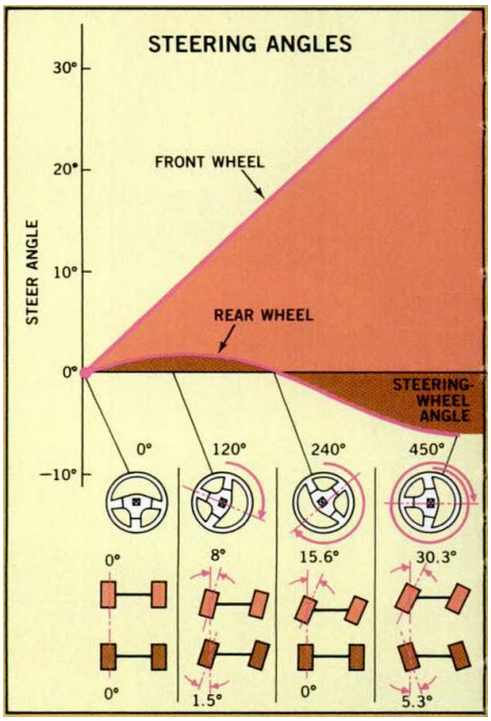

(b) Honda Prelude

Figure 1.7: Control logic for the rear wheels [12].

The Honda Prelude, however, does not use a computer. What Honda does instead is turn the rear wheels as a function of the steering wheel only. The Prelude uses a center shaft to connect the front steering gearbox to a rear steering gearbox. From there, a planetary set of gears controls the steering linkages in the rear. Because it is purely mechanical, the rear wheel always move when the steering wheel is moved no matter what the maneuver or vehicle speed. Through the first 140 degrees of steering wheel angle, the rear wheels turn with the front wheels in phase. After 140 degrees, they straighten out until the steering wheel is turned beyond 246 degrees. Then the rear wheels turn opposite to the front wheels. At full lock, the car's turning radius is 31.4 feet (almost three and a half feet less than the 2WS Prelude). The reasoning behind this is explained by Yoshimi Furukawa of Honda R&D, "At High speeds, the driver's steering angle stays small, and the rear wheels steer in the same direction as the front. At low speeds, steering angle is large. This causes the rear wheels to steer in the opposite direction of the front for greater maneuverability [12]." This control decision is shown in Figure 1.7(b).

Dan McCosh from Popular Science tested these 4WS vehicles vs their 2WS counterparts for a month [13]. He was quick to notice that the 4WS was easier to control and went through the handling grid faster than the 2WS cars. The 4WS in the prelude helped overcome some of the understeer tendencies the 2WS had, providing significantly more "bite" at the rear wheels. However, he concluded that at the adhesion limit of the tires, there was only a small difference in time between the 2WS and 4WS car and that the suspension design and balance could easily offset any 4WS advantage. Testing in low-speed cone maneuvering showed little difference between 4WS and 2WS. These tests were at the speed range where the rear steers don't move (around 25 mph for the Mazda logic). Therefore it would make sense that they behave the same; the 4WS was basically a 2WS vehicle at that speed. However, McCosh argues that there were many real world benefits to 4WS that would not show up in typical performance tests. At medium-speed, cornering on wet surfaces felt "as if an invisible hand were patting the rear axle back on track [13]." This handling security is supposed to be enhanced on snow and ice, but McCosh did not have the opportunity to test in those conditions. The 4WS cars "handled buffeting crosswinds like an M-1 tank." Also, "both four-wheel-steer cars put Amtrak to shame on the freeway for straight-line stability." And of course there was the parking lot capabilities where the turning radius of the 4WS had a significant advantage.

Consumer Report's review of the RWS Honda Prelude commented that the routine handling of the 4WS Honda Prelude was "as sharp, accurate, and steady as anyone could expect. The 4WS was most noticable in tight, low-speed turns, when the rear end moved out sharply to help tighten the turn. [14]" Also, the emergency handling was "excellent. The Prelude set a new speed record through our avoidance-maneuver course, and proved extremely accurate and controllable in hard turns at the track." Although, they also commented about a quirk in the design where "if you turn the wheels sharply when the car is parked, the rear end will swing out a bit when you start to move forward. So you have to take care when parked next to a wall or next to another car."

In their road test of the Mazda 626, they reported that the routine handling was "very quick and precise. The four-wheel steering sharpened low-speed turns, but we didn't notice

it otherwise. [15]" On its emergency handling, they said that it was "very responsive. We felt a trace of fishtailing, but it was easy to correct." Similar to the prelude, the 626 had its own quirk: "Brisk acceleration in a low-speed turn makes the steering wheel try to tug itself loose from your hands."

Ordering the 4WS option included additional upgrades (anti-lock brakes, alloy wheels, automatic transmission, electric door locks, etc). McCosh estimates that the RWS alone costs about $650 for the mechanical Prelude and $1,100 for the electric RWS system in the 626. He was optimistic that fine tuning in the future would improve the 4WS in parking, centralized electronics would bring down the cost, and that the system would be as commonplace as power steering and automatic transmissions were at that time.

Consumer Reports asked: although 4WS is an improvement in practice (or theoretically), is it a big improvement [14]? In larger cars with less disciplined handling, it seems like it would be a big improvement. However, in the Honda Prelude's case, it adds little improvement on typical performance metrics. The Prelude without 4WS handled so well that adding the 4WS system made a small difference in the small sporty car. James Cobb of the New York Times agrees with the sentiment, saying "Those already nimble cars didn't benefit much, and buyers rejected the added cost and complexity [16]." In two days of testing, two Car and Driver editors simply could not detect any handling differences between the 2WS and 4WS vehicles. They wondered "just how many buyers will cough up about $1500 for the 4WS option if the differences aren't obvious [17]."

1.3.4 Notable Rear-Wheel Steering Systems

A large number of automakers have offered RWS on a small number of cars. It was common that the RWS option was only offered in the country or area of origin. For example, in 1989 the fifth generation (T180) in Toyota Celica offered RWS models in the Japanese market only. In 1992, the BMW 850Csi was released with rear wheel steering (Aktive Hinterachs-Kinematik) as the standard option, however, only in the European market. RWS in the marketplace began to phase out after the initial boom. As described by Peter Herold of BMW, "After their high tide in the 1990s, almost all the all-wheel steering systems disappeared from the market again. The reasons were the high add-

on costs and functional deficits in the driving dynamics. [...] Another reason was the availability of cheaper brake control systems, like ESP, that could realise the purpose of driving stabilization in the upper limit range for much less costs. [18]"

However the Japanese market was the exception to this trend. Nissan consistently offered RWS through its HICAS and super HICAS technology on its Skylines (and other cars) starting with the 1985 Skyline (R31) until it was dropped from the Skyline models in 2007 (R35). RWS then began to show up on its Inifinity brand.

The Mitsubishi 3000GT was first released in the Fall of 1990 and included RWS. This system takes advantage of the the company's rear-toe link design and uses hydraulics to give actuation of up to 1.5 degrees in phase with the front tires to increase high-speed stability. The system begins working at around 30 mph, and does not actuate at speeds below. According to the company's research, low-speed or opposite-direction RWS is undesireable [19]. "The Mitsubishi system provides extremely precise control over the car, allowing the driver to slither through turns at high speed. On the negative side, by steering all four wheels the car can at times feel twitchy and oversensitive, with every slight steering input translated into a change in direction. [20]"

General Motors and Delphi Automotive Systems worked together to implement their "Quadrasteer" system as an option on some GM trucks starting in 2002 [16]. This system combines the front wheels' conventional hydraulic system with electric RWS which allows the Sierra Denali to turn 20% tighter with a rear steering angle of up to 12 degrees. This allows the vehicle to behave like a vehicle that is four feet shorter. The shortening of the virtual wheelbase can be seen in Figure 1.8. The system also steers the rear in phase with the front at speeds above 40 mph with a rear steering angle of up to 1-2 degrees. Another notable improvement was when the vehicle towed large trailers. When backing a trailer into a stall, the Quadrasteer system made this task easier. However, the Quadrasteer option was dropped in 2005 [21]. Only 16,500 vehicles with Quadrasteer were sold since the system was an option in 2002. One problem with the system was that it was too pricey. When it was first available, it added $4,495 on top of a luxury truck. Even when the price of Quadrasteer was dropped to $2,000, consumers didn't understand the

advantages and capabilities of the system. Delphi still hopes to sell the their system to other automakers. RWS in large pickup trucks may not be dead, however. Andrew Ganz reported that ZF fit its experimental RWS system into the Ford F-150 in 2017 [22].

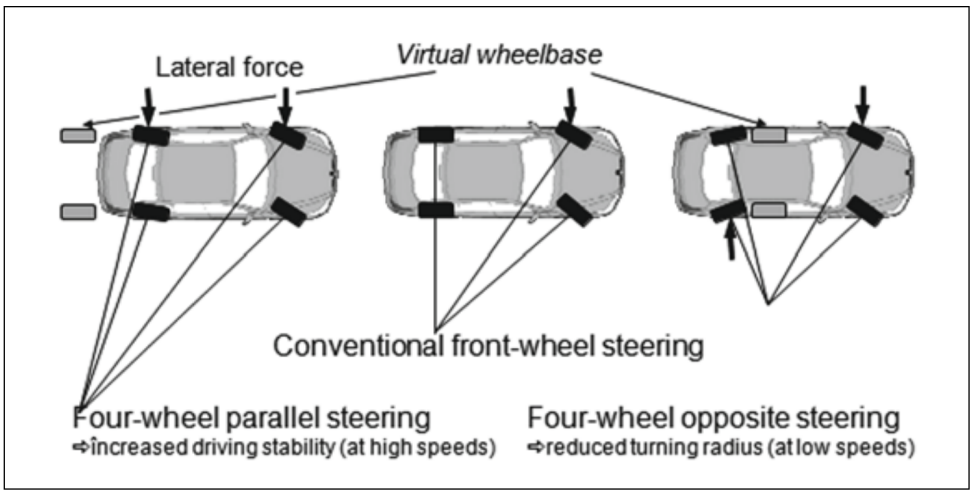

Figure 1.8: Virtual wheelbase and turning radius of RWS [23].

1.3.5 Rear-Wheel Steering Currently

There are a number of companies that offer RWS as an option. Some have RWS as standard. In 2013, Porsche released their new 911 GT3 with RWS as standard. It featured two independent electric actuators to give the rear up to 1.5 degrees of actuation which improves manouverability at high speed and "[makes] the GT3 feel as if its wheelbase were 20 inches longer at speed." [24]. The German supplier ZF has been selling its active kinematics control (AKC) system to Porsche, Ferrari, Audi, Cadillac, and BMW, and recently celebrated its one hundred thousandth AKC system produced [25]. Sixty thousand use a central actuator system, which is used in the Porsche Panamera, Audi Q7, Cadillac CT6, and the BMW 7 series. Forty thousand use a two actuator system, which is used in the Porsche 911 Turbo, 911 GT3, and the Ferrari GTC4Lusso.

The French company Renault announced in 2015 that their new generation Mégane GT will have their 4Control technology as standard which adds RWS [26]. What is special about this vehicle is that it is much more affordable compared to the other vehicles in the market with RWS. Typically RWS is found only in high performance vehicles and luxury

Figure 1.9: ZF's single actuator Active Kinematics Control system [25].

vehicles.

1.4 Problem Statement

There are two main advantages in RWS that are implemented by the industry already. The first is the easier maneuverability and better agility at low speeds. This done by steering the front and rear opposite to each other, which effectively shortens the wheel base by moving the center of rotation as shown in Figure 1.8. This helps in parking lot efforts but parallel parking takes practice. All vehicles can be improved with this, but the biggest benefit seems to be on vehicles with a long wheelbase.

The second advantage is high speed directional stability and better handling dynamics at high speed cornering. This is done with the rear wheels steering in-phase with the front tires. This has already been taken advantage of by passive systems through kinematic means, but also implemented actively on high performance vehicles. It makes it possible to negotiate corners at high speeds better and faster, and possibly make cornering safer on wet surfaces and snow. For the Honda Prelude, "[Honda] also found that, for maximum stability, the rear tires should steer only about one-fifth as much as the fronts. In Honda's

tests, this was the strategy that produced the quickest response and the greatest stability in transient maneuvers, particularly on slippery surfaces. (Steady-state behavior is not affected by 4WS)[17]."

These two ideas are often implemented in commercially sold passenger vehicles. It is desired to explore additional uses and capabilities that RWS can offer, since steering has a direct effect on the lateral dynamics of the vehicle. This opens the door for various schemes for control and design depending on the configuration of the vehicle. Two main ideas for investigation are proposed. The first is how the dynamics of a vehicle can benefit from the use of RWS. The second is from a safety standpoint, are there advantages to the use of RWS?

Chapter 2

Literature Review

Chapter 1 introduced a brief history and overview of RWS from the perspective of journalists and the general public. It discussed at how RWS was introduced and received in the marketplace. RWS was typically seen as an expensive add on which offered little benefit to the regular consumer, and usually offered on expensive high performance vehicles or top-of-the line models.

Regardless, there are real advantages to RWS that engineers agree on. Here, academic and engineering works are discussed. In the literature, numerous papers make use of RWS, but a majority seem to use the same reference and signals. The focus of many papers is the control algorithm. An important question that seems to be ignored is: what should the system do? The emphasis of this chapter is placed on discussing the reasoning behind augmenting the vehicle lateral dynamics, and what the rear wheels should do.

This literature review is split into three sections. The first explores the use of RWS only. The second looks at research that use active front and rear wheels together. The final section looks at research that specifically compare RWS and other actuation methods for the purpose of stability.

2.1 Rear-Wheel Steering Design

RWS has been around with numerous papers discussing its benefits and methods of implementation. Previous surveys of RWS technolgies [27],[28],[29],[30] discuss such improvements. Some major improvements are:

1. The vehicle response can be augmented
2. Improved low-speed maneuverability
3. Improved high-speed stability
4. Better response near limits of adhesion

These items are not necessarily independent of each other, but encapsulate the general characteristics that RWS can affect.

The biggest effect of RWS is the augmentation of the vehicle response, primarily its lateral dynamics. This was a big issue with the sporty vehicles of the 80s with RWS. Many were tuned to handle exceptionally, where the addition of RWS had a negligible effect on performance. Changes can be made but defining an improvement for the driver is a difficult task because of its subjectivity. An important question is by how much is performance changed and can a typical driver detect this change.

One possible methodology to make a more noticable improvement is to use RWS for handling while the rest of the car is tuned for something else. As Fijalkowski describes, "if the desired vehicle character is for a smoother ride through a softer suspension, the [4WS control] may be used to help regain the deisred handling by [dynamcially adjusting] the rear-wheel angle according to a vehicle behaviour physical model [27]." An interesting work from Fiat [31] investigates the integration of suspension design and RWS control. The idea is to soften the suspension for better ride comfort. However, the decrease in handling would be made up by steering the rear wheels. The design is tested using a combination of ADAMS and MATLAB. A multilink suspension system for the rear is used as the nominal case, which is compared to a Mc-Pherson strut with worse lateral handling performance. The suspension is designed to maximize longitudinal comfort performance. The work concluded that RWS can compensate for a softer suspension.

Changes in lateral dynamics can be accomplished passively through kinematic effects of the suspension, called bump steer or roll steer [32]. The typical tuning of the rear is to have the wheels toe out slightly during straight line driving, and toe in during a turn [33]. During a turn, the weight of the vehicle shifts from the inside tires to the outside, which

compresses the suspension and turns the wheels in, resulting in toe in or steering in the same direction as the front wheels. This reduces the amount the rear end of the vehicle slides out, reduces body-slip angle, and improves vehicle cornering stability. In addition, lateral acceleration and roll angle can be reduced more by using bump steer in the rear compared to the front. However there are natural design limits to the amount of bump steer that can be added without losing straight line stability. In addition, some handling lag may be experienced due to the dependence on the vehicle body to roll.

One step removed from RWS is active geometry control (or active suspensions), where the rear bump-toe geometry is controlled [34]. This idea from Hyundai controls the rear suspension link mounting point which affects the kinematics and how much bump steer is created. This technology improves on passive bump steer, but still requires the vehicle to roll in order to create the toe angle. Direct control of the rear-wheel angle allows for direct and faster changes in toe.

Typically in RWS studies, suspension and heave motion are ignored, concentrating on the change in lateral dynamics only. In the case of low-speed maneuverability, the effect of RWS is often compared to virtually shrinking the wheelbase of the vehicle, as seen in Figure 1.8. In order to significantly improve maneuverability, large actuating angles are needed in the rear. Subjective testing done [35] shows that the decrease in turn radius is perceptible if the rear angle exceeds -4 degrees for the particular vehicle that was tested.

At very low speeds (parking lot speeds), slip angles are negligible and side forces are small enough such that many papers that analyze the improvements of RWS by only looking at the geometry and not the dynamic equations [36],[29]. The typical metric of improvement for RWS is simply the minimum turning radius of the vehicle and the off-tracking [30]. This is found by extending the front and rear tire's axle line finding the intersection.

At high velocities, 4WS is said to be capable of achieving better stability than a 2WS vehicles. To show how it improves the system, time domain testing is often done where a RWS vehicle is compared to a vehicle without rear wheel steering. Standard testing conditions are used such as lane change, double lane change, step steering, or slalom tests.

Frequency domain studies are also conducted.

Many different metrics are used which are categorized under the broad definition of stability. The exact definition differs depending on the literature. In addition, an important distinction needs to be made when speaking about the vehicle as a system, which is described by Furukawa [37] and Whitehead [29]. The systems that can be studied can be categorized into two types: the vehicle system alone and the driver-vehicle system where the driver closes the loop. The first tends to use classical control terms, open-loop tests, and objective metrics. The second includes the driver's sense of stability and tends to use metrics correlated to how the driver senses the vehicle and controls it. This is a much more difficult system to study without real human drivers recording their subjective impressions.

When the vehicle system is studied alone, the dynamics of a vehicle and response characteristics can be looked at relatively easier. Models and linear analysis tools can be straight forward to apply. The system input and outputs typically looked at are the steering wheel input to the lateral acceleration or yaw rate of the vehicle. This is sometimes referred to as the handling stability in literature. Robust stability is often discussed when feedback controls are applied. This is a typical metric used to say the stability is improved in literature. An examples for defining how robustly stable a system are the stability margins, which are the gain and phase margin.

The conventional definition of stability for linear time invariant (LTI) systems is also discussed within this framework, where a system is stable if all real parts of its eigenvalues are less than zero, or if all of the system's poles are on the left side of the s-plane. This is nominal stability where there is no model uncertainty. Adding classic feedback control still adheres to this definition: the system is stable if the closed-loop poles are to the left side of the real-imaginary system.

When the driver-vehicle system is discussed, usually real-world testing is done with drivers that give subjective feedback. In computer simulation, it is difficult to quantify the overall performance of the whole system because of the use of a driver model. Attempts are made in literature to correlate the vehicle's different response characteristics with

the level of its control ease. Conclusions about how the driver reacts and controls the vehicle is dependent on how the driver model is tuned, which may need to be adapted depending on conditions or vehicle. Any subjective information extracted from these models may have very different results in real world testing since a driver's feeling is extremely complex and not easily described. The driver feeling, however elusive, is still an important consideration. Irie's work shifted focus from fixed control "to the idea of free control, which takes into account the driving operations executed by the driver. It became clear that the entire man-machine system had to be considered if vehicle dynamics were to be improved [38]."

Stability in driver-vehicle systems can refer to the ability of the driver model to control the vehicle. The driver behaves as a controller and attempts to keep the vehicle on the road. Driver stability can encompass any issue that impedes on the driver's ability to control the vehicle in a predictable manner. An example is when Ackermann [28] speaks on yaw stabilization. This is the ability of the vehicle to self-damp unexpected yaw motions, including the ability to damp out disturbances. If only the vehicle system is looked at, then the system is stable as yaw oscillations eventually damp out. When the driver is in the loop and attempts to control a vehicle with bad damping abilities, the driver can find it difficult to control and the vehicle might feel unstable. These disturbances are typically from wind or split μ scenarios, where the driver's intention through the steering wheel is not satisfied by the vehicle. For disturbance rejection, the vehicle needs some measurement fed back to determine if it is performing the driver's intention. The addition of feedback allows for change in the closed loop poles of the system. Typically, with this feedback system, it is desirable for the closed loop poles of the system be faster and farther to the left of the real-imaginary plane as it can damp out disturbances quicker. The sensitivity function of the closed loop is an indicator of how well the system can reject disturbances.

There are many known and unknown metrics that have to do with the sense of stability or performance to the driver. Along with yaw damping, it could include body slip angle [39], lateral acceleration phase lag [37], disturbance rejection [30], response times, heading

angles, efficiency of tires, frequency range reduction in emergency maneuvers, and the free control weave mode [29]. Irie [38] characterizes the outward deflection of the rear end at high speeds as unstable behavior. However, this list is not thorough because of the difficulty to relate subjective feelings to objective metrics.

2.1.1 Conventional Design

Conventional RWS uses the driver's steering angle and the vehicle's forward speed to dictate how much the rear wheels should turn. The most common control system structure is showed in Figure 2.1, which consists of a prefilter F_r [28]. δ_f is front steer angle without any filtering. The rear steering signal, δ_r however, uses the front steering angle information along with F_r.

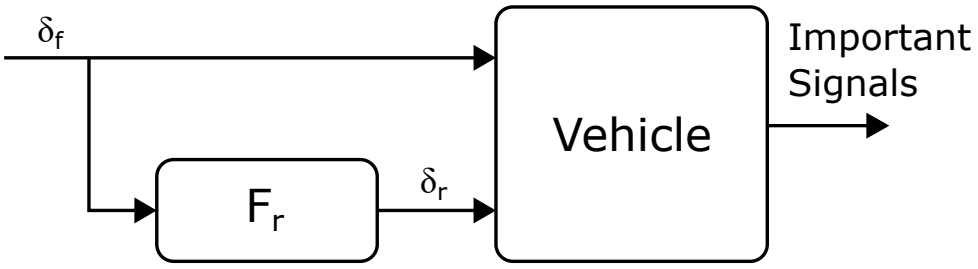

Figure 2.1: The most common control system structure (adapted from [28]).

This prefilter may be just a gain that is mapped with the forward speed $k(v_x)$. An a example mapping is shown in Figure 1.7 (a). However, a more complicated prefilter may be used. A filter example from a German BMW paper is of the following form:

$$F_r(s, v_x) = k(v_x)\frac{1 + T_D(v_x)s}{1 + T_1(v_x)s} \tag{2.1}$$

However, many papers discuss a variable gain $k(v_x)$ prefilter without a memory component. Analysis is typically done with a bicycle model of a car at constant forward speed. One example is a classic paper from Honda R&D in 1986 [36]. First, a transfer function of the vehicle from the steering input to lateral acceleration output and yaw rate output are derived with the inclusion of the gain $k(v_x)$. This can be done with $\delta_r = k(v_x)\delta_f$ as follows:

$$a_y = \left(\frac{a_y}{\delta_f}\right)\delta_f + \left(\frac{a_y}{\delta_r}\right)\delta_r \tag{2.2}$$

$$= \left(\frac{a_y}{\delta_f} + k\frac{a_y}{\delta_r}\right)\delta_f \tag{2.3}$$

$$= \frac{\frac{1}{m}(C_f + kC_r)s^2 + \frac{C_fC_r(a+b)}{mJ_zv_{x0}}(b+ka)s + \frac{C_fC_r(a+b)}{mJ_z}(1-k)}{D}\delta_f \tag{2.4}$$

Similarly, the relationship for the yaw rate is as follows:

$$\omega_z = \frac{\frac{1}{J_z}(aC_f - kbC_r)s + \frac{C_fC_r(a+b)}{mJ_zv_{x0}}(1-k)}{D}\delta_f \tag{2.5}$$

A simplified system is presented in order to help with interpretation. When the car is assumed to be near neutral steer, i.e. $bC_r = aC_f$, the yaw rate relationship of Equation 2.5 can be simplified as follows:

$$\omega_z = (1-k)\frac{\frac{aC_f}{J_z}s + \frac{C_fC_r(a+b)}{J_zmv_{x0}}}{D}\delta_f \tag{2.6}$$

When the gain k changes, it only changes the overall gain of the yaw rate. This indicates that the phase of the yaw rate is largely unaffected by the gain, which cannot be said of the lateral acceleration transfer function. At higher speeds, positive values of k decrease the difference in phase delays between the yaw rate and lateral acceleration. The work finds that decreasing the phase delay of the lateral acceleration at higher forward speeds is subjectively better in testing. This is also reported in another work done by Honda R&D [40], where steering the rear tires in the same direction as the front improves nearly straight line driving maneuvers at medium and high speeds. This gives a shorter delay in lateral acceleration response that is desirable.

The phase delay in lateral acceleration exists because the rear wheels do not immediately generate the necessary force to sustain a turn. The vehicle must turn, generating a body slip angle, which then creates the necessary slip angles at the rear to hold the turn [36]. A method for reducing the delay is to use high-performance tires that produce a great lateral force with a small body slip angle. Additionally, the suspension system can be improved which helps keep the tire performance efficient. However, this type of

set up is not appropriate for conventional vehicles because of the negative effect on ride and other qualities. Steering the rear in the same direction as the front would create the necessary rear forces faster.

Using this idea, the authors describe the natural progression in reducing the lateral acceleration phase delay. "If the rear wheels are controlled properly by this method to keep the body side-slip at zero in [a steady-state turn], vehicle rotation around [the vehicle's] center of gravity is no longer needed and it can start turning the moment the steering input is operated. This can reduce the delay in lateral acceleration response to steering [36]." Enforcing the body slip to be zero at the steady state, the gain k can be derived as follows:

$$\begin{aligned}
\beta &= \frac{v_y}{v_{x0}} \\
&= \frac{1}{v_{x0}} \left[\left(\frac{v_y}{\delta_f} \right) \delta_f + \left(\frac{v_y}{\delta_r} \right) \delta_r \right] \\
&= \frac{1}{v_{x0}} \left(\frac{v_y}{\delta_f} + k \frac{v_y}{\delta_r} \right) \delta_f \\
&= \frac{\frac{1}{mv_{x0}}(C_f + kC_r)s - \frac{1}{J_z}(aC_f - kbC_r) + \frac{C_f C_r (a+b)}{J_z v_{x0}^2 m}(b + ka)}{D} \delta_f
\end{aligned}$$

Taking the limit of this transfer function ($\frac{\beta}{\delta_f}(s)$) as $s \to 0$ yields the steady state value in response to a step input. Solving then for $\frac{\beta}{\delta_f}(s)|_{s \to 0} = 0$ yields:

$$k = \frac{-b + \frac{ma}{C_r(a+b)} v_{x0}^2}{a + \frac{mb}{C_f(a+b)} v_{x0}^2} \tag{2.7}$$

Phase reduction is beneficial for the driver, where a 4WS vehicle "can make lane changes more stably and requires less correction steering because its phase delay in lateral acceleration response to steering is shorter [36]."

An example curve is plotted in Figure 2.2. When this curve is traced as the forward velocity increases, it is found that at low velocities, a negative ratio is needed while at higher velocities, a positive ratio is needed. This corresponds with traditional tuning found in the literature.

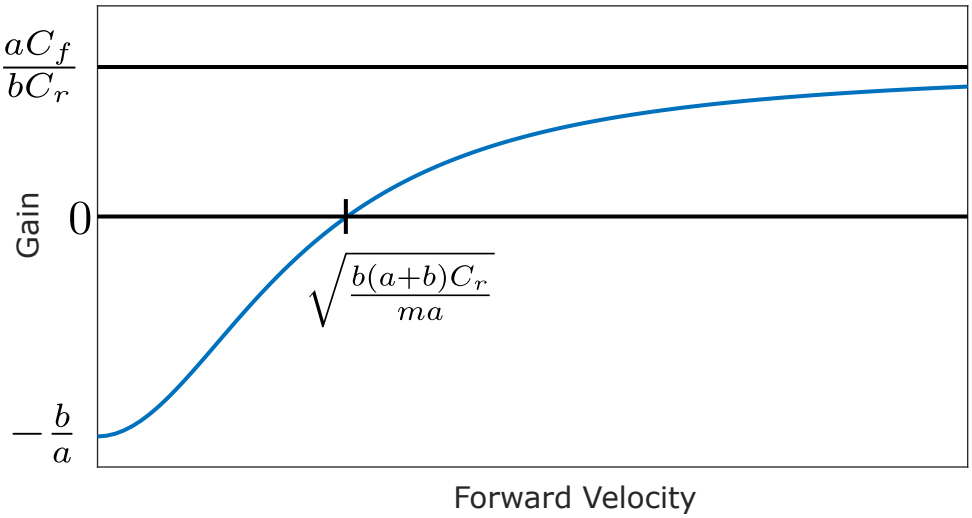

Figure 2.2: Example of gain k vs forward velocity v_x curve of Equation 2.7 (adapted from [36]).

Literature published by other companies agree with this assesement, such as Nissan who claimed that in a typical compact car, at higher speeds without RWS, the the rear end deflects more to the outside and produces rear-end sway [39]. This causes a decline in perceived steering performance when changing lanes at high speed. Reducing the body slip is better ergonomically since the vehicle will proceed in the forward direction when steered [41].

However, there's a limit to how much the rear should be steered with the front. Research by Honda investigated how lateral acceleration and yaw rate response affects the driver-vehicle system [37]. The work describes testing on a lateral motion simulator, shown in Figure 2.3. The test vehicle was specifically built so that the yaw or lateral acceleration response could be changed independently from each other. This proposed test vehicle would need to be a neutral steer vehicle with equal front and rear distribution, and RWS. The testing procedure included two tests, a lane change and a course tracking test, where the objective was to keep the vehicle's C.G. as closely in line with the target in front of them as possible. The error is integrated and weighted in order to describe the control performance of the driver.

Results showed that the driver's control performance is not affected as much by steady-state gain as by the phase delay in lateral acceleration response. It was found that

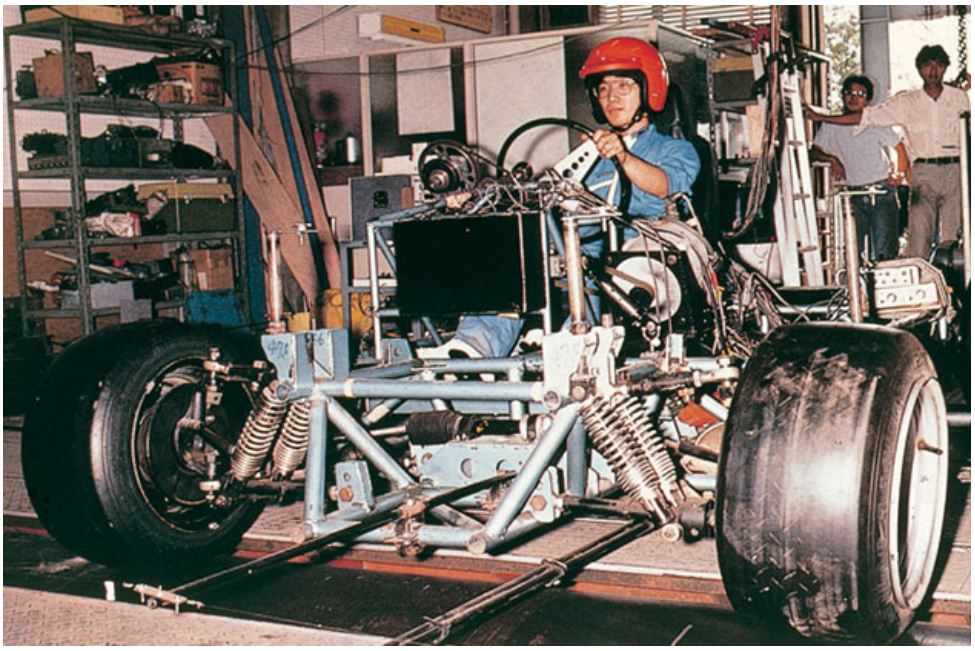

Figure 2.3: Experiemental facility at the Shibaura Institute of Technology allowing large lateral motion of vehicles on wide drums [6].

increasing the gain for high speeds improved driver control performance significantly, up to a point. Any more decrease in phase delay did not yield better improvement in a real driving test with experienced and inexperienced drivers.

Further research by the team investigated the power spectrum density of the driver's steering wheel angle during course tracking tests. The driver's actions was at its peak around 0.75 Hz, which is attributed to the driver's action for correcting steering error.

Additionally, the lane change and course tracking test were experimented with different indicators. In addition to the C.G. indicator, a heading indicator was tested which gave the driver accurate information regarding its vehicle heading. When the yaw velocity and lateral acceleration were changed independently, it is found that keeping either phase delay low improved driver performance. Using the C.G. indicator had consistently better results than the heading indicator during the lane change test. However, using the heading indicator had consistently better results than the C.G. indicator during the course tracking test. The work concludes that the driver uses lateral displacement more during a vehicle's evasive maneuvers, and uses heading angle more during normal driving.

Work from Mazda generated similar results regarding the study of the phase of the lateral acceleration and yaw rate [35]. The response of a 2WS and 4WS with a variable rear-to-front steering ratio was evaluated. A frequency response was performed on a test vehicle with RWS, which yielded similar results to the mathematical analysis. Analyzing across multiple system gains and forward speeds, following trends were generated:

- Regardless of forward speed, same-phase steering reduces the static gains in yaw rate, lateral acceleration, and roll angle. Anti-phase steering does the opposite.
- Regardless of forward speed (in the steering frequency range), same-phase steering increases the yaw rate phase slightly and decreases the phase lags in lateral acceleration and roll angle. Anti-phase does the opposite.
- Higher vehicle speed and larger steering ratios accentuate the trends.

These results are similar to the analytical study done by Honda, however, here the vehicle is not a neutral steer vehicle. This leads to the yaw rate phase changing a small amount, which is expected.

Subjective evaluation was done at two speeds with multiple steering ratios. In one test where the vehicle drives at 50 km/hr on a winding track, drivers preferred a 4WS vehicle with -.2 steering ratio front to rear, meaning that some anti-steering was preferred. In another test where the vehicle drives at 100 km/hr doing a lane change, it was found that a steering ratio of 0.2 was preferred. The conclusion is that the objective measure that correlates best with the subjective evaluation is the difference in yaw rate phase lag and lateral acceleration phase lag.

For these two tests, it was found that the phase lag using the appropriate steering ratio that drivers preferred brought the phase lags in lateral acceleration and yaw rate together to the range value at frequencies below 0.6 Hz. This was tested again with a different suspension with drivers and again drivers preferred steering ratios where the difference in phase lags of lateral acceleration and yaw rate were minimized.

Putting together these two observations, what should be done for a better handling vehicle is to have the lateral acceleration and yaw rate phases be equalized and minimized.

A possible reason given is that "the time lag between the two motions presumably makes the driver feel uneasy [35]." In the paper, the ratio necessary to equalize the phases at a particular frequency can be derived analytically. This is done by setting equal the phase calculation of Equation 2.5 and Equation 2.4. Since the denominator of both transfer functions are the same,$\Phi^D_{a_y} = \Phi^D_{\omega_z}$, they cancel. The following steps can be taken, where Φ represents the phase, the superscript N represents the numerator portion, and the superscript D represents the denominator:

$$\Phi^N_{a_y}(s) = \Phi^N_{\omega_z}(s) \tag{2.8}$$

$$\Rightarrow \arctan\left(\frac{\mathrm{Im}(N_{a_y})}{\mathrm{Re}(N_{a_y})}\right) = \arctan\left(\frac{\mathrm{Im}(N_{\omega_z})}{\mathrm{Re}(N_{\omega_z})}\right) \tag{2.9}$$

$$\Rightarrow \mathrm{Re}(N_{\omega_z})\,\mathrm{Im}(N_{a_y}) = \mathrm{Re}(N_{a_y})\,\mathrm{Im}(N_{\omega_z}) \tag{2.10}$$

$$\Rightarrow a_1 k^2 + a_2 k + a_3 = 0 \tag{2.11}$$

where

$$a_1 = a\left(\frac{C_f C_r(a+b)}{v_{x0}}\right)^2 + mJ_z b C_r^2 \omega^2 + mC_f C_r^2 b(a+b) \tag{2.12}$$

$$a_2 = (b-a)\left(\frac{C_f C_r(a+b)}{v_{x0}}\right)^2 + mJ_z(b-a)C_f C_r \omega^2 - mC_f C_r(a+b)(aC_f + bC_r) \tag{2.13}$$

$$a_3 = -b\left(\frac{C_f C_r(a+b)}{v_{x0}}\right)^2 - mJ_z a C_f^2 \omega^2 + mC_f^2 C_r a(a+b) \tag{2.14}$$

The quadratic equation can be solved at a particular frequency ω. The optimal frequency to set the phase equal was argued to be between 0.5 Hz and 1 Hz, since the steering frequency is usually between these frequencies. This also agrees with the previous Honda study, where the work presumes that 0.75 Hz is the frequency where driver steering correction takes place. The results of this choice of gain is similar to the gain derived when setting the steady state value of the body slip to zero. A comparison is shown in Figure 2.4. When the frequency ω is made zero, the curves match[1].

Mazda also investigated the subjective perceptions at low speeds where parking and u-turns were considered. When the maximum allowed rear steer angle was greater than

[1]Note: the quadratic equation has two solutions. At zero the other upper limit $\frac{aC_f}{bC_r}$ is the limit for the frequency zero.

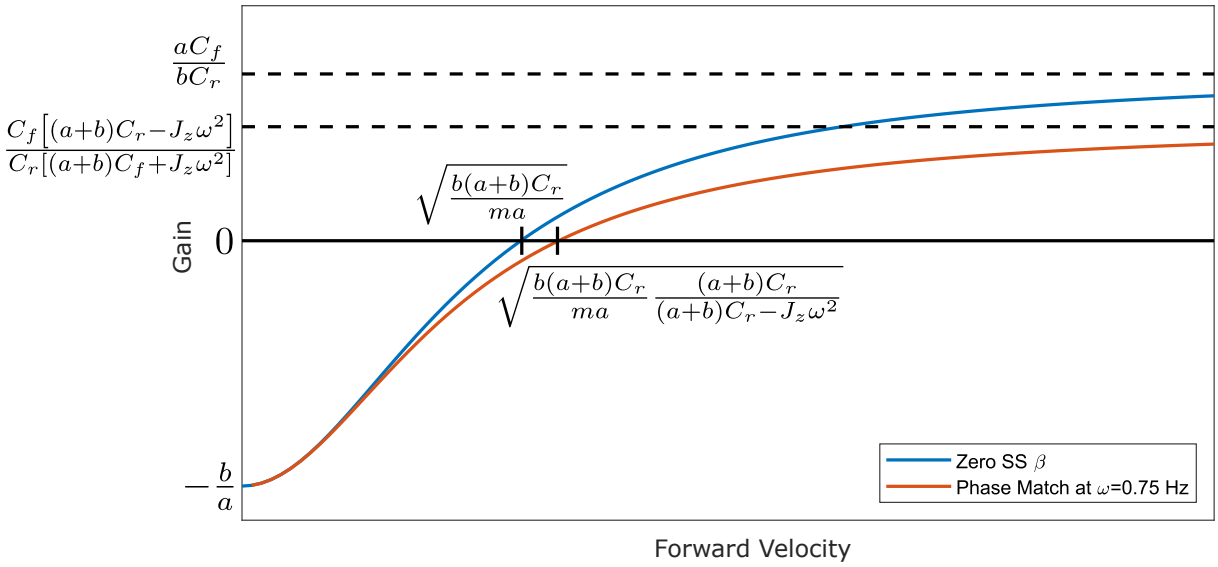

Figure 2.4: Comparing zero SS body slip and 0.75 Hz phase matching.

4°, test drivers could perceive the decrease in turn radius. Some drivers found parking more difficult when the rear steer angle exceeded 6.5°. Therefore, it is suggested that for these low speed situations the optimal maximum steer angle of the rear should be 5°.

Work from Nissan is in agreement with the previous works discussed. Nissan's work proposes that in a 2WS vehicle at high speeds, the rear wheels deflect to the outside of a turn. This situation is what causes a decline in perceived steering performance. Increasing the slip angle at the front is done by steering more, but to produce more slip at the rear the vehicle attitude must change and swings out more. This issue can be resolved by steering the rear in. 4WS also makes it possible to vary the equivalent corning power of the tires at will.

Subjective testing showed that the system should be controlled by making the phases the same. It is also stated that "Eliminating the phase difference of lateral acceleration in relation to the yaw rate would have the same effect as reducing the dynamic sideslip angle at the vehicle's center of gravity to zero [38]."

Although there are benefits from zero body slip at high speeds, it does not come without downsides. One major problem identified is the deterioration the yaw rate response. The deterioration of yaw response is described as a yaw rate reduction in gain, along with a delay in rise time. This is described as "strong understeer characteristics [39]." The

gain reduction is easily seen in the equation for the yaw rate for a neutral steer vehicle in Equation 2.6. As the steering ratio k increases, the overall gain decreases. However, the change in yaw-rate phase happens because vehicles are generally designed with an understeer characteristic, where $bC_r/aC_f > 1$.

Another drawback is that the transient body slip can occur in the opposite direction from a system with RWS, which can be "disconcerting to the driver [41]." A solution was explored for the transient problems by testing several filter designs. These filters are used to augment the rear wheel output when the zero body slip condition from Equation 2.7 is used in order to improve the transients, especially the yaw rate transient.

First, a first-order lowpass filter is added. The purpose is to delay the generation of side force at the rear wheels just long enough to allow the necessary yaw rate to be obtained. The lateral acceleration response does suffer, but a large improvement is seen in the yaw rate.

The second filter is a first-order advance control, which would steer the rear wheels opposite as a response to the driver's steering input. The overall filter would be $\delta_r = (k - T_r s)\delta_f$, where T_r is tuned, and k is the necessary ratio to make the steady-state body slip zero. This would respond to the driver's steering wheel angular velocity. The idea is to give more yaw when a driver turns by steering the rear wheels opposite, before settling on same phase steering in steady state. There is a limit on setting T_r, because if its too high, the vehicle's lateral acceleration generated can be in the opposite direction, which can disconcert the driver.

Finally, to overcome the limitations of a single input from the rear-wheel actuator, the front wheel is controlled as well. This development is expanded on in another section below.

The experimental results saw the best improvement when the front and rear wheels were both controlled, followed by the first-order advance control, followed by the first-order delay control. The first-order delay was described as making the vehicle behavior natural. The advance filter was described as providing crisp and sharp steering [41].

In practice, the gain would not span the range derived in Figure 2.4 because the rear

wheels have saturation limits. The theoretical values reach close to 1:1 and 1:-1. While the front tires are limited to around 30°, the rear is limited to about a third of that or less due to packaging and costs. Specialized test vehicles may allow large rear steer angles, but consumer vehicles do not.

Work done by Whitehead analyzes RWS control at low and high velocities [29]. The high speed control strategies are compared to a front-wheel steer case. A gain-based conventional control is case 1, while a control methodology that keeps the body slip at zero during steady state and transients is case 2. Bode plots are used to study the responses. The outputs studied are the displacement of the front axle and the heading angle, while the input is the front steering angle. The response delay interpreted through the phase plots of the bode indicates that case 1 reduces phase lag, while case 2 eliminates it. Another conclusion is that the tires are used more efficiently by a RWS vehicle during transient maneuvers.

The author also tests the driver's ability to affect the car at high frequency inputs. In an experiment, drivers were asked to steer on a dummy steering wheel. What was concluded was that at the most, above 10 radians per second, the driver would only be able to move the vehicle laterally by 70 mm, which is negligible. Therefore, studying frequencies above this limit would be pointless. Below 10 radians per second, the drivers were able to steer the vehicle enough to exceed the tire adhesion limits.

Another claim by the author is that RWS should not be expected to enhance a vehicle's ideal slalom performance when the Honda Prelude is considered. This is derived from studying the tire forces frequency response and assuming that the maneuver is basically a lateral sine wave 0.9 m in amplitude and near 3 rad/s frequency. The advantage of RWS for reducing rear tire force peaks occurs at higher frequencies, so it is argued to not expect enhancement in the slalom maneuver.

However, lane change should see improvements. Quick lane changes can have significant frequency content up to 10 rad/s. Therefore, the whole spectra can influence the response. The author estimates that the most rapid lane change must have fundamental frequency components as low as 2 rad/s. The optimum emergency lane change maneuver

must have frequency content up to 6 rad/s. Considering these frequency components, it is determined from frequency responses that RWS can maximize the efficiency of tire utilization at these higher frequencies. In addition, a lane change with 2WS is expected to be 15% slower than a RWS vehicle due to phase lag and delay in the lateral displacement response. The heading angle deviation required is also reduced by 4WS.

The author goes on to postulate that the stability improvements of RWS over front-wheel steering might be a combination of reasons such as faster response time, smaller heading angles, and more efficient use of tires during maneuvers, and that less frequency content above 6 rad/s is required in emergency maneuvers. Another possible contributor is the free control oscillation of a vehicle at 6 rad/s. This is basically how the vehicle responds when the driver has no hands on the wheel and the return moment of the front tires creates an oscillatory mode typically around 1 Hz. To study this, the author modifies an eight order free control model of an automobile by Segel to not include dynamics in the steering wheel. Simulating shows the weave mode crops up during high forward speeds. This weave mode could be a contributing factor to driver overcorrection during a high speed emergency maneuver. It is "to have an unexpected extra pair of hands applying force to the [...] steering wheel in the direction of the overshoot." RWS improves on this weave mode as well.

Therefore, the paper comments on three possible improvements that might be perceived as stability improvements of RWS vehicles: High frequency (6 rad/s) driver inputs have lower delay, the weave mode is less excited, and reducing the rear tire force peaks (i.e. more evenly distributing force across front and back).

2.1.2 Non-conventional Design

One of the first RWS vehicles that came to the consumer market used one of the most unique control designs. The work done by Honda led to the understanding that on winding roads, it is desired to have the rear wheels steer opposite. During near straight line driving, it is desired to steer the wheels in phase. However, the driver's intention and road conditions are not readily available through direct measurement. In order to satisfy both conditions, a system was designed [40] where when the steering wheel was

turned only a little, the rear tires turned in phase with the front. When the steering wheel was turned at a much larger angle, the rear wheels turned opposite of the front. This system only uses the steering angle information to control the rear mechanically. This nonlinear dependence on the steering wheel angle is able to satisfy two objectives which were seemingly at odds. The benefits are that at high speeds, using only a small amount of steering wheel angle input gives the better lateral acceleration feel (low phase delay). When winding roads are negotiated, the large steering wheel inputs gives the better yaw response. The steering angle is used as an indicator of the type of negotiation the driver is trying to accomplish, and speed is not used.

Antother non-conventional design is the work done by Bosch and General Motors [42]. The rear steer controller algorithm is made up of a linear and a nonlinear component. The linear component allows for tuning of the steering ratio, while the nonlinear component can change the transient dynamics. Two tests were performed comparing different steering ratios, a slow and a high steering input test. When the steering input was kept slow (100 deg/s), steering the rear wheels opposite gives a larger yaw response, which could give a feeling of a nimble or sporty vehicle. Steering the wheels together provided subdued dynamics for the passenger. However when the input was fast (500 deg/s), steering the rear wheels opposite would result in a response drivers described as "two-stage," where the rear axle force was distinctly felt after the front axle. Steering the rear wheels together increased the lateral jerk.

Tests comparing tire types (winter, summer,all weather) were also performed. Depending on the tires used, the body slip angle can be significantly altered, even if yaw rates are similar.

The author notes that there is a limit to how much RWS can be used comfortably. In addition, care should be taken when tuning the body slip angle. Tuning the body slip too small leads to a vehicle that awkwardly points away from the turn, while tuning it too large can resemble driving a car with a flat tire or snow tires.

2.1.3 Feedback Control of the Rear Wheels

Another common control structure in literature is the feedback control structure. Feedback allows for robust manipulation of the system's signals which can handle disturbances and parameter changes of the vehicle. It separates the desired signal created by the reference generator and the controller which attempts to keep the error at zero. Manipulation of output signals can also be done with the previous feedfoward strategy, but loses the robustness advantages and can be complicated.

Figure 2.5 shows an example of this, which consists of a prefilter F_r and compensator/controller H_r. The prefilter can be interpreted as a the reference generator, which takes in the driver's intention in the form of their steering wheel input. Other inputs can be used as well. Typically the signal that is being controlled is the yaw rate, but lateral acceleration or a combination can also be used, along with body slip angle. However, the body slip would need to be estimated.

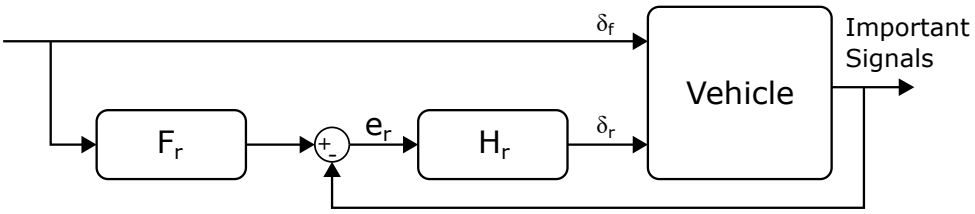

Figure 2.5: Feedback control structure (adapted from [28]).

Sato from Toyota worked on the RWS system introduced on the 1991 Toyota Soarer [43]. The system uses a combination of feed forward and feedback in order to improve the vehicle response. The system keeps the slip angle at zero, even in transient behavior. This leads to a convergence of yaw rate and lateral acceleration response with respect to the steering input.

The main addition to the system is a feedback term using the yaw rate signal. This adds some robustness to stability in regards to disturbances from side winds or road surface irregularities. The reference for the system is created with lookup tables that are dependent on the forward speed, v_x, the front steering angular velocity $\dot{\delta}_f$, and the front steering angle. This is shown below, where k_1,k_2,k_3 are values determined by tuning maps. k_1 is the opposite-direction steering angle proportional gain, k_2 is the tuning gain

of steering velocity, and k_3 is the yaw rate proportional gain.

$$\delta_r = k_1(v_x)\delta_f + k_2(\dot{\delta}_f, v_x)k_3(v_x)\omega_z \tag{2.15}$$

The purpose of responding to the derivative of the front steer angle is because there is a delay associated with the actuator, and it improves the initial response of the vehicle. When the vehicle is driving in a straight line, the yaw rate proportional value is dominant. This is good for wind rejection, which decreases the driver input and the ride is more stable.

Work from Seul University [44] uses a control scheme where the RWS control is split up into a steady-state component, and a transient component. This is similar to the work by Bosch and General motors described in a previous section, however, this work uses feedback. The steady-state component is designed by using an understeer gradient ratio, which is a ratio of understeer gradients from the front steering input and rear steering input. However, it was designed such that the body slip is zero. The transient component uses a gain on the feedback from the lateral acceleration and yaw rate. The combination of the signals is based on the derivative of the body slip. It is generated through the relationship as follows:

$$a_y = \dot{v}_y + w_z v_{x0}$$

$$\dot{v}_y = a_y - w_z v_{x0}$$

and

$$\dot{v}_y = \dot{\beta} v_{x0}$$

Therefore, $\dot{\beta} = a_y/v_{x0} - w_z$. It is assumed that the forward velocity does not change.

2.1.3.1 Reference Generators

For a single-input single-output system, the controllers used are typically standard and not interesting. Works that describe how the vehicle should behave and feel, or offer alternative methods for setting the reference generators of the vehicle give better insight into the lateral dynamics of the vehicle and offer unique ideas into what can be done.

Creating the reference signal or identifying the ideal feeling a car should have is a difficult task. Some papers have asserted what the ideal vehicle should do. For instance, an engineer from Nissan Motor Co. asserts that the ideal theoretical vehicle would have a frequency response characteristic from the steering wheel input to the yaw rate and lateral acceleration where "the gain would be at a given constant level and the phase lag equal to zero. This vehicle [behavior] is obtained through [] phase reversal control at the rear wheels and differential control at the front wheels. [38]" This idea came from analyses on a vehicle model. Although this type of response is ideal for any controlled system, where the response is the same at all frequencies, it is uncertain if this is ideal for the driver. This would require vehicle would steer the rear wheels opposite momentarily in the transient, before steering in phase.

A driver model is created based on the assumption that the driver steers the vehicle according to the error between the vehicle's position and the target point the driver aims to pass through, it is asserted that the vehicle must coincide with the actual direction of forward movement. This is because "in order to steer the vehicle accurately, the vehicle must provide high fidelity outputs in relation to the driver's steering inputs. [38]" When the body slip is zero ($\beta = 0$), the claim is satisfied, along with keeping the delay low in the frequency characteristic from steering wheel to yaw rate.

This can be deduced by studying the lateral acceleration equation. The lateral acceleration is $\dot{v}_y + v_{x0}\omega_z$. If it is desired to make the lateral acceleration and yaw rate phase equal at all frequencies, then $\dot{v}_y = 0$ should be enforced over all frequencies. This is equivalent to making the body slip zero over all frequencies, since the gain of the system does not affect the phase and the two signals would have the same poles and zeros,

Another reason for keeping the body slip zero comes from Fijalkowski, where the claim is that if the body slip angle is large, the driver drives with an "inclined line of vision," which is a reason for driving difficulties [27]. This is a physical attribute of the driver which is not often considered.

Mobis [45] introduced a unique model reference called yaw center control. The concept shifts the C.G. location while keeping the overall length of the model vehicle the same.

This changes the yawing behavior of the vehicle. The yaw rate of the model reference is then used to create the error in the system. The advantage of the system is that only one parameter is used to tune the system. The optimal location of the C.G. is not discussed, but possible methods of controlling the location are suggested, such as a lookup table dependent on vehicle speed or a comfort mode.

Work by Daimler AG [46] introduced a similar concept called pivot point distance. Given a front and rear wheel angle, the instantaneous center of rotation can be found from the kinematic bicycle model. When a line is drawn from this point to the vehicle body such that its orthogonal to the body, that intersection is called the pivot point. When this point is manipulated, both states of the bicycle car model (lateral velocity and yaw rate) are affected.

Typically in the literature the yaw rate is controlled directly. A choice is made in what to control as the yaw rate and lateral acceleration (or body slip) are inherently coupled, and a compromise between improving either signal is inevitable. One technique for compromizing comes from the aircraft industry. The term "C* criterion" is a new variable that is made up of a blend of two signals. Specifically, when pilots control the pitch axis of the aircraft, they respond to different sensations or motion cues depending on the speed of the aircraft. At lower speeds, the pitch rate is used. At higher speeds, the pilot's load factor (related to heave acceleration) is used. Therefore, a normalized blend of the two signals (pitch rate and normal acceleration) is created called C*. A criteria for the directional axis is also created, where the blend of lateral load factor (lateral acceleration) and sideslip is used. This is called D* [47].

Ito from Nissan implements this control strategy in his work [48]. He states that during normal driving, a person steers with an emphasis on the yaw rate. During emergency avoidance, a person steers with an emphasis on the lateral acceleration. He designs a reference model for the vehicle and compares three different systems. The reference is tracked using only yaw rate, only lateral acceleration, and a linear combination of both lateral acceleration and yaw rate. It is important to distinguish that in Ito's paper, D* refers to the linear combination of lateral acceleration and yaw rate, which differs from

the aero industry use of load factor and sideslip.

The definition for D* created by the paper is $D^* = da_y + (1-d)v_x\omega_z$, where $0 \leq d \leq 1$. The feedback loop is made up of three gains, which are derived using LQR. These gains are a function of the vehicle speed. Using the D* definition, both signals/movements are achieved at a high level, as described by Ito.

Other methods of considering multiple signals is the use of optimization. In one example, from work by Cho [49], LQR optimization is used to determine what the rear wheels should do. The system includes a driver model to simulate a driver following a path, so the objective of the controller is to support the driver model. With LQR, it is assumed that the control system has access to all the signals of the vehicle, even the ones that might be impossible to measure such as information the driver has regarding tracking the road. However, the work does not consider feasibility. Three different strategies were used in order to tune the optimization. The first strategy was to minimize all the state variables, including the lateral deviation of the vehicle from the path and its rate, the yaw angle and rate, and finally the front steering angles. In the second strategy, the side slip velocity is minimized. The third strategy minimizes both the side slip velocity and angular velocity. The argument for this is that it is considered that it reflects ride comfort better than just the side slip velocity. However, in simulations the vehicle exhibited some undesired responses, such as the rear wheels steering more than the front.

Cho introduced another controller concept, in which the objective is to maximize the stability of the system. A lookup table is used to define the steering ratio, similar to other lookup tables to keep the body slip zero. Stability in the work is defined by the location of the poles of the system, where the largest negative real root is looked at.

2.2 Active Front and Rear-Wheel Steering

Many early papers determined that keeping the body slip of the vehicle at zero was the best thing to do. Systems with only active rear wheel steering were used for this objective. However, this often led to worse yaw response characteristics. Specifically, the yaw gain dropped significantly. In order to remedy this, many authors looked to using

active front steering along with active rear steering. Many different configurations have been done such as an open loop or as depicted by Figure 2.6, closed loop. The closed loop configuration could be multi-input multi-output (MIMO) or multi-input single-output (MISO). The error signal e in the figure may be a vector of errors, where F is a reference generator.

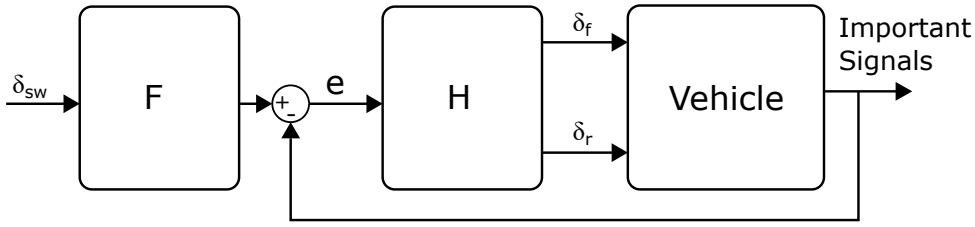

Figure 2.6: A generalized feedback structure (adapted from [28]).

Here, some papers are presented to discuss the reference generation, and some ways to achieve better vehicle handling.

2.2.1 Open Loop

Work from Nissan has been discussed already regarding its RWS only implenataion, but it also consists of active front steering in combination with RWS [39]. One important issue that led to integrating active front steering is the excessive drop in vehicle response gain in relation to steering maneuvers. This is at higher speeds with a control strategy that reduces the body slip to zero. The turning radius would also sharply increase when the vehicle forward velocity increased during a turn. This could cause the driver to plow and head off the road when accelerating and turning at the same time.

In order to circumvent this understeer characteristic, active steering at the front could be applied to change the steering ratio from the driver to the front wheels. With this amount of actuation, the system is designed to have the steady-state gain characteristics of yaw and lateral acceleration identical to a 2WS vehicle, and the frequency characteristics to have zero phase lag. At low speeds the active steering of the front steers at a fraction of what it would steer previously. At higher speeds the front steers more. The authors calls the system the optimum control method for four-wheel active steering.

First, an open loop MIMO controller is developed which takes into account the cross

coupling between the yaw rate and lateral acceleration. The plant can be described as follows.

$$\begin{bmatrix} \frac{\omega_z}{\delta_f} & \frac{\omega_z}{\delta_r} \\ \frac{a_y}{\delta_f} & \frac{a_y}{\delta_r} \end{bmatrix} \begin{bmatrix} \delta_f \\ \delta_r \end{bmatrix} = \begin{bmatrix} \omega_z \\ a_y \end{bmatrix} \tag{2.16}$$

In order to control the front and rear wheels, a controller needs to be developed. A simple approach would be to use the inverse of the plant, and to use the desired properties of the plant as an input. This can be described as

$$\begin{bmatrix} \frac{\omega_z}{\delta_f} & \frac{\omega_z}{\delta_r} \\ \frac{a_y}{\delta_f} & \frac{a_y}{\delta_r} \end{bmatrix}^{-1} \begin{bmatrix} \omega_{zdes} \\ a_{ydes} \end{bmatrix} = \begin{bmatrix} \delta_f \\ \delta_r \end{bmatrix} \tag{2.17}$$

The controller generated has improper transfer function entries. In addition, since the plant has a transmission zero at $s = 0$ (discussed in more detail in Section 4.3, the controller with have an integrator in the entries. The improper entries can be realized with added poles to the controller and/or combining the controller with a reference generator. Since a driver is still controlling the system through a steering wheel, the desired yaw rate and lateral acceleration can be described through the following:

$$\begin{bmatrix} \frac{\omega_{zdes}}{\delta_{sw}} \\ \frac{a_{ydes}}{\delta_{sw}} \end{bmatrix} \delta_{sw} = \begin{bmatrix} \omega_{zdes} \\ a_{ydes} \end{bmatrix} \tag{2.18}$$

Using these relationships, the input into the plant through the tire angles can be rewritten as

$$\begin{bmatrix} \frac{\omega_z}{\delta_f} & \frac{\omega_z}{\delta_r} \\ \frac{a_y}{\delta_f} & \frac{a_y}{\delta_r} \end{bmatrix}^{-1} \begin{bmatrix} \frac{\omega_{zdes}}{\delta_{sw}} \\ \frac{a_{ydes}}{\delta_{sw}} \end{bmatrix} \delta_{sw} = \begin{bmatrix} \delta_f \\ \delta_r \end{bmatrix} \tag{2.19}$$

$$\begin{bmatrix} G_{c1} \\ G_{c2} \end{bmatrix} \delta_{sw} = \begin{bmatrix} \delta_f \\ \delta_r \end{bmatrix} \tag{2.20}$$

where

$$G_{c1} = \frac{\frac{a_y}{\delta_r}\frac{\omega_{zdes}}{\delta_{sw}} - \frac{\omega_z}{\delta_r}\frac{a_{ydes}}{\delta_{sw}}}{\frac{\omega_z}{\delta_f}\frac{a_y}{\delta_r} - \frac{\omega_z}{\delta_r}\frac{a_y}{\delta_f}} \tag{2.21}$$

$$G_{c2} = \frac{\frac{\omega_z}{\delta_f}\frac{a_{ydes}}{\delta_{sw}} - \frac{a_y}{\delta_f}\frac{\omega_{zdes}}{\delta_{sw}}}{\frac{\omega_z}{\delta_f}\frac{a_y}{\delta_r} - \frac{\omega_z}{\delta_r}\frac{a_y}{\delta_f}} \tag{2.22}$$

These derived open loop filters are used by Shibahata. Although the plant may have non-minimum phase zeros in some entries, the open loop MIMO controller here does not directly cancel out right-half plane zeros with unstable poles. The desired transfer functions of the yaw rate and lateral acceleration are the steady state gains of a conventional vehicle. Therefore, the theoretical response would be a flat gain at all frequency inputs and no phase lag. The results prevent excessive enlargement of the turning radius when the vehicle is accelerated while making a turn, as well as preventing the drop in steering response gain at high speeds. This would theoretically have a great response according to the paper.

Additional work from Nissan has discussed the use of filters to augment the transient response of the vehicle while also keeping the steady state bodyslip angle at zero [41]. One of the methods to combat the yaw rate gain drop (which deteriorates the cornering performance) was to add an additional filter to augment the front wheels. A first-order advance control is used on the front wheels in addition to an advance filter to the rear. The derivation leads to flat vehicle characteristics (constant gain and zero phase), similar to the previous work discussed. This is tested in an experimental vehicle. The results compared to other RWS algorithms show that controlling the front and rear wheels had the best yaw rate rise time characteristic, the best performance for lateral acceleration, and had good balance of stability and response at high levels. Evaluators commented that zero body slip at all times made the vehicle easy to drive with accurate tracking performance.

2.2.2 Closed Loop

Nagai [50] explored the use of a model reference to control a vehicle. The model reference outputs the body slip angle and yaw rate, which is then controlled by a gain matrix derived from LQR. The LQR was designed such that there was a higher weight on the body slip error. The model reference is a conventional front steered vehicle. The real car's front and rear wheels are controlled to track the model reference states. The model reference was tested with designs that exhibited weak understeer, strong understeer, and strong oversteer. The work was able to conclude that the virtual vehicle could be tracked successfully, even with significant changes in the virtual vehicle's parameters. Including feedback helped with stability against crosswind disturbance.

Further work with LQR and choice of model reference is studied by another author [51]. The transfer functions of the body slip and yaw rate of the conventional vehicle and their relationship with the forward velocity are analyzed. The steady-state gain of the body slip becomes zero at a lower speeds, and the steady-state gain of the yaw rate increases as the speed increases. Analyzing the poles of the transfer function show that the resonant frequency decreases with increasing speed, which means the transient steering responses become worse at high speeds. Using this information, the desired performance of the model reference vehicle is determined to be the same performance at the forward speeds of $16.6m/s$, where the steady state side slip angle is zero. This should result in eliminating the unnecessarily large yaw motion at high speed turning, and improve transient steering response at high speeds. Results are made with open loop and closed loop tests, where a driver model is included. Some improvements include less steering effort by the driver using a 4WS system compared to a 2WS system, and higher stability in response to side gusts of wind with a feedback system. It is possible to design an arbitrary performance of stability and handling by controlling the front and rear steer angles cooperatively.

Ackermann proposes a unique control methodology different from the work previously discussed [52],[28]. A control law is used where the derivative of the steering wheel angle controls the yaw rate error of the vehicle through feedback. This choice can lead to a robust compensator for vehicles where the front-axle lateral acceleration is decoupled from the

yaw rate. The decoupling means that the other states in the system are unobservable from the front-axle lateral acceleration. Therefore, the driver only has to control the lateral acceleration subsystem by trying to keep the point at the front axle on the road through the lateral acceleration. However, this depends on the assumption that the moment of inertia is $J_z = abm$.

The system designed has poor damping characteristics at higher speeds. Therefore, rear wheel steering is used to place the poles in the desired configuration. This gives the vehicle's yaw model better characteristics. Simulation results show robustness against disturbances such as side winds or braking under split mu condition. Adding a prefilter that is a function of the forward velocity, the steering wheel can command the reference of the lateral acceleration of the front axle.

Canale uses internal model control (IMC) in order to track both the yaw rate and body slip angle [53]. A simple mapping taking in the vehicle speed and handwheel angle is used to provide the reference yaw rates and body slips. The more interesting contribution is its use of IMC. This is mathematically similar to a Youla-Kuchera control design. However, the internal model control is an enhanced version where actuator saturation is considered. This creates a nonlinear controller overall. The work also considers multiplicative uncertainty which represents parametric uncertainty for vehicle speed, inertial characteristics, cornering stiffness's, and tire relaxation lengths. These are considered in the design of the controller for robustness. To solve for the controller, the use of an H_∞ norm is used. Simulations performed shows good robustness and stability properties.

2.2.3 Reference Generators

The inclusion of the front and rear wheels can lead to interesting ideas on how to control the vehicle. One idea is the use of the center of percussion of the vehicle. This is described as the point on the vehicle where an impact force on the wheels causes no lateral acceleration. Two points exist on the vehicle, one with respect to the front wheels, and one with respect to the rear wheels. Hiraoka [54] considers using the center of percussion with respect to the rear wheels as the point to control. A control law is developed using the front wheels, where the lateral acceleration of the point considered becomes proportional

to the steering wheel angle input. The influence of yaw rate and body slip angle fall out of the equations.

However, the body slip response and the yaw rate of the overall vehicle was worse with this control law. Therefore, another control law was proposed to be added where the rear wheel keeps the body slip to zero. To make the system robust against uncertainties and the nonlinear characteristics of the tire, a sliding mode controller and reference vehicle model are introduced as well. Computer simulations using CarSim and a driver model show that the vehicle follows the target path adequately while keeping the body slip near zero, even in bad road conditions such as on a packed snow road. It is robust against crosswind disturbances as well.

Russell and Gerdes [55, 56] have a special application of front and rear wheel steering control. The purpose of their work was to create a car that behaves as though it is on low-μ friction while operating on dry asphalt. The reference model is a low-μ front steered vehicle. A combination of feed forward and feedback is used to control the vehicle, however, special consideration is taken into account. The high body slip angles require large rear steered angles, which are prone to saturation. Therefore, when the rear wheels saturate, the controller objective becomes track the model yaw rate instead of both yaw rate and body slip.

Emulating the dynamics of other vehicles has also been done in Lee's work on the Variable Dynamics Testbed Vehicle (VDTV) [57, 58]. The goal was to determine how well their VDTV with four-wheel steering can emulate the lateral dynamics on a wide variety of vehicle models, from small to full size. Work done by Akar also shared this goal [59], where the vehicles emulated range from a compact size vehicle up to a bus. The control methodology consisted of feeding back the body slip and yaw rate of the vehicle and the use of sliding mode control.

2.3 Electronic Stability Control

In order to better understand how RWS can be used for stability purposes, especially in an emergency situation, its important to understand what is currently being used. This

background can guide how RWS can be applied and for the purposes of comparison.

The National Highway Traffic Safety Administration (NHTSA), an agency part of the U.S. Department of Transportation, created the Federal Motor Vehicle Safety Standard (FMVSS) No. 126. This safety standard required implementation of electronic stability control (ESC) on all vehicles starting in 2012. The documents include the docket, the final impact analysis, and the laboratory testing procedures [60, 61, 62]. These documents include an enormous amount of information, including costs of the system, its effect on fuel efficiency due to weight, human lives it could potentially save, along with a myriad of other estimates. The most important information in the documents is the standard that is used to show what is considered stable and the arguments surrounding it. In addition, there are comments from interested parties, including automobile suppliers, safety advocacy groups, and others. These can be beneficial to understanding how stability should be defined.

The main argument for ESC is that keeps the vehicle headed in the direction intended by drivers, which can keep the vehicle on the road to prevent run-off-road crashes. This is a circumstance which can lead to single-vehicle rollovers. The agency at the time was very concerned with rollovers, which comprised a large share of single-vehicle crashes. This led the agency to add a rollover resistance rating in 2001 which is based on the C.G. height and track width of a vehicle.

The standard introduces a definitional requirement and a dynamic performance test the ESC system would need to pass. The agency uses a definition based on the SAE Surface Vehicle Information Report J2564. The definition includes what the system can measure or estimate, the actuator (brakes) it uses, its capabilities, etc. If one strips away any mention of brakes, a list of necessary components for a method of stabilization can be created. The main ideas that could apply to any actuation method are

- ESC augments vehicle directional stability to induce a corrective yaw moment
- ESC is a computer-controlled system which uses a closed-loop algorithm to limit vehicle oversteer and understeer

- ESC is operational over the full speed range except for less than 15 kph (9.3 mph)
- ESC must be operational during all phases of driving including acceleration, coasting, and deceleration (braking) unless deactivated
- ESC must remain capable of activation even if the antilock brake or traction is also activated

This of course means that the actuation method needs to have enough control authority at limit-handling conditions. However, having a combination of actuation methods may improve current ESC technologies.

The standard also defines a lateral stability and a responsiveness criteria which together achieves an acceptable stability performance. At the time of writing, the final rule does not specify any understeering performance criteria. The testing method only induces oversteering and only oversteering related performance criteria must be met.

The test, which is a sine with dwell, will initiate oversteer intervention by every ESC tested and will "discriminate strongly" between vehicles with and without ESC. In addition, the maneuver is representative of steering inputs produced by human drivers in an emergency obstacle avoidance situation. More information on the testing is discussed later in Section 6.2.

2.3.1 Comments from the Public

Documents surrounding the safety standard include public comments from companies. These show interesting ideas and topics that go beyond ESC with brakes. For example, companies such as BorgWarner Torq Transfer Systems, Delphi Corporation, RLP Engineering, the Association of International Automobile Manufacturers, and the Alliance of Automobile Manufacturers, argued that ESC standard should only define the performance standards and not the method, as the method can be any actuator that influences the tires and friction. Defining ESC as using friction brakes is limiting.

Delphi for example, had various alternative technologies in various stages of development including: active steering systems (active front steering, active rear steering, steer by wire, electronic power steering), active drivetrains (active differentials, electronic limited

slip differentials, electric motor/generator devices for propulsion/braking), and active suspensions (active stabilizer bars, active dampers, active springs.) An argument from Delphi is that other technologies could operate across a range of linear-handling to limit-handling conditions while braking systems are restricted to limit-handling conditions. Active front steer and active rear steer may prevent the vehicle's tires from reaching total saturation in the first place, thereby avoiding unstable and unresponsive situations.

The NHTSA rejected the change because no information was provided to demonstrate the efficacy of the ESC-related technologies as an alternative to brake-based ESC systems. In addition, in response to Delphi's comment that active steering intervention could operate at driving conditions well below critical levels of tire saturation and produce a more responsive vehicle, the NHTSA commented that the steering interventions may not be very helpful at or near the limit of traction. This arguably is the critical situation at the heart of the rule making. Braking forces have an advantage over steering forces because they can create a more powerful yaw intervention when the vehicle is at the limit of traction (Liebemann et al, Safety and Performance Enhancement: The Bosch Electronic Stability Control (ESP), 2005 ESC Conference).

2.3.2 Bosch 5 Years of ESP Experience

Bosch [63] published an informative paper that describes the practical problems that are encountered when implementing ESC. They make a case that vehicle slip angle is a "crucial indicator for maneuverability." They also make reference to the work by Shibahata's β method study [64], which is described in more detail in later sections.

First, utilizing the β-method, it is shown why it is difficult for a driver to control the vehicle near the limits. Figure 2.7 shows the yaw moment produced by the vehicle under various steering angles and body slip angles. The larger the yaw moment, the larger the change in yaw rate. However, the body slip affects the yaw moment as well. When the body slip is large, the steering has much less influence on the yaw moment, which is difficult for drivers to control.

Second, an additional method to analyze the system is referenced which uses the $\beta - \dot{\beta}$ phase plane. This shows that the slip angle stability margin is reduced in the direction

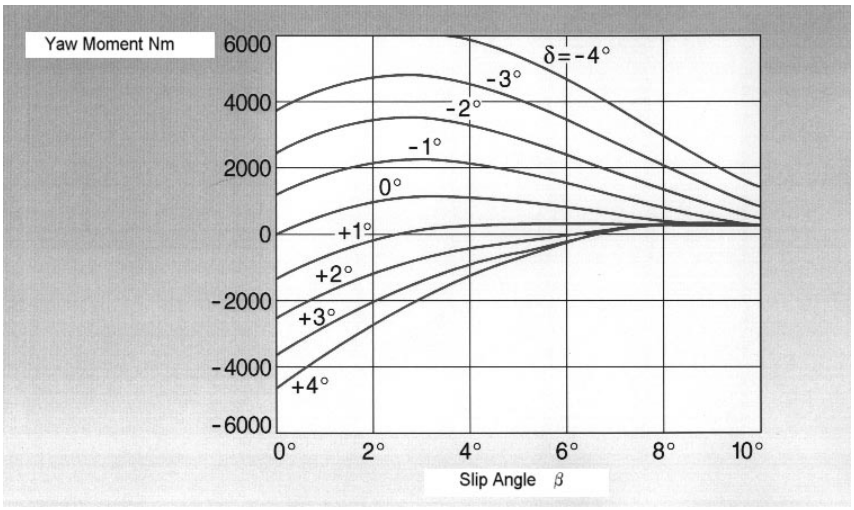

Figure 2.7: β-method diagram from [63].

of steering for non-zero steering angles. For large steering angles, the stability margin disappears. Both analysis methods show the same trend. According to the author, the physical limit on asphalt roads is approximately $\pm 12°$ of slip angle, while on ice this is approximately $\pm 2°$. Under normal driving, average drivers will not exceed slip angles of $\pm 2°$. At high speeds, the author dictates that the slip angle of the car should not exceed $6°$.

An important consideration that is brought up is the tire model. A tire model is needed in order to compute side forces that are not measured directly for a full car model that estimates necessary signals. Changes between tire types or even tire wear changes the parameters of the system. The HSRI tire model is used, where a simple relationship between lateral and longitudinal force can be derived from it. The relationship discussed is as follows:

$$F_y = \frac{C_y \tan \alpha}{C_x \lambda} F_x \tag{2.23}$$

The significance of this relationship is that it can use a ratio of lateral to longitudinal tire coefficients, which the author asserts is robust with respect to changes from summer to winter tires, or changes in tire wear.

The ESC uses yaw rate error and body slip error to create a desired yaw moment, which is fed to the brake slip controller and traction slip controller. The specifics of the

control logic is not discussed. Only the model used for estimating the signals.

A special case for ESC is discussed, which is the split-μ case. According to the author, the control cannot interpret the steering angle as a cornering desire. ESC has a closed loop control of the asymmetric brake forces on the front and rear tires, which depends on the driver's countersteering. The yaw moment of the brake force imbalance is countered by the lateral forces of the tires. Therefore, the ESC needs to account for the speed at which the driver applies the countersteering. If its slow, then the yaw moment from the asymmetric brake forces must not be increased fast. If the driver is fast, then it can be increased fast. This system results in braking distance being increased by 15% compared to production anti-lock braking system (ABS). Production ABS uses only open loop control[2] on the front tires, while using low control on the rear tires to keep the car under control.

The author gives many examples of special cases. Even more special is split-μ straight line driving at low speed. Here, traction is of the highest importance. In order to improve the traction under this condition, the low-μ side of the driven axle needs the brakes applied. This results in an involuntary yaw movement which must be compensated by countersteering.

The ESC logic and production ABS without ESC is tested on a lane change maneuver during full braking on ice. The test results in the driver using less effort to steer the ESC car. In the ABS only system the driver needed to heavily countersteer. The ESC logic utilizes a Kalman filter to estimate the lateral velocity, which is based on a full vehicle model. Experience has shown that during full braking tests, slip angle estimates are quite accurate. However, during free rolling of the tires, the observer cannot be used and slip angle estimates have to be derived from different estimators, specifically, integrating the equation for the derivative of the slip angle.

On a constant radius test, a vehicle with ESC and without are compared. The speed is slowly increased. At up to 7 m/s^2 lateral acceleration, both systems behave identically. At 7.5 m/s^2, the vehicle without ESC loses control. The vehicle with ESC limits the

[2]This is the paper's assertion at the time, but depends on the ABS type.

engine output torque to keep the vehicle within the limits of adhesion.

The paper does well in talking about all the specifics of ESC, and informative regarding the split-μ case.

2.4 Comparison of Rear-Wheel Steering for Stability

One of the benefits of RWS is the improvement of stability at higher speeds by steering the rear wheels in phase with the front. This traditional method of RWS control fundamentally changes the dynamics of the vehicle, and how the vehicle responds to the driver's steering compared to a vehicle without RWS. This stability improvement is always on, responding to the driver's inputs. However there are many other actuation methods that can help stabilize a vehicle, such as using the brakes at a corner of the vehicle to induce a yaw moment which turns on when detecting a stability issue. This type of stability improvement is known as ESC. In order to make a persuasive argument, RWS or integration of RWS with other actuation methods needs to be compared the current state-of-the-art for stability, as well as other alternatives. The standard stabilizing method in current vehicles is ESC. Also known as electronic stability program (ESP by Bosch), this system uses the brakes strategically to keep the vehicle from oversteering or understeering.

In order to explore stability in RWS, this section looks at papers that compare different stability methods. Some papers [64, 65, 66, 67] have looked into comparing these different approaches to RWS, such as active rear wheel differential, roll stiffness distribution, and ESC.

2.4.1 Stability Cases

Interesting stability cases that can be explored include fishtailing, split-μ roads, oversteering vehicles above its critical speed, and understeering vehicles. Fishtailing is a driver induced instability where the driver attempt to stabilize their vehicle through steering. The driver over-corrects exacerbating the problem until finally the vehicle loses control, typically taking three turns of the wheel to finally induce the loss of vehicle control. This type of stability testing would require a driver steering model which over-corrects the steering, and RWS would sense this and stabilize the vehicle.

Typically, split-μ road tests are for braking tests where the difference in μ create an imbalance of braking forces on the left and right side of the vehicle, inducing yaw motion. RWS could potentially steer to correct the yaw, however, this could use up the little remaining tire forces on the wheel with low mu. It would still be an interesting test to explore.

Finally, oversteering vehicles that exceed their critical speed is a straightforward way of testing stability. However, this oversteering can be induced in traditionally understeering vehicles through aggressive steering maneuvers. This is what is done by the NHTSA testing.

2.4.2 Comparison of ESC and 4WS

Authors from the vehicle laboratory in the National Technical University of Athens, Greece published a paper comparing the behaviour a vehicle equipped with RWS, ESC, and the comintation of both [66]. For both ESC and RWS, the control system uses two proportional gains on two error signals, the body slip and the yaw rate. RWS has an additional open loop component that steers the rear relative to the front. The functions that calculate the desired signals are derived from the bicycle model of a vehicle. In the paper the road friction is assumed to be known.

RWS control system has a saturation of 5°, while ESC has a deadband so that the system is not on at all times. Additionally, ABS is used to prevent wheel locking with ESC.

In order to compare the systems on an even playing field, optimization was used to choose the parameters of the controls, as well as the driver model. This seems reasonable, but is dependent on the objective function. Careful assessment of the metrics must be done in order to ensure it defines stability well enough.

Three test cases are performed using their respective objective functions: a sine wave, obstacle avoidance, and a track lap. The sine wave input test comes from ISO/TR 8725, where outputs from the vehicle are compared to the input in order to create metrics, such as how much the signal lags. The obstacle avoidance comes from ISO 3888-2, which is a closed loop test dependent on the driver model. This test looks to maximize the entrance

speed where the maneuver can still be completed, without touching the cones. Finally, a test lap around a track is done where a successful lap is one where the vehicle does not exceed the limits of the track.

The paper found that for the sine wave test, RWS was better than ESC. In the obstacle avoidance and the racing track, ESC performed better than RWS. ESC and RWS combined performed better across all tests. However, this is dependent on how the author defines the metrics. In the test lap on the track, it is desirable to complete the track in the fastest time. RWS completed the track in the fastest time, followed by a vehicle without any stability control. The author weighs maximum speed the driver model attempts to follow high. Therefore in the results, ESC and RWS has a lower cost function.

The paper concludes that RWS performs better than ESC in the open loop tests according to their objective function, while in the closed loop test ESC performed better. When used in combination, the system performs best overall.

2.4.3 Comparison Between Braking and Steering Yaw Moment Control

Authors from two universities in South Korea [68] compared two methods for vehicle stability. Brake yaw moment control (BYMC) uses the brakes to add a moment on the vehicle, which operates like ESC. However, only the brakes at the rear wheels are used to affect the yaw motion. On the other hand, steering yaw moment control (SYMC) steers the rear wheels to stabilize the vehicle. Both methods use ABS, which uses a more advanced sliding mode control scheme. In the case of SYMC, ABS is used only to keep the longitudinal stability, meaning it doesn't let the tires lock. The yaw motion controller is the upper controller which creates either the rear wheel angle or desired slips necessary to stabilize the vehicle. It limits the slip angle in order to prevent vehicle spin. It also maintains the slip angle below a characteristic value to preserve yaw momenta gain. The argument is that if the slip angle reaches the characteristic value, the yaw momenta will be low and the driver will notice they are beginning to lose control.

The BYMC's strategy is to control the slip of the inner rear wheel. The strategy uses

a PID controller for controlling the yaw motion. The tests cases done are simultaneous braking and cornering maneuvers over various road conditions, sinusoidal steering input with full braking applied, and a lane change maneuver with a driver model. The reference yaw rate uses a measurement of the friction coefficient which is assumed can be estimated. The conclusion from the tests is that by creating smaller slip angles, SYMC performs better than BYMC.

Each test has the driver applying full brakes. When full braking is applied, the ESC cannot apply more braking torque on the front outside tire to prevent oversteer. It will need to relieve some braking torque on the inside tires, specifically, the rear inner tire. The author asserts that the rear inner tire has the greatest effect on vehicle direction, referencing the Bosch paper discussed previously.

Braking on split-μ is also tested. The steering wheel is kept straight and the brakes are fully applied. When a vehicle equipped with only ABS is tested, a large deviation from the center line is seen when compared to the other strategies.

2.4.4 Comparisons based on 4WS, Brake, Brake-FAS, and IMC techniques

Authors from the Shanghai Jiaotong University [69] compare various strategies for stabilizing the vehicle. They implemented internal model control (IMC). The vehicle sideslip angle and the yaw rate of the vehicle are used to formulate the errors.

The first strategy is called 4WS IMC, where active front and RWS are used by the controller. The second strategy is a brake strategy which is similar to the ESC braking strategy, where the inner-rear tire is actuated to prevent understeer, while the outer-front is used to prevent oversteering. However, extra steps were taken for control. The system uses a pseudo-linear system where the inverse system theory is applied. This theory uses feedback to linearize a nonlinear system. Since the brakes alone use only one actuation input at a time, the system is a multi-input single-output system.

Brake and front active steering (Brake-FAS) expands on the brake strategy by adding front steering by a controller. Similar to the brakes only strategy, a pseudo-linear system is created for the IMC controller. The front steering and a brake torque are the inputs

into the vehicle.

Open and closed loop tests with a driver model were used to compare the systems. Sine steering tests and double-lane change tests over various road coefficients were made. In addition, a test with white noise into the measured yaw rate sensor was also done to test the disturbance rejection characteristics.

The controller parameters for each filter that was tuned were time constants that were tuned for each controller. For the braking strategies, the tuning had to be done for the different driving scenarios. The tuning for 4WS IMC could cover each driving situation. The authors conclude that 4WS IMC achieved comparatively good results where good yaw tracking and small sideslips were maintained with small steer angles, and kept the speed of the vehicle near constant. In contrast, the brake only strategy had fast yaw rate tracking but the sideslip was large and oscillatory. In addition, the vehicle speed would decrease. Brake-FAS had a mix of the two.

The steerability, measured by the ability of the vehicle to track the yaw rate, was best with the braking strategy. Stability however, characterized by the sideslip angle, was best kept small by the 4WS IMC strategy.

2.4.5 Comparison among Active Front, Front Independent, 4-Wheel and 4-Wheel Independent Steering Systems

The author from the Soul National University investigated different steering strategies for vehicle stabilization [70]. The strategies are as follows: active front steering (AFS), front wheel independent steering (FWIS), 4WS, and four wheel independent steering (4WIS). The control system uses control allocation to determine the steering angles for generating the desired yaw moment. AFS and 4WS use the same steering angles for the left and right, but the other two and independently change their left and right tire angles. In this research when the author use the terms 4WS and 4WIS, they mean that the front wheels are also actively controlled. The author used CarSim for their simulations, where driver model comes from CarSim as well with a 0.75 s preview time. The steering actuators were modeled as first order filters with a time constant of 0.05 s.

The control allocation uses an objective function which minimizes the normalized

lateral tire forces to create the yaw moment. The objective function is subject to the geometry of the vehicle, and how it contributes to the yaw moment. Once the lateral tire forces are extracted through an algebraic solution of the problem, the required tire angles are generated through an inversion of the linear tire force relationship. In addition to the linear tire force relationship, other inverse methods are used, such as using a hyperbolic tangent model of the tire force relationship.

The paper concludes that the independent tire methods of FWIS and 4WIS were superior to their coupled counterparts of AFS and 4WS. However, using the rear wheels were much better than only using the front wheels for the particular situation simulated, which was a closed loop moose test.

2.4.5.1 Optimization of Control Allocation with ESC, AFS, ARS, and TVD in Integrated Chassis Control

An author from the previous paper also published other works. The control allocation and objective functions are the same in both papers. The author's main concern is with studying vehicle maneuvers where the front tires are saturated in a turn [71].

The actuators that can be controlled are the front wheels, the rear wheels, and the longitudinal forces of the wheels. The objective functions are now a combination of longitudinal and lateral forces of each wheel. Torque vectoring (TVD) is done only on the rear wheels. The author uses a separate optimization to determine the "amount of actuator" to use in each combination. Fourteen combinations are used. The metric to determine if the system is good is the maximum yaw rate error, maximum vehicle side slip, and the difference in forward velocity once the test is complete. Each metric is optimized separately to determine the combinations.

The author finds that using rear-wheel steering (ARS) has comparable results to various combinations that yield good results, regardless of the saturation of the lateral forces at the front. This was for a closed-loop steering on a moose test track.

2.4.5.2 Coordinated control with ESC and Active Steering

Here [72], the same author looks at ESC with active steering specifically. Various combinations of actuation are used including ESC applied at the front, applied at the

rear, AFS, and RWS (called active rear steering in the paper - ARS). The same allocation method is used. In addition, a parameter sensitivity study is done around the actuator effectiveness. The paper finds that ARS is satisfactory for yaw moment control. AFS and ARS produces larger body slip angles than ESC methods. The author's work concludes that ESC is necessary to use in order to reduce the body slip angles.

2.4.6 Vehicle Stability Control Through Optimized Coordination of ARS and Drive/Brake

Authors from Wuhan University and Dongfeng Motor Corporation [73] investigated vehicle stability control through optimized coordination of RWS and differential driving/braking. An upper controller creates the desired rear steering angle and the desired yaw moment. The yaw moment then goes through an allocator which determines the longitudinal tire forces at each wheel. This set up is interesting since other allocation methods also allocate the rear tire angle instead of directly being determined by the upper controller. In addition, the same set up is done using AFS instead of RWS for comparison.

The reference models are two independent first order transfer functions. The steady state gain and time constants can be derived from vehicle parameters.

The allocation control uses optimization, which uses a combination of equality and inequality constraints. The paper does not discuss how the optimization problem is solved.

The conclusions drawn are that hierarchical control scheme can help achieve substantial enhancements in handling performance and stability. AFS was found to reduce both the body sideslip and yaw rate, which results in understeer. The drive/braking system generates additional yaw moment to compensate for the deficiency of yaw rate. RWS causes an oversteering system which requires the drive/braking system to correct.

2.4.7 Comparison of Three Active Chassis Control Methods

Work by Honda's R&D center [64] explores stability of the vehicle during acceleration and braking. Combined driving and braking torque of the rear wheels, RWS, and longitudinal roll stiffness distribution control are compared. The work makes heavy use of

"β-method", which are diagrams that describe the stabilizing yaw moments. These diagrams allow analysis of vehicle characteristics over a full range of motion. This includes non-linear regions and transient states.

The diagrams are created by constraining the vehicle to move in a straight line. With a change in body slip, a stabilizing moment is required to keep the vehicle from turning. Therefore, the stabilizing moment is equal and opposite to all the moments from the tire forces created with a given body slip. This is calculated analytically with consideration to changes in normal force and the nonlinearity of the tires. Without a yaw rate, the tire slip angles are simplified and the dynamic motion of the vehicle can be expressed as combinations of front-wheel and rear-wheel slip angles. The difference between the front and rear slip angles is simply the steering angle of the front tires. An examples of the β-method are shown in Figure 2.8. Analyzing the slopes of the plots give information about the dynamic characteristic. When the slope is positive, the vehicle is understeering, and when the slope is negative, the vehicle is oversteering. The concept of a quasi steady state is applied in order to calculate the vehicle characteristics during acceleration and braking. The effects of acceleration emerge primarily as an increase or decrease in the necessary yaw moment to stabilize the vehicle caused by load transfer between the front and rear wheels.

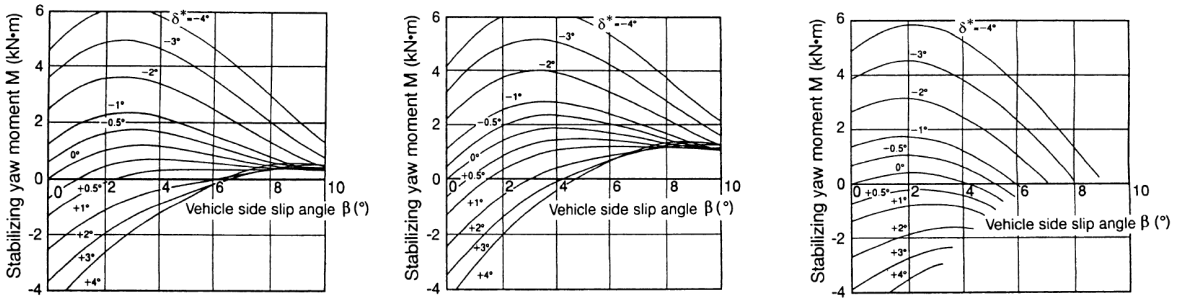

Figure 2.8: β Yaw-moment diagrams

This essentially shows the maximum yaw moment for each stability method. Shimada proposes that in order to improve a vehicle's stability, the characteristics of the vehicle while it accelerates or decelerates should remain the same. His study concludes that

controlling the distribution of roll stiffness is not effective at a lateral acceleration less than $4m/s^2$, and the effect varies depending on the longitudinal weight distribution. Controlling the rear wheel steering angle is most effective with a small side slip angle. Increasing the angle reduces the range in which stabilizing yaw moment is controllable, especially during deceleration. It can compensate for changes in the characteristics at a lateral acceleration of up to $7m/s$. And finally, controlling the drive and braking forces of the individual rear wheels, the characteristics can be compensated over a full range of motions.

2.4.8 Comparing RWS and Rear Active Differential

This work from Italy compares two approaches for vehicle stability control, which are the use of RWS and rear active differential [65]. A reference generator in the form of a nonlinear mapping is implemented, which uses the vehicle's speed and steering angle to output a yaw rate for tracking. This reference is constructed numerically, taking into account the nonlinear vehicle and the saturation limits of each actuator. A brute force search of feasible steady-state motions is done, which includes nonlinearities in the tire. The vehicle is manipulated using the rear tire angle for each front tire angle and forward velocity pair. This was also done with a yaw moment which would represent the rear differential.

The reference generation itself determines the stability regions that each actuation method can reach, along with the saturation limits. These limits are 5° of rear steering and $\pm 2500Nm$ of yaw moment generated from the rear wheel's differential. The working region of the control systems shows that with rear-wheel steering is better suited for modifying and improving the maneuverability of vehicles up to about $7m/s^2$ of lateral acceleration, while using rear active differential is better suited for higher lateral accelerations, as shown in Figure 2.9. A lower understeer gradient is perceived as a higher handling quality. Therefore, at low lateral accelerations, a reference understeer gradient is used to create the map. At higher lateral accelerations (or non linear region), the mapping is created to maximize the lateral acceleration.

The paper also explores the robustness of each controller which uses an H_∞ design. Each controller is designed for its respective actuator using multiple open loop tests. Two

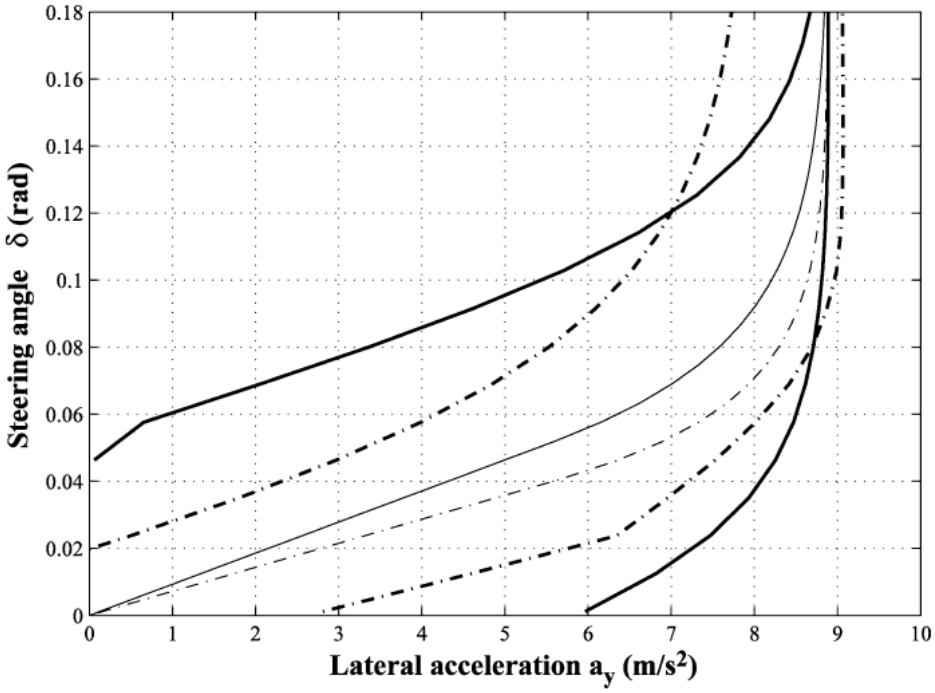

Figure 2.9: Control system working region, delimited by bold lines, for RWS (solid) and RAD (dash-dot) systems and uncontrolled (thin solid line) and reference (thin dash-dotted line) vehicle steering diagrams. Speed: 100 km

particularly challenging tests for the controllers are a steer reversal test at decreased road friction (wet road) and a 0.7 Hz sine with dwell test. The tests show that the rear active differential fails due to excessive longitudinal slip, whereas the problem is mitigated with rear-wheel steering. The control system for the rear-active differential appears to have issues with correcting extreme oversteering behaviors, whereas RWS achieve very good results in all of the considered tests. However it must be remarked that using a forward active differential can overcome these issues, as well as systems that use braking forces such as ESC. The work concludes that RWS can greatly improve both vehicle safety and maneuverability in all driving situations.

2.4.9 Integrated Control of 4WS and Individual Wheel Torques

Work from Honda makes a comparison of three different strategies [67]. These are RWS, wheel torque control on all four wheels, wheel torque control with active front and rear-wheel steering. The stability tests conducted were braking at $0.4g$ while the driver

input a sinusoid, and a split-μ braking test. A nonlinear predictive controller is used for each controller strategy which tries to track zero slip, a desired yaw rate, and the forward speed from the driver's braking command. The controller is an optimization problem that penalizes the error and inputs. The controller input is solved through approximations from a series expansion.

Results show that under the sinusoidal test, RWS is not as effective compared to four-wheel torque or the combination of the two. RWS has the largest difference in individual wheel workload, calculated by dividing the resultant tire force by the maximum available tire force. This is because the RWS is trying to track two errors. The other two systems have the workloads of each tire almost equal and near the maximum. The split-μ brake test only compares four-wheel torque with the combination of active front and rear wheel steering and four-wheel torque. Results show that the integrated control performs better than four-wheel torque only, indicating that RWS can improve safety systems when combined.

2.4.10 Supervisory Control to Manage Brakes and 4WS

Work presnted by Delphi integrates RWS with a braking system [74]. The main concern that is studied is conflict between RWS and controlled brake systems when they are not aware of one another. The example used to show the conflict is a system where both systems use separate and unique feedback control mechanisms that use state error for yaw rate and side-slip. In order to fix this issue, the authors introduce a supervisory control system which coordinates the actuators.

The control system is only expressed through a written description, and no mathematical models or equations are shown. The control system is broken up into three components. The first is the reference signal, which create the desired yaw rate and side-slip. The second is the state estimator, which calculates the side-slip. The final component is the feedback control, which prioritizes the steering before braking is used. This is done by considering the information on road surface friction and the degree of actuation saturation. Steering is prioritized because it is seen as less intrusive in nature when compared to using the brakes.

Two test cases are simulated. One is an emergency lane change on snow, and the other is a split-μ test. For the lane change test, a coordinated system and non-coordinated system is compared. The results show that coordination gives less side-slip angle, less brake actuation, and less handwheel input from the driver. For the split-μ test, a system with ABS only was compared to the coordinated system. With brake control systems, there is a compromise between deceleration and lateral stability. This is done by limiting the braking pressure on the front wheel on the high μ side. However with coordination of RWS, better performance can be had with better deceleration and lateral stability. The simulation showed less driver intervention to stabilize the vehicle.

2.5 Literature Review Conclusion

The papers reviewed above explored the evolution of RWS technology, and its how it was integrated with other actuators to develop better stability control. Once the technology was compared to ESC, the definition of stability shifted to the driver-vehicle model which considers the driver's actions. With this definition of stability, papers compare systems using a small number of specific maneuvers, or map out the stability regions and offer a more in-depth analysis. All of the comparisons require actuator limitations in order to compare the different stabilization systems. The main takeaway is that at the absolute maximum of tire performance, some sort of differential tire braking or direct yaw control is better than RWS. However, combining RWS with other stabilization concepts outperform the individual systems.

The performance of the individual systems can be loosely ordered in stabilizing ability from the papers. RWS is high on the list, second only to ESC where all four wheels can be controlled. Controlling the torque of only the rear wheels tends to suffer under certain conditions that RWS can handle. And finally, controlling the longitudinal stiffness has performance issues at lower accelerations. Therefore, RWS is still an interesting actuation method for stabilization, where at the limits it should be combined with traditional ESC.

An important consideration is how to make apple-to-apple comparisons of different actuation methods, since they are measured in different units, use different amounts of

power, and saturation limits. Many metrics can be considered beyond motion of the vehicle. The maximum amount of tire force generation could be considered since stability tends to concentrate on the extremes of tire grip.

Chapter 3

Modeling

In this chapter, various models used in this research are constructed and described. The linear bicycle model has already been described in Section 1.1. The first model in this chapter is a nonlinear planar vehicle model, used for preliminary results. The system has enough fidelity to reflect realistic vehicle dynamics, and is simple enough to test easily. It is then validated by comparing it to another paper's more advanced model.

3.1 Nonlinear Planar Vehicle Model

The bicycle model of a vehicle is a linear system with two degrees-of-freedom: yaw and lateral motion. The 2-state system can accurately predict vehicle dynamics with small slip angles at a constant forward speed. This is a good starting place for control design, however, it would need to be tested on a more realistic vehicle model. Therefore, a study of a nonlinear vehicle is introduced here.

3.1.1 Dugoff Tire Model

The most important aspect of the vehicle is the tires. This is where the system generates its forces. Therefore, having realistic tires will make the vehicle response in simulation more realistic, especially when the system is performing maneuvers with large slip angles. When the maneuvers are extreme, tire force saturation and the roll of the vehicle becomes important because of the normal force variation's effect on the tire forces.

The tire force relation to the slip angle is a nonlinear relationship. Popular tire models

includes the magic tire formula, the brush model, and the Dugoff model [75].

The model implemented here is the Dugoff model [76], which uses Equations 3.1 - 3.5.

$$F_{tx} = \begin{cases} F_{txd}, & \text{if } \lambda_f \geq 1 \\ F_{txd} 2\lambda_f \left(1 - \frac{\lambda_f}{2}\right), & \text{if } \lambda_f < 1 \end{cases} \tag{3.1}$$

$$F_{ty} = \begin{cases} F_{tyd}, & \text{if } \lambda_f \geq 1 \\ F_{tyd} 2\lambda_f \left(1 - \frac{\lambda_f}{2}\right), & \text{if } \lambda_f < 1 \end{cases} \tag{3.2}$$

λ_f is calculated by

$$\lambda_f = \frac{\mu}{2\sqrt{\left[\frac{F_{txd}}{F_{tz}}\right]^2 + \left[\frac{F_{tyd}}{F_{tz}}\right]^2}} \tag{3.3}$$

where μ is the coefficient of friction between the tire and road. F_{txd} and F_{tyd} are calculated by

$$F_{txd} = \frac{C_x \kappa}{1 - |\kappa|} \tag{3.4}$$

$$F_{tyd} = \frac{C_y \tan(\alpha)}{1 - |\kappa|} \tag{3.5}$$

where κ is the longitudinal slip, C_y is the nominal cornering stiffness. F_{tz} is the normal force on the tire. The subscripts i and j are used to identify the tire (i identifies left or right, j identifies front or rear).

3.1.2 Slip and Slip Angles

Longitudinal and lateral tire forces are generated through deformations of the tire contact patch, which is the patch of tire that is in contact with the road. Tire models relate the wheel motion to the force it is generating through the slip and slip angles. Additional properties of the tire can be included, such as the camber angle, turn slip, and self-aligning torque. These increase the complexity of the model and generally do not have as big of an influence on the tire forces. They can be included in full simulation software such as CarSim, which is used for some of the simulations here.

The slip angle α is defined as the angle between the velocity vector of the tire and the x-axis of the tire. The velocity vector is decomposed into its x and y components, shown as v_{tx} and v_{ty} in Figure 3.1. The slip angle relationship used is as follows:

$$\tan \alpha_{ij} = -\frac{v_{tyij}}{v_{txij}} \tag{3.6}$$

This slip angle sign convention is used so that a positive slip angle yields a positive force.

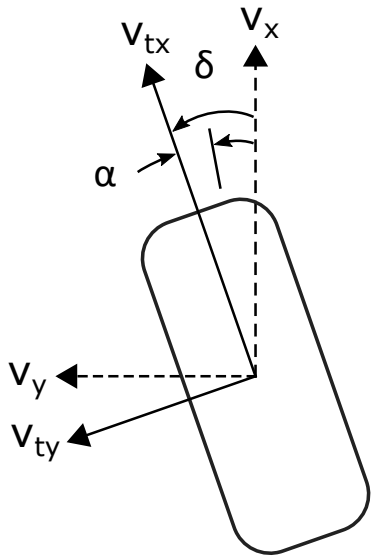

Figure 3.1: Slip angle of a tire.

The tire is assumed to be rigidly connected to the vehicle. Therefore, the velocity of the tire at the contact patch can be derived through a velocity transfer from the vehicle. A velocity diagram showing the velocity at the corners is shown in Figure 3.2. This is a planer vehicle model with no suspension. The velocities at the corners can be derived as

$$v_{yL1} = v_{yR1} = v_y + a\omega_z \tag{3.7}$$

$$v_{yL2} = v_{yR2} = v_y - b\omega_z \tag{3.8}$$

$$v_{xL1} = v_{xL2} = v_x - c\omega_z \tag{3.9}$$

$$v_{xR1} = v_{xR2} = v_x + c\omega_z \tag{3.10}$$

where the L and R stand for the left and right side of the vehicle, while 1 and 2 stand for the front and rear of the vehicle, respectively. Since many of the velocities are duplicates of the other, they can be represented as

$$v_{yL1} = v_{yR1} = v_{y1} \tag{3.11}$$

$$v_{yL2} = v_{yR2} = v_{y2} \tag{3.12}$$

$$v_{xL1} = v_{xL2} = v_{xL} \tag{3.13}$$

$$v_{xR1} = v_{xR2} = v_{xR} \tag{3.14}$$

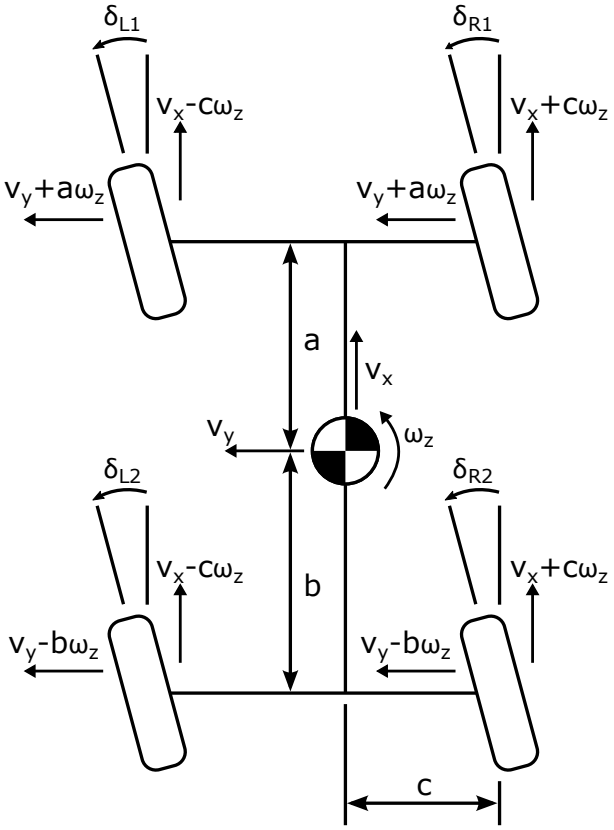

Figure 3.2: Velocity Diagram.

Converting from the vehicle's reference frame to the tire's reference frame can be done with a rotation matrix

$$R_{ij} = \begin{bmatrix} \cos\delta_{ij} & \sin\delta_{ij} \\ -\sin\delta_{ij} & \cos\delta_{ij} \end{bmatrix} \tag{3.15}$$

with the following relationship:

$$\begin{bmatrix} v_{txij} \\ v_{tyij} \end{bmatrix} = R_{ij} \begin{bmatrix} v_{xij} \\ v_{yij} \end{bmatrix} \tag{3.16}$$

With the proper velocities aligned with the tire's frames, the slip angle calculation can be done as in Equation 3.6. Certain assumptions can help reduce the complexity of the slip angles. The tire angles and slip angles are generally small, which leads to trigonometric simplifications such as $\sin\theta \simeq \theta$, $\cos\theta \simeq 1$, and $\arctan\theta \simeq \theta$. Some values such as v_x are very large relative to v_y, and when small terms are multiplied they can be neglected.

In addition, the relationship between slip and the force generation is defined as the force the wheel outputs to the road. When integrated in a vehicle model, it is desired to have the road force as an input into the vehicle system. Therefore a negative sign is required. This leads to the following slip angle equations:

$$\alpha_{L1} = \delta_{L1} - \frac{v_{y1}}{v_{xL}} \tag{3.17}$$

$$\alpha_{R1} = \delta_{R1} - \frac{v_{y1}}{v_{xR}} \tag{3.18}$$

$$\alpha_{L2} = \delta_{L2} - \frac{v_{y2}}{v_{xL}} \tag{3.19}$$

$$\alpha_{R2} = \delta_{R2} - \frac{v_{y2}}{v_{xR}} \tag{3.20}$$

The longitudinal slip κ is a relationship between the angular velocity of the wheel and the longitudinal velocity of the wheel center, expressed as a percentage. A slip velocity s_v can be defined as the difference between the speed at which the circumference of the wheel rolls and the speed of the wheel center in the longitudinal direction. This can be calculated by $s_v = r_e\omega - v_x$, where r_e is the effective rolling radius and ω is the angular velocity of the wheel. Figure 3.3 shows a diagram of a wheel rolling. The ratio of the slip velocity to the speed of the wheel center is the slip, expressed as:

$$\kappa = -\frac{v_x - r_e\omega}{|v_x|} \tag{3.21}$$

When the wheel locks up during braking ($\omega = 0$), the slip expression gives a value of -1 (or -100%). When the wheel angular velocity is excessive on slippery roads during

traction/driving, Equation 3.21 can exceed a value of 1. Therefore, an alternative equation can be used to limit its value [77].

$$\kappa = -\frac{v_x - r_e\omega}{|r_e\omega|} \tag{3.22}$$

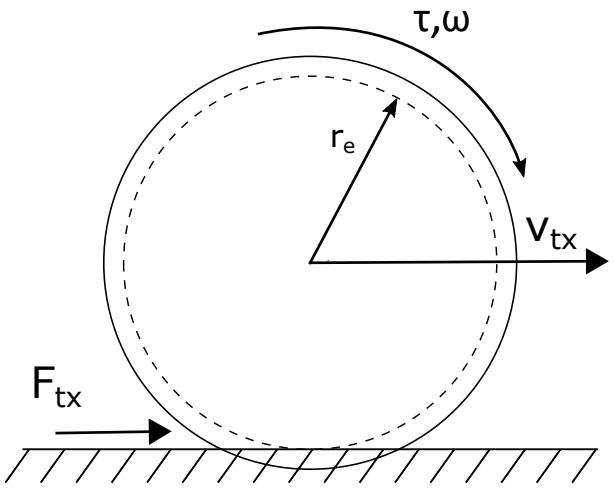

Figure 3.3: Longitudinal velocity of tire.

The equations used for the slip at each wheel for the model are as follows:

$$\kappa_{L1} = -\frac{v_{xL} - r_e\omega_{L1}}{v_{xL}} \tag{3.23}$$

$$\kappa_{R1} = -\frac{v_{xR} - r_e\omega_{R1}}{v_{xR}} \tag{3.24}$$

$$\kappa_{L2} = -\frac{v_{xL} - r_e\omega_{L2}}{v_{xL}} \tag{3.25}$$

$$\kappa_{R2} = -\frac{v_{xR} - r_e\omega_{R2}}{v_{xR}} \tag{3.26}$$

3.1.3 Normal Force Calculation

The normal force varies during vehicle maneuvers and this effect must bi included in order to have more realistic saturation effects of the vehicle. The extended bicycle model is used in order to characterize the change at each tire. The extended bicycle model has four separate wheels and is seen in Figure 3.4.

The normal forces on the tires can be approximated from force and moment equilibrium equations for the planar vehicle. This assumes that there are no dynamics in the

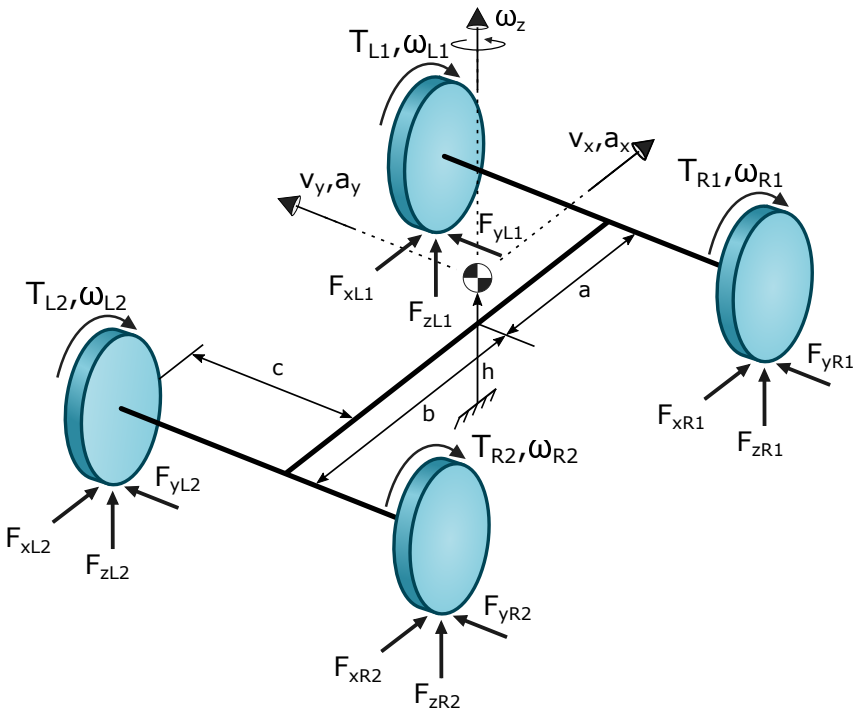

Figure 3.4: Diagram of an extended bicycle model.

roll or pitch direction. A steady-state relationship is assumed between the longitudinal acceleration, lateral acceleration, and the normal force variation, generating an algebraic relationship relating the terms. The following can be derived from the figure.

$$\Sigma F_x = ma_x \tag{3.27}$$

$$\Sigma F_y = ma_y \tag{3.28}$$

$$\Sigma F_z - mg = 0 \tag{3.29}$$

$$\Sigma M_x = 0 \tag{3.30}$$

$$\Sigma M_y = 0 \tag{3.31}$$

First, the moment equation aligned with the y-axis (pitch) is considered. The sum of the moments expanded is as follows:

$$-h\Sigma F_x - (F_{zL1} + F_{zR1})a + (F_{zL2} + F_{zR2})b = 0 \tag{3.32}$$

This can be simplified with the assumption that the normal force on the left and right

due to forces in the x-direction are equal. Therefore, the equation simplifies slightly as follows with substitution of Equation 3.27

$$ma_x h = 2(F_{z2}b - F_{z1}a) \tag{3.33}$$

Next, the forces in the z-direction are expanded, keeping the assumption that the forces left and right are equal.

$$2F_{z1} + 2F_{z2} - mg = 0 \tag{3.34}$$

Substituting Equation 3.34 into Equation 3.33 and solving for the normal force, the following can be derived.

$$F_{z1} = F_{z01} + \Delta F_{z1x}$$
$$F_{z2} = F_{z02} + \Delta F_{z2x}$$

where

$$F_{z01} = \frac{1}{2}\frac{mgb}{a+b} \tag{3.35}$$
$$F_{z02} = \frac{1}{2}\frac{mga}{a+b} \tag{3.36}$$
$$\Delta F_{zx1} = -\frac{1}{2}\frac{ma_x h}{a+b} \tag{3.37}$$
$$\Delta F_{zx1} = \frac{1}{2}\frac{ma_x h}{a+b} \tag{3.38}$$

When the wheels roll freely without forces acting on them in the lateral or longitudinal direction, the nominal normal force is represented by the F_{z0} terms above. When the vehicle accelerates longitudinally, the normal force variation is represented by the ΔF_{zx} term.

Now the moment equation in the y direction (roll) is considered.

$$h\Sigma F_y + (F_{zL1} + F_{zL2})c - (F_{zR1} + F_{zR2})c = 0 \tag{3.39}$$

Similar to the previous derivation, the sum of the forces in the y-direction can be replaced by the mass-acceleration term using Equation 3.28. Furthermore, the equation

can be rewritten to introduce the shift of normal force between the left and right. The change in normal force in the front and rear can be expressed (through symmetry) as, $\Delta F_{z1} = F_{zR1} - F_{zL1}$ and $\Delta F_{z2} = F_{zR2} - F_{zL2}$. This leads to the following expression.

$$ma_y h = \Delta F_{z1} c + \Delta F_{z2} c \tag{3.40}$$

Introducing roll stiffnesses at the front and rear and the roll angle θ yields the following:

$$\Delta F_{z1} c + \Delta F_{z2} c = (k_{t1} + k_{t2})\theta \tag{3.41}$$

where k_{t1} corresponds to the roll stiffness at the front of the vehicle, while k_{t2} corresponds to the rear. These can be related to the normal force shifts at the front and rear. Equations for the change in normal force as a function of the lateral acceleration can be derived:

$$\Delta F_{z1} = \frac{k_{t1}}{k_{t1} + k_{t2}} ma_y \frac{h}{c} \tag{3.42}$$

$$\Delta F_{z2} = \frac{k_{t2}}{k_{t1} + k_{t2}} ma_y \frac{h}{c} \tag{3.43}$$

Assuming a symmetric vehicle along the longitudinal axis, the outside tires will receive $+\frac{1}{2}\Delta F_z$ while the inside tires receive $-\frac{1}{2}\Delta F_z$. Furthermore, assuming the roll stiffness at the front and rear are equal ($k_{t1} = k_{t2}$) and integrating Equations 3.35-3.38 leads to

$$F_{zL1} = F_{z01} + \Delta F_{z1x} + \Delta F_{zLy} \tag{3.44}$$

$$F_{zR1} = F_{z01} + \Delta F_{z1x} + \Delta F_{zRy} \tag{3.45}$$

$$F_{zL2} = F_{z02} + \Delta F_{z2x} + \Delta F_{zLy} \tag{3.46}$$

$$F_{zR2} = F_{z02} + \Delta F_{z2x} + \Delta F_{zRy} \tag{3.47}$$

$$\tag{3.48}$$

where

$$\Delta F_{zLy} = -\frac{1}{4} ma_y \frac{h}{c} \tag{3.49}$$

$$\Delta F_{zRy} = \frac{1}{4} ma_y \frac{h}{c} \tag{3.50}$$

Simulating the algebraic relationships results in an error due to the dependence on the lateral acceleration and the lateral acceleration's dependence on the lateral force. The implicit nature of the equations can be circumvented by using the normal force calculated at the previous time step in simulation.

3.1.4 Equations of Motion

The tire forces are defined relative to their respective coordinate systems. The same rotation matrix from Equation 3.15 can be used. The tire forces are shown in the force diagram of Figure 3.5.

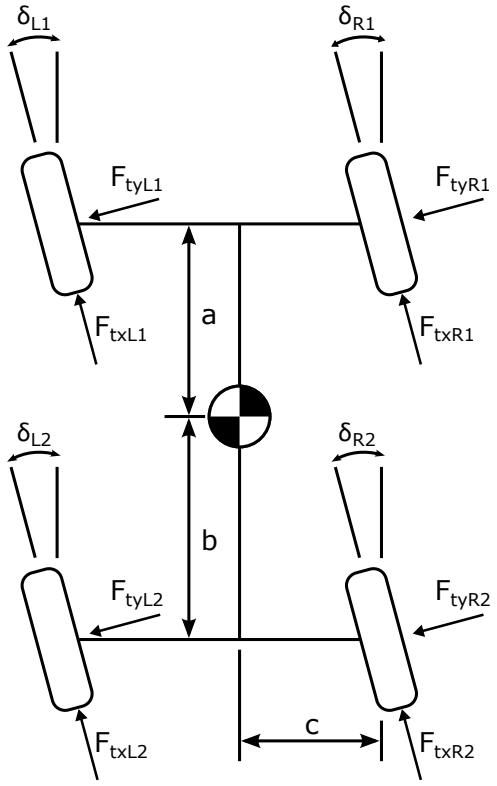

Figure 3.5: Force Diagram.

The forces need to be transformed to forces in the body coordinate frame. Therefore, the following can be derived.

$$\begin{bmatrix} F_{xij} \\ F_{yij} \end{bmatrix} = R_{ij}^{-1} \begin{bmatrix} F_{txij} \\ F_{tyij} \end{bmatrix} \tag{3.51}$$

Table 3.1: Description of state variables.

Description	Symbol	Unit
Momentum in the x-direction	p_{vx}	N-s
Momentum in the y-direction	p_{vy}	N-s
Angular momentum in the z-direction (yaw)	p_{Jz}	N-m-s
Angular momentum of the i-jth wheel	$p_{J\omega ij}$	N-m-s

With the proper coordinate transformation, the equations of motion can be derived. However, the tires do not exhibit large angles. The small angle approximation is used to simplify the forces.

With the modeling assumptions made, a bond graph [78] of the vehicle can be made. This includes independent steering at each wheel and wheel torques if desired. This can be seen in Figure 3.6.

The equations of motion can be derived as follows.

$$\begin{aligned}\dot{p}_{vx} = m\omega_z\frac{p_{vy}}{m} + F_{xL1} + F_{xR1} + F_{xL2} + F_{xR2} \\ -F_{yL1}\delta_{L1} - F_{yR1}\delta_{R1} - F_{yL2}\delta_{L2} - F_{yR2}\delta_{R2}\end{aligned} \tag{3.52}$$

$$\dot{p}_{vy} = -m\omega_z\frac{p_{vx}}{m} + F_{yL1} + F_{yR1} + F_{yL2} + F_{yR2} \tag{3.53}$$

$$\begin{aligned}\dot{p}_{Jz} = a(F_{yL1} + F_{yR1}) - b(F_{yL2} + F_{yR2}) \\ + c\left[F_{xR1} + F_{xR2} - (F_{yR1}\delta_{R1} + F_{yR2}\delta_{R2})\right] \\ - c\left[F_{xL1} + F_{xL2} - (F_{yL1}\delta_{L1} + F_{yL2}\delta_{L2})\right]\end{aligned} \tag{3.54}$$

$$\dot{p}_{Jwij} = \tau_{wij} - R_e F_{xij} \tag{3.55}$$

In total seven equations of motion are necessary for the model, three to describe the body momentum and four for each of the tires with respect to their spin axis. This model is used for simulations where braking in the vehicle is an important ability, such as in

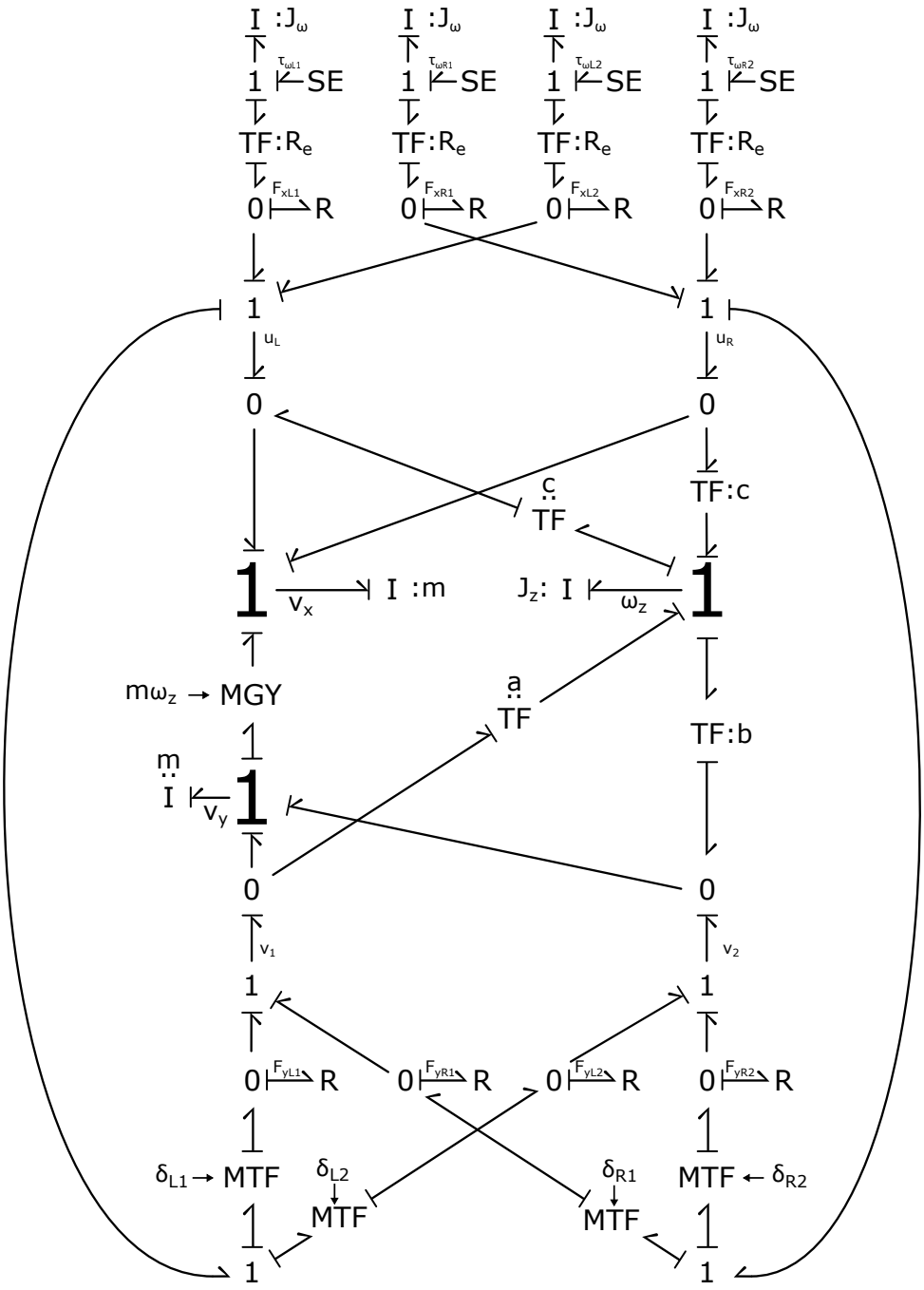

Figure 3.6: Bond graph of the extended bicycle model with independent steering at each wheel.

ESC. However, a simpler model can be used when the vehicle's forward speed is assumed constant.

3.2 Simplified Planar Model

Similar to the bicycle model, the extended bicycle model can also have a constant forward speed. With a bond graph, is implemented with a source flow of v_{x0}. Therefore, only the yaw rate and the lateral velocity can move freely. This model is easier to use and still keeps important characteristics that are desired to study front and rear steering. The bond graph of the model is shown in Figure 3.7.

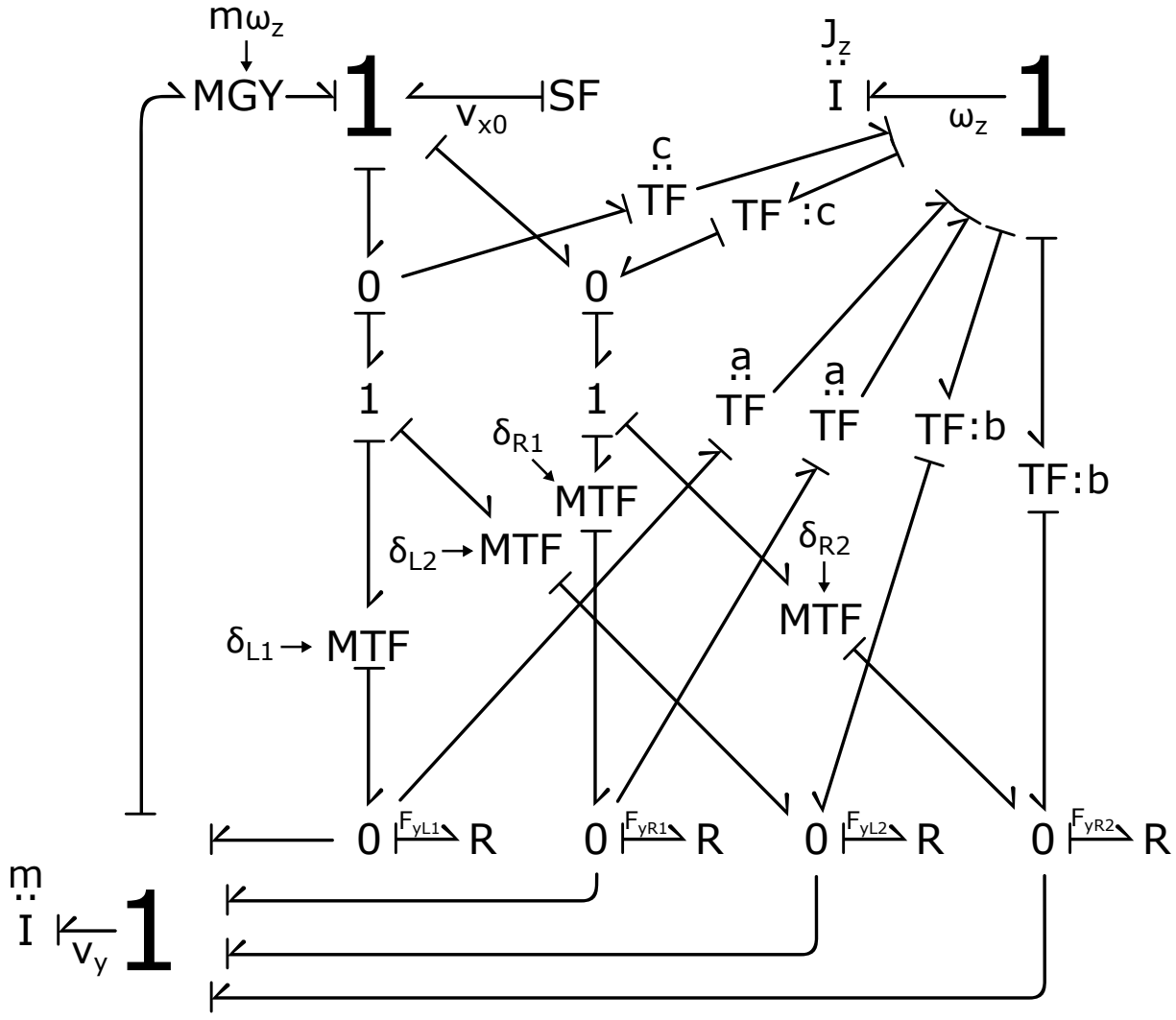

Figure 3.7: Bond graph of planar vehicle with independent steer.

The equations of motion consists of only two equations, as follows:

$$\dot{p}_{vy} = -m\omega_z v_{x0} + F_{yL1} + F_{yR1} + F_{yL2} + F_{yR2} \tag{3.56}$$

$$\begin{aligned}\dot{p}_{Jz} = {} & a(F_{yL1} + F_{yR1}) - b(F_{yL2} + F_{yR2}) \\ & + c(F_{yL1}\delta_{L1} + F_{yL2}\delta_{L2}) - c(F_{yR1}\delta_{R1} + F_{yR2}\delta_{R2})\end{aligned} \tag{3.57}$$

The tire model used is the Dugoff tire model with the normal force variations as developed in a previous section.

3.2.1 Validation

The simplified planar model from Section 3.2 is validated against a model with greater fidelity. The model comes from a paper done by Andrzej [79]. The goal of the paper was to present a vehicle model which is capable of simulating the dynamic behavior of a passenger car and includes effects that are ignored in the bicycle model. The model includes a roll degree of freedom along with a kinematic suspension and camber variation. The tire model used is done with Calspan tire data, a semi-empirical model [79].

The simulation results of the simplified planar model are overlaid on the data from the paper. Figure 3.8 shows the results of the lateral acceleration and yaw rate of the vehicle with a step input. The overlaid data use the traditional blue and red colors from Matlab, whose legend can be seen on the top right which read “4WS” and “2WS”. The original data from the paper is in black and white with 4 curves. The two curves that are important here are the “TWO WHEEL STEER” and the “PROPORTIONAL” curves which are the solid black curve and dashed curve, respectively. They represent a typical front wheel controlled vehicle and a 4WS vehicle where a ratio from front to rear is used to control the rear wheels.

The simulations use the same data and running conditions. The comparison shows that both models exhibit almost the same characteristics. The only mismatch is the amplitude of the subsequent oscillation after the initial peak, where the results from the paper exhibit larger amplitudes and the model proposed shows more of a damped characteristic. This effect may be from the lack of a suspension model which would add damping and compliance to the system.

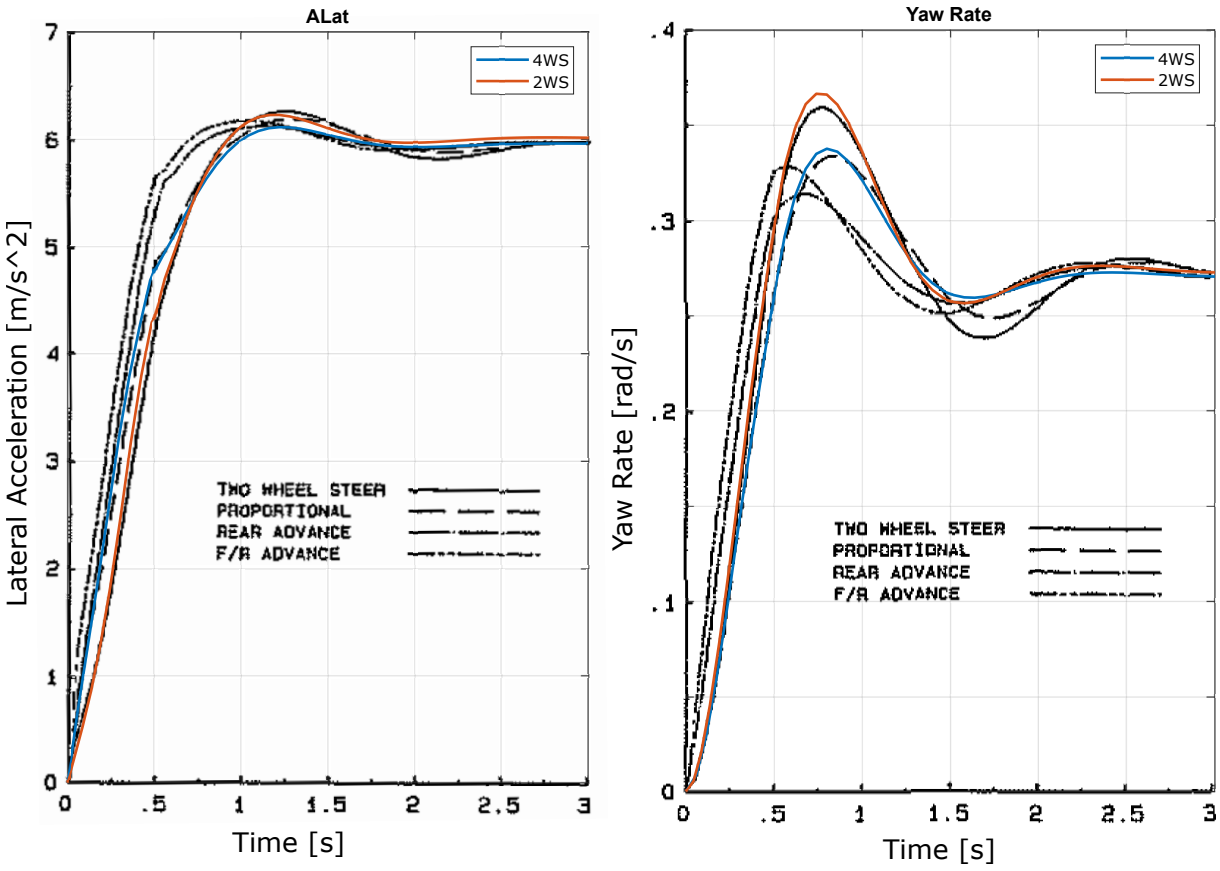

Figure 3.8: Lateral acceleration and yaw rate comparison of different models.

This simplified planar model is useful for initial investigations of the vehicle system where nonlinear effects are important. However, for handling at the limits a high fidelity CarSim model is used for validation.

3.3 CarSim

In instances where it is desired to test a controller on a vehicle that can exhibit all the characteristics of a real car CarSim is used [80]. This high fidelity simulation software is used by automotive engineers, OEMs, and tier 1 suppliers for its accuracy and details.

CarSim has a standard interface to Matlab/Simulink. Integrating CarSim with control algorithms developed in this dissertation is a matter of passing the correct signals from Matlab/Simulink into CarSim. These signals include the steering angle input , brake moments on each wheel for the ESC algorithm, and rear steering angles for RWS. Outputs include the forward velocity, the slip of each wheel, and the yaw rate among other signals.

The vehicle selected for all instances of CarSim use is a Class-D sedan.

Other features that can be used is a built in driver model for tracking a trajectory.

Chapter 4

Variable Wheelbase Control

Chapter 1 discussed some of the explanations for RWS by industry. Figure 1.8 shows an explanation of RWS as a virtual wheelbase that can elongate and shrink. This idea is taken literally in this chapter. What if the vehicle can vary its wheelbase?

The vehicle in this chapter cannot change its wheelbase literally, but with a model reference the real vehicle can behave like it is. This model reference is a reference generator which generates the signals of a vehicle that can change its wheelbase. In turn, the real vehicle will use its front and rear wheels to track these reference signals. If the driver makes a steering input, then the only control decision left is how and when to change the wheelbase.

This chapter explores the model reference, a controller for tracking the signals, and proposes a control law for the virtual wheelbase.

4.1 Background

The concept of making a vehicle behave like another is not new. Chapter 2 discusses works in which the dynamics of another vehicle were emulated through control[55, 56, 57, 58, 59]. However, these works only sought to emulate another vehicle with static properties. Work from [45] uses the concept of a yaw center rotation, which it then moves in order to change how the vehicle handles. The work here and in [81] proposes two ideas. The first is a novel model reference where a physical vehicle parameter is transformed into an input to the reference. This allows adjustments of the model reference to be made

online, changing the vehicle's properties through a single intuitive input. It is often seen in literature that the control of the rear wheels can be thought of as a vehicle with a changing wheelbase. This virtual wheelbase becomes longer when the rear wheels steer in the same direction as the front, and becomes shorter when the rear wheels are steered opposite to the front. This explanation of rear-wheel steering can be implemented as described using the proposed model reference. The wheelbase of the model reference is used to change the characteristics of the vehicle. The model reference behavior is tracked by the real vehicle using active front and rear wheels. A MIMO controller is designed which uses feedback to track the reference vehicle's motions. Previous works used signals that are not readily available or had to be estimated in commercial vehicles.

The second idea proposed is a control law for the virtual wheelbase length. This system assumes it can measure the curvature of the road, and a relationship between the current curvature and the virtual wheelbase is developed. This serves as an example for controlling the wheelbase and shows the flexibility of integrating the variable wheelbase into a global scheme.

4.2 Model Reference

The model reference begins with the bicycle model as described in Section 1.1. A bond graph of the model is shown in Figure 4.1.

For the model reference, a vehicle with only front steering is considered. Therefore, the rear tire angle δ_r is not used, and can be considered zero for all time. Given this, the equations of motion can be derived as follows:

$$\dot{p}_{vy} = -\frac{C_f + C_r}{m v_{x0}} p_v - \frac{1}{J_z}\left(m v_{x0} + \frac{a C_f - b C_r}{v_{x0}}\right) p_{\omega_z} + C_f \delta_f \tag{4.1}$$

$$\dot{p}_{\omega_z} = -\frac{a C_f - b C_r}{m v_{x0}} p_v - \frac{a^2 C_f + b^2 C_r}{J_z v_{x0}} p_{\omega_z} + a C_f \delta_f \tag{4.2}$$

where p_{vy} and p_{ω_z} are the lateral momentum and angular momentum of the vehicle, respectively.

The wheelbase of the model reference, $L = a + b$, will now be considered an input into

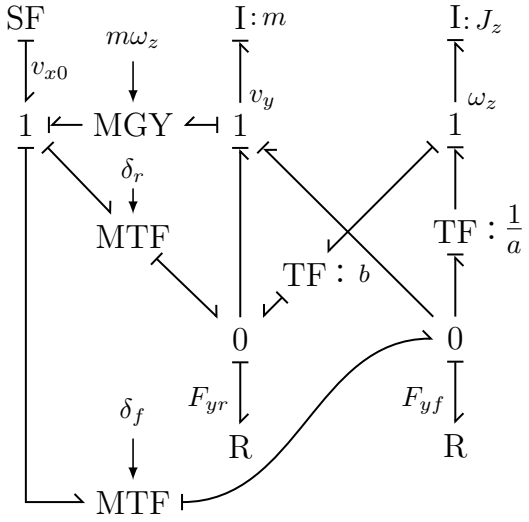

Figure 4.1: Bond graph of a bicycle model.

the system. The lengths of a and b can both change. Their ratio will be kept constant thus keeping the center of gravity fixed while varying the length. Therefore, the lengths can be rewritten as follows:

$$a = \frac{L}{\frac{b}{a} + 1} \tag{4.3}$$

$$b = \frac{L}{\frac{a}{b} + 1} \tag{4.4}$$

Some intermediate parameters are introduced to simplify the writing:

$$\alpha = \frac{1}{\frac{b}{a} + 1} \tag{4.5}$$

$$\beta = \frac{1}{\frac{a}{b} + 1} \tag{4.6}$$

Therefore,

$$a = \alpha L \tag{4.7}$$

$$b = \beta L \tag{4.8}$$

In this manner, the parameters a and b are now functions of the wheelbase, simplifying the number of variables needed to be changed to just one. The ratio between a and b, $\frac{a}{b}$, is kept constant while the front and rear axles grow and shrink proportionately.

Another consideration is that changing the wheel base would change the mass distribution and therefore the moment of inertia of the vehicle. A good relationship to assume [82] for the moment of inertia which is common among vehicles is

$$J_z = \kappa_J mab \tag{4.9}$$

where κ_J is a dimensionless number, typically $\kappa_J = 1$. However κ_J is included for finer tuning if desired. Using this relationship allows the moment of inertia to change with the wheelbase. Rewriting this with the equations for the lengths a and b yield the following:

$$J_z = \kappa_J m\alpha\beta L^2 \tag{4.10}$$

In reality, however, changing the wheelbase arbitrarily changes the moment of inertia, which takes energy that is not accounted for in the model reference in addition to many other issues that are not accounted for. This is not a problem since the goal of the model reference is not to create a realistic model of a car that can actually change its wheelbase. The model approximation will be sufficient to create outputs for the real vehicle to follow.

Equations 4.7, 4.8, and 4.10 can be combined with the equations of motion from Equations 4.1 and 4.2, which yields the following:

$$\dot{p}_{vy} = -\frac{C_f + C_r}{mv_{x0}} p_v - \frac{1}{\kappa_J \alpha\beta}\left(v_{x0}\frac{1}{L^2} + \frac{\alpha C_f - \beta C_r}{mv_{x0}}\frac{1}{L}\right) p_{\omega_z} + C_f\delta_f \tag{4.11}$$

$$\dot{p}_{\omega_z} = -\frac{\alpha C_f - \beta C_r}{mv_{x0}} p_v L - \frac{\frac{\alpha}{\beta}C_f + \frac{\beta}{\alpha}C_r}{\kappa_J mv_{x0}} p_{\omega_z} + \alpha C_f L\delta_f \tag{4.12}$$

Rewriting the equations of motion in this manner allows for easy modulation of the wheelbase L. The system is clearly nonlinear. The model reference will now use two inputs: L and δ_f. Since the inertia properties change in the derived equations, the system's equations of motions are in terms of its momenta instead of its velocities.

4.2.1 Linearization

Because the wheelbase L is a parameter in the typical bicycle model and is now considered an input to a new model reference system, the system is nonlinear. An investigation into its characteristics by linearizing the system is done.

The nonlinear system can be defined as follows:

$$\dot{x}(t) = f(x(t), u(t)) \tag{4.13}$$

where

$$x(t) = \begin{bmatrix} p_{vy}(t) \\ p_{\omega_z}(t) \end{bmatrix}$$
$$u(t) = \begin{bmatrix} \delta_f(t) \\ L(t) \end{bmatrix}$$

The linearization process can be thought of as the deviation from an equilibrium point, $x(0) = \bar{x}$ and $u(0) = \bar{u}$. We can define the deviations as

$$\eta(t) = (x(t) - \bar{x})$$
$$\nu(t) = (u(t) - \bar{u})$$

and we can construct the linear system as

$$\dot{\eta}(t) = A\eta(t) + B\nu(t) \tag{4.14}$$

where

$$A = \left.\frac{\partial f}{\partial x}\right|_{\substack{x = \bar{x} \\ u = \bar{u}}}$$
$$B = \left.\frac{\partial f}{\partial u}\right|_{\substack{x = \bar{x} \\ u = \bar{u}}}$$

To recover the states after simulation would simply be $x(t) = \eta(t) + \bar{x}$.

4.2.1.1 Partial Derivatives

Here the partial derivatives are taken for the state equations and evaluated at the equilibrium points:

$$\left.\frac{\partial \dot{p}_{vy}}{\partial p_{vy}}\right|_{\substack{x=\bar{x}\\u=\bar{u}}} = -\frac{C_f + C_r}{m v_{x0}} \tag{4.15}$$

$$\left.\frac{\partial \dot{p}_{vy}}{\partial p_{\omega_z}}\right|_{\substack{x=\bar{x}\\u=\bar{u}}} = -\frac{1}{\kappa_J \alpha \beta}\left(v_{x0}\frac{1}{\bar{L}^2} + \frac{\alpha C_f - \beta C r}{m v_{x0}}\frac{1}{\bar{L}}\right) \tag{4.16}$$

$$\left.\frac{\partial \dot{p}_{\omega_z}}{\partial p_{vy}}\right|_{\substack{x=\bar{x}\\u=\bar{u}}} = -\frac{\alpha C_f - \beta C_r}{m v_{x0}}\bar{L} \tag{4.17}$$

$$\left.\frac{\partial \dot{p}_{\omega_z}}{\partial p_{\omega_z}}\right|_{\substack{x=\bar{x}\\u=\bar{u}}} = -\frac{\alpha/\beta C_f + \beta/\alpha C_r}{\kappa_J m v_{x0}} \tag{4.18}$$

$$\left.\frac{\partial \dot{p}_{vy}}{\partial \delta_f}\right|_{\substack{x=\bar{x}\\u=\bar{u}}} = C_f \tag{4.19}$$

$$\left.\frac{\partial \dot{p}_{vy}}{\partial L}\right|_{\substack{x=\bar{x}\\u=\bar{u}}} = -\frac{1}{\kappa_J \alpha \beta}\left(-2v_{x0}\frac{1}{\bar{L}^3} - \frac{\alpha C_f - \beta C_r}{m v_{x0}}\frac{1}{\bar{L}^2}\right)\bar{p}_{\omega_z} \tag{4.20}$$

$$\left.\frac{\partial \dot{p}_{\omega_z}}{\partial \delta_f}\right|_{\substack{x=\bar{x}\\u=\bar{u}}} = \alpha C_f \bar{L} \tag{4.21}$$

$$\left.\frac{\partial \dot{p}_{\omega_z}}{\partial L}\right|_{\substack{x=\bar{x}\\u=\bar{u}}} = -\frac{\alpha C_f - \beta C_r}{m v_{x0}}\bar{p}_v + \alpha C_f \bar{\delta}_f \tag{4.22}$$

4.2.1.2 Linearized State Space

The state space matrices can be written as the following:

$$A = \begin{bmatrix} -\frac{C_f + C_r}{mv_{x0}} & -\frac{1}{\kappa_J \alpha\beta}\left(v_{x0}\frac{1}{\bar{L}^2} + \frac{\alpha C_f - \beta Cr}{mv_{x0}}\frac{1}{\bar{L}}\right) \\ -\frac{\alpha C_f - \beta C_r}{mv_{x0}}\bar{L} & -\frac{\alpha/\beta C_f + \beta/\alpha C_r}{\kappa_J m v_{x0}} \end{bmatrix} \tag{4.23}$$

$$B = \begin{bmatrix} C_f & -\frac{1}{\kappa_J \alpha\beta}\left(-2v_{x0}\frac{1}{\bar{L}^3} - \frac{\alpha C_f - \beta C_r}{mv_{x0}}\frac{1}{\bar{L}^2}\right)\bar{p}_{\omega_z} \\ \alpha C_f \bar{L} & -\frac{\alpha C_f - \beta C_r}{mv_{x0}}\bar{p}_v + \alpha C_f \bar{\delta}_f \end{bmatrix} \tag{4.24}$$

These are the state space matrices for the nonlinear Equations 4.11 and 4.12.

The equilibrium points can be found next, where if the system is started at $\bar{x}$ with $\bar{u}$, the states will remain fixed at $\bar{x}$. The equilibrium points are the points about which the system would be linearized. This can be solved using the nonlinear equations and setting the derivatives to zero. Solving for $\bar{p}_v$ and $\bar{p}_{\omega_z}$ gives

$$\bar{p}_{vy} = \frac{(\beta\bar{L} - \alpha m v_{x0}^2/C_r)mv_{x0}}{\bar{L} + K_{us}v_{x0}^2}\bar{\delta}_f \tag{4.25}$$

$$\bar{p}_{\omega_z} = \frac{v_{x0}\kappa_J m\alpha\beta\bar{L}^2}{\bar{L} + K_{us}v_{x0}^2}\bar{\delta}_f \tag{4.26}$$

where K_{us} is the understeer coefficient. The understeer coefficient is invariant to changes in the wheelbase. Therefore, it can be represented using the typical parameters of the vehicle or with the substitution of Equation 4.7 and Equation 4.8.

$$K_{us} = \frac{m(bC_r - aC_f)}{(a+b)C_f C_r} = \frac{m(\beta C_r - \alpha C_f)}{C_f C_r}$$

4.2.2 Controlling the Wheelbase

The choice in wheelbase affects how the vehicle will respond to a driver's inputs. A common metric for comparing the steering responses are the steady state gains. These can be found by starting with the transfer functions of the yaw rate to front steering and lateral acceleration to front steering. These were presented in Equation1.4 and Equation 1.10. Setting the derivatives to zero by taking $s \to 0$, the steady-state gains are found.

The yaw rate gain and lateral acceleration gain of the standard bicycle model are derived as the following:

$$G_{\omega_z} = \frac{v_{x0}}{(a+b) + K_{us} v_{x0}^2} \tag{4.27}$$

$$G_{a_y} = G_{\omega_z} v_{x0} \tag{4.28}$$

In order to investigate the yaw rate gain of the model reference, we will assume L is held constant or changes very slowly. Essentially, the linear system is studied with varying wheelbase length. Therefore, substituting the terms defined previously, the following is derived:

$$G_{\omega_z} = \frac{v_{x0}}{(\alpha+\beta)L + K_{us} v_{x0}^2} \tag{4.29}$$

$$G_{a_y} = G_{\omega_z} v_{x0} \tag{4.30}$$

It is clear from the equations that increasing the wheelbase reduces the yaw rate and lateral acceleration gains, while decreasing the wheelbase increases the gains.

The stability of the linear system can also be explored. The poles of the model reference with various wheelbases are shown in Figure 4.2. The parameters used can be found in Table 4.2.

Figure 4.2 shows the effect of the wheelbase on the poles of the system, where L_{nom} in the legend is the nominal wheelbase. Increasing the wheelbase lowers the value of the imaginary component of the poles. This also increases the damping and lowers the natural frequency, but keeps the time constant of the system constant. Increasing the wheelbase has the opposite effect.

The effects of changing the wheelbase only appears during a turn with a steering wheel input. This is obvious from the yaw rate gains and lateral acceleration gains, but also in the input matrix of Equation 4.24. With zero steering input, $\bar{p}_{vy}$ and $\bar{p}_{\omega_z}$ are zero. This makes the second column in the B matrix a column of zeros, indicating that if the system is linearized about these conditions, L would have no effect.

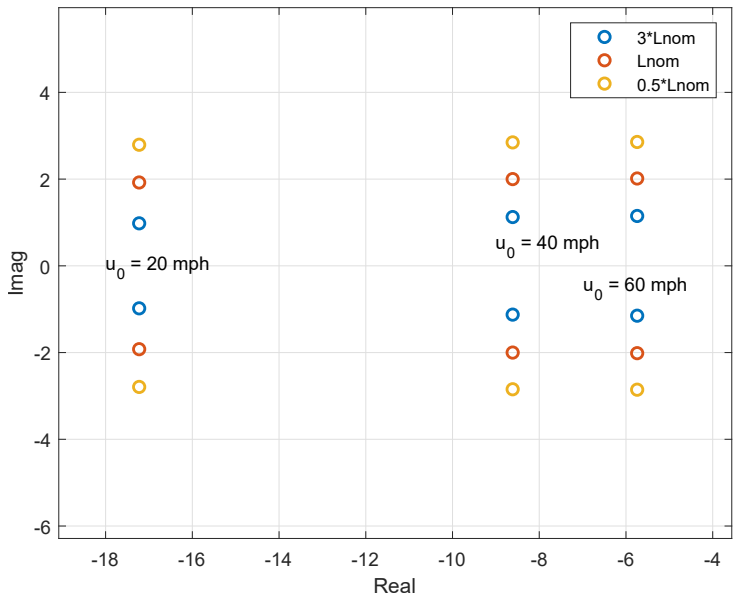

Figure 4.2: Linear system poles on the s-plane as the wheelbase is modulated over various forward velocities.

Taking this into consideration, the wheelbase of the model reference is not treated as a direct input that changes the outputs directly. It would make more sense to treat it as an input that changes the properties of the vehicle. Therefore, a control law should be formulated that creates desirable properties during certain conditions. This is explored in a later section.

4.3 Feedback Controller Design

The plant used for the design of the controller consists of a bicycle model of a car with added rear-wheel steering. The equations of motion are repeated here for convenience:

$$\begin{bmatrix} \dot{v}_y \\ \dot{\omega}_z \end{bmatrix} = \begin{bmatrix} -\frac{C_f+C_r}{mv_{x0}} & -\left(v_{x0}+\frac{aC_f-bC_r}{mv_{x0}}\right) \\ -\frac{aC_f-bC_r}{J_z v_{x0}} & -\frac{a^2C_f+b^2C_r}{J_z v_{x0}} \end{bmatrix} \begin{bmatrix} v_y \\ \omega_z \end{bmatrix} + \begin{bmatrix} \frac{C_f}{m} & \frac{C_r}{m} \\ \frac{aC_f}{J_z} & -\frac{bC_r}{J_z} \end{bmatrix} \begin{bmatrix} \delta_f \\ \delta_r \end{bmatrix} \tag{4.31}$$

Typical signals easily available in vehicles are the yaw rate and lateral acceleration. If these signals are used for feedback, the transfer functions of the plant are derived and shown below.

$$\frac{\omega_z}{\delta_f}(s) = \frac{\frac{aC_f}{J_z}\left[s + \frac{(1+\frac{b}{a})C_r}{mv_{x0}}\right]}{D(s)} \tag{4.32}$$

$$\frac{\omega_z}{\delta_r}(s) = -\frac{\frac{bC_r}{J_z}\left[s + \frac{(1+\frac{a}{b})C_f}{mv_{x0}}\right]}{D(s)} \tag{4.33}$$

$$\frac{a_y}{\delta_f}(s) = \frac{\frac{C_f}{m}\left[s^2 + \frac{b(a+b)C_r}{J_z v_{x0}}s + \frac{(a+b)C_r}{J_z}\right]}{D(s)} \tag{4.34}$$

$$\frac{a_y}{\delta_r}(s) = \frac{\frac{C_r}{m}\left[s^2 + \frac{a(a+b)C_f}{J_z v_{x0}}s - \frac{(a+b)C_f}{J_z}\right]}{D(s)} \tag{4.35}$$

where

$$D(s) = s^2 + \left[\frac{C_f + C_r}{mv_{x0}} + \frac{a^2C_f + b^2C_r}{J_z v_{x0}}\right]s + \frac{(a+b)^2C_fC_r}{mJ_z v_{x0}^2} + \frac{bC_r - aC_f}{J_z} \tag{4.36}$$

The transfer function matrix can be arranged as follows:

$$G(s) = \begin{bmatrix} \frac{\omega_z}{\delta_f}(s) & \frac{\omega_z}{\delta_r}(s) \\ \frac{a_y}{\delta_f}(s) & \frac{a_y}{\delta_r}(s) \end{bmatrix} \tag{4.37}$$

The system configuration is shown in Figure 4.3, where a MIMO controller needs to be generated for the term K.

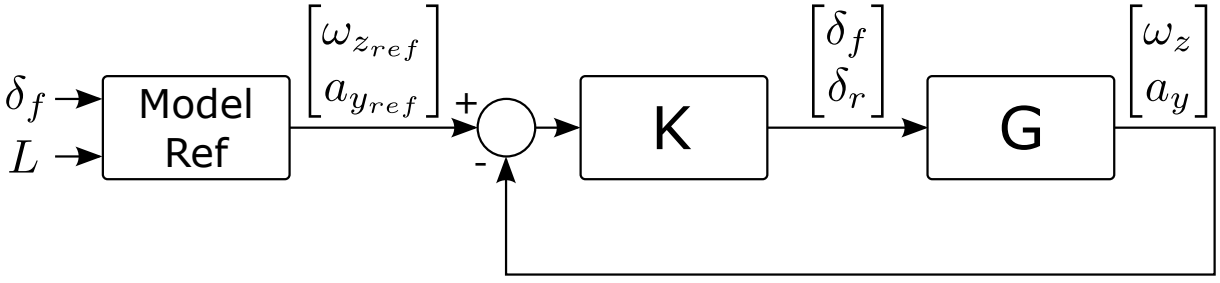

Figure 4.3: System Configuration.

From inspection of the plant, it is found that the transfer function matrix loses rank at $s = 0$. This indicates a transmission zero that can be seen in Equation 4.38. Decoupling the outputs of the plant at all frequencies is not possible. This is evident from the equation

for the lateral acceleration, $a_y = \dot{v}_y + \omega_z \times v_{x0}$. At steady state where the derivatives are zero, the lateral acceleration is dependent on the yaw rate. This limits what can be done for control for steady state.

$$\begin{bmatrix} \frac{\omega_z}{\delta_f}(s \to 0) & \frac{\omega_z}{\delta_r}(s \to 0) \\ \frac{a_y}{\delta_f}(s \to 0) & \frac{a_y}{\delta_r}(s \to 0) \end{bmatrix} = \frac{1}{D(s \to 0)} \frac{(a+b)C_f C_r}{mJ_z} \begin{bmatrix} 1 & -\frac{1}{v_{x0}} \\ 1 & -1 \end{bmatrix} \tag{4.38}$$

where

$$D(s \to 0) = \frac{(a+b)^2 C_f C_r}{mJ_z v_{x0}^2} + \frac{bC_r - aC_f}{J_z}$$

4.3.1 Input/Output Scaling

A crucial step in norm-based MIMO control design and loop shaping is input and output scaling. This is especially important in MIMO systems, where the sensitivity function is dependent on the scaling. The error signals need to be comparable in magnitude. The inputs and outputs should be scaled according to the maximum expected value or allowed change. This is critical for input selection consideration, singular value directions, and condition numbers.

For the active front and rear wheel steering system, the maximum front and rear tire angles can reach about a value of 30° and 10° respectively. However, it is not wise to steer the wheels to their maximum. In a pure slip maneuver without normal force variation, the peak lateral force a tire generates happens when the slip angle lies somewhere between $5° - 10°$. The maximum allowed tire angle would be the angle that generates these slip angles. The slip angles depend on both tire angles on the front and rear, along with the forward velocity. When the front and rear wheels are steered in opposite directions, this creates the largest slip angles. Taking this into consideration, the scaling is chosen based on the steady-state values of the slip angles when a nominal forward speed is chosen while the front and rear wheels are steered opposite.

The lateral acceleration cannot exceed the maximum grip available, which is about μg, while for the yaw rate is $\frac{\mu g}{v_{x0}}$. However, the output is done according to the maximum allowed error instead of the maximum allowed value, since a major concern is minimizing the error between the reference and real value. Here an arbitrary value is chosen based on

experience for the lateral acceleration error (1 m/s^2). Again to simplify the choices, the yaw rate error will be calculated based on the steady state value of the lateral acceleration. The scaling decisions are listed in Table 4.1.

Table 4.1: Scaling choices for analysis.

Description	Symbol	Value	Unit
Max Lateral Acceleration Error	e_{ay-max}	1	m/s^2
Max Yaw Rate Error	e_{wz-max}	$2.5\left(\frac{\pi}{180}\right)$	rad/s
Max Front Steering Angle	δ_{f-max}	$5\left(\frac{\pi}{180}\right)$	rad
Max Rear Steering Angle	δ_{r-max}	$5\left(\frac{\pi}{180}\right)$	rad

With these scaling values, diagonal scaling matrices can be generated for scaling the plant. The error scaling matrix D_e and the input scaling matrix D_u can be used as follows: $G = D_e^{-1}\hat{G}D_u$, where $\hat{G}$ is the unscaled plant.

4.3.2 RGA Analysis

Relative gain array (RGA) analysis is typically used for considering decentralized control. Although this paper uses a decoupling controller, there are still some useful properties that can be discussed regarding RGA. The inputs considered are the front steering angle and rear steering angle of the vehicle. The RGA of the square matrix can be calculated in order to identify particular input-output pairs for control structure selection. Originally RGA was proposed as a study at the steady-state condition. The gains of specific input-output pairs can be considered at two extremes, where the other control loops are open and closed. If an input u_j and output y_i are considered, the gains $\left(\frac{\partial y_i}{\partial u_j}\right)$ can be described as the following:

$$\text{Other loops open:} \quad \left(\frac{\partial y_i}{\partial u_j}\right)_{u_k=0,k\neq j} = g_{ij} = [G]_{ij}$$

$$\text{Other loops closed:} \quad \left(\frac{\partial y_i}{\partial u_j}\right)_{y_k=0,k\neq i} = \hat{g}_{ij} = [G^{-1}]_{ji}$$

The interpretation here is that g_{ij} is the gain when all other outputs are uncontrolled, and $\hat{g}_{ij}$ is when all other outputs are perfectly controlled. The relative gain is the ratio of these

values, where $\lambda_{ij} = g_{ij}/\hat{g}_{ij}$. Perfect control is only possible at the steady state when the other outputs have integral action. However, considering the frequency dependent RGA at the bandwidth being considered is argued as more important and useful for analysis.

There are two pairing rules when using RGA that are associated with decentralized control. They are as follows:

1. Prefer pairing such that the rearranged system, with the selected parings along the diagonal, has an RGA matrix close to identity at frequencies around the closed-loop bandwidth.

2. Avoid (if possible) pairing on negative steady-state RGA elements.

Additionally, some control properties are also useful from RGA:

1. Large RGA elements (typically, 5-10 or larger) at frequencies important for control indicate that the plant is fundamentally difficult to control due to strong interactions and sensitivity to uncertainty.

2. If the sign of an RGA element changes as we go from $s = 0$ to $s = \infty$, then there is a RHP-zero in G or in some subsystem of G.

Figure 4.4 shows the magnitudes of the RGA elements.

The figure shows that at low frequencies as $s \to 0$, the magnitudes of the RGA elements increase. This indicates that the system should not be controlled at low frequencies, especially with the knowledge that a transmission zero exists at $s = 0$. The magnitude of the RGA exceeds 10 at around 0.1 hertz (not plotted). At 4 hertz, the RGA elements cross over. This indicates that if we choose a bandwidth frequency lower than 4 Hz, controlling the system on the diagonal is preferred. However, at frequencies above 4 hertz, the off diagonal pairing is preferred. However, since a decoupling controller is being used instead of decentralized control, the choice in which input should correspond to which output is not important.

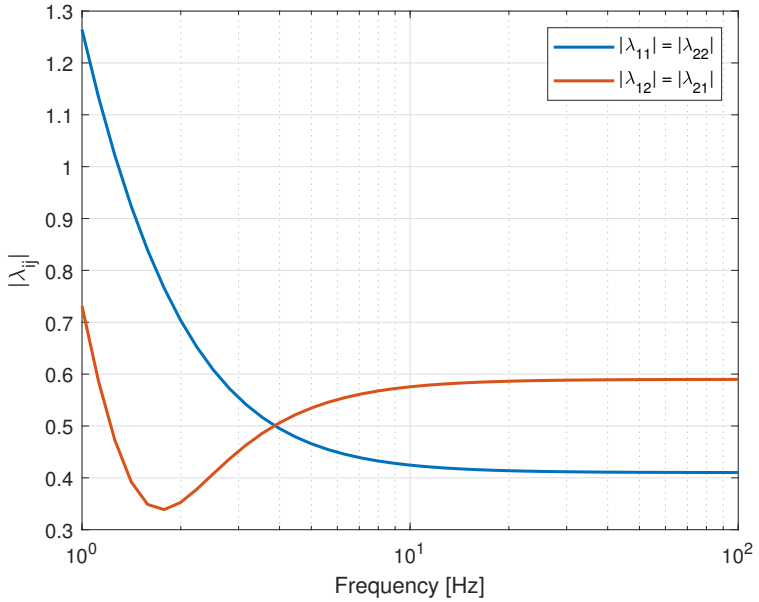

Figure 4.4: Frequency based RGA for inputs δ_f and δ_r

4.3.3 Condition Number

In addition, the condition number as a function of frequency can be studied. The condition number is a ratio between the largest and smallest singular value. It is defined as:

$$\gamma(G) = \frac{\overline{\sigma}(G)}{\underline{\sigma}(G)} \tag{4.39}$$

The singular values can be determined from a singular value decomposition. Large condition numbers (larger than 10) may indicate control problems. Small condition numbers indicate that multivariable effects of uncertainty are not likely to be serious [83].

The condition number over a frequency range (0.5 hertz − 20 hertz) is derived and plotted in Figure 4.5.

The range plotted indicates that control in this range should be good.

4.3.4 Controller Design

The system to be controlled is 2×2 and coupled, so the MIMO control design is explored using Youla parameterization [84]. The transmission zero in the plant requires the following interpolation condition to be satisfied in order to avoid unstable pole zero cancellation in the design: $y_z^H T(z) = 0$, where z is the zero and y_z is output direction of

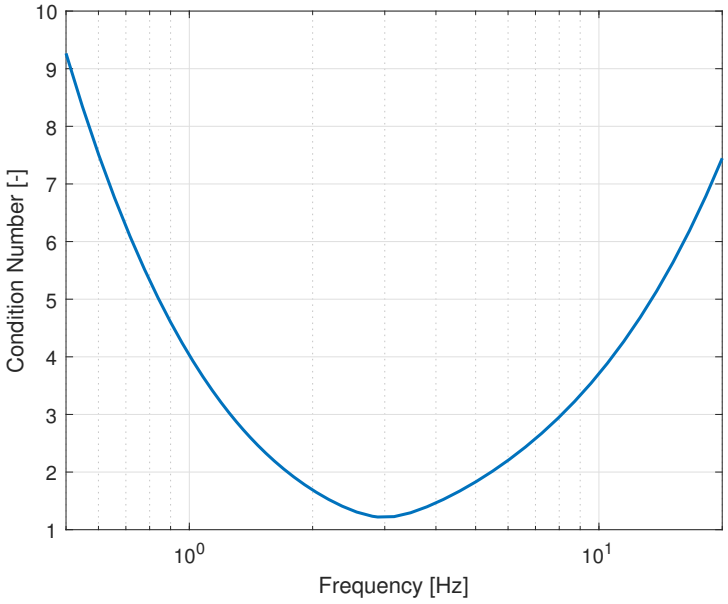

Figure 4.5: Frequency based condition number for inputs δ_f and δ_r

the zero [83]. The output direction can be derived from a singular value decomposition or a generalized eigenvalue problem.

The controller design and sensitivity loop analysis will be done with the scaled plant $G(s)$. The output zero directions depend on the relative scaling of the outputs. Therefore, the zero direction at steady state is re-derived. Because of the choices in scaling where the yaw rate and lateral acceleration differ by the value v_{x0}, the zero direction corresponding to the singular value of $\underline{\sigma} = 0$ is simply

$$y_z^H(s=0) = \frac{1}{\sqrt{2}}[1 \ \ -1] \tag{4.40}$$

A design proposal for the closed loop is presented below. T_{ay} tracks the lateral acceleration at all frequencies while the yaw rate is not tracked at low frequencies.

$$T_{a_y}(s) = \begin{bmatrix} \frac{s}{(s+\omega_1)}\frac{\omega_2^2}{(s+\frac{2}{\sqrt{2}}\omega_2 s+\omega_2^2)} & \frac{\omega_1}{(s+\omega_1)} \\ 0 & \frac{\omega_2^2}{(s+\frac{2}{\sqrt{2}}\omega_2 s+\omega_2^2)} \end{bmatrix} \tag{4.41}$$

It can be seen that the interpolation condition for the zero, where $y_z' T_o(s=0) = 0$, is satisfied.

The frequency ω_2 is the bandwidth of the controller while ω_1 does two things. In row 1 column 1, ω_1 is a high pass filter that does not track the yaw rate at low frequencies. In row 1 column 2, ω_1 is a break frequency for a low pass filter that is needed to satisfy the interpolation condition. This filter essentially couples the required lateral acceleration response to the yaw rate.

In addition to tracking the lateral acceleration at low frequencies, the yaw rate can also be tracked. This results in the following closed-loop transfer function choice $T_{\omega z}$:

$$T_{\omega_z}(s) = \begin{bmatrix} \dfrac{\omega_2^2}{(s + \frac{2}{\sqrt{2}}\omega_2 s + \omega_2^2)} & 0 \\ \dfrac{\omega_1}{(s+\omega_1)} & \dfrac{s}{(s+\omega_1)} \dfrac{\omega_2^2}{(s + \frac{2}{\sqrt{2}}\omega_2 s + \omega_2^2)} \end{bmatrix} \tag{4.42}$$

From here, the controller can be derived. The singular values for the loop transfer functions for the closed loop T_o, sensitivity S_o, and the controller output Y_o are plotted in Figure 4.6 where the break frequencies of $\omega_1 = 0.01$ Hz and $\omega_2 = 10$ Hz are chosen. The figure shows that either choice in tracking at steady state yields almost identical results with a sensitivity peak of 2.1 dB.

A concern encountered is the amount of time it takes for the actuators to settle. It is desirable to have the steering actuators to quickly settle to their final value. This is dependent on the high pass and low pass filter break points which use the frequency ω_1. This pole is designed around the closed loop transfer function T_o, which then comes into the transfer function of the actuator $Y_o = KS_o = G^{-1}T_o$. The control design calls for a small frequency for ω_1.

When ω_1 is very small, the system tries to keep the outputs decoupled at low frequencies. This results in the actuators slowly coming to their steady state values. Figure 4.7 shows a step response for when the yaw rate and the lateral acceleration are separately tracked. When the lateral acceleration is tracked (T_{ay} is the blue line), it can be seen that the lateral acceleration comes to a value of 1 very quickly in subplot (d) due to the bandwidth chosen where $\omega_2 = 10$ Hz. Subplot (c) shows no response from δ_f to the lateral acceleration. This is a good decoupled design. However, when the yaw rate response is considered for T_{a_y}, subplots (a) and (b) show a very slow response. The dominant pole

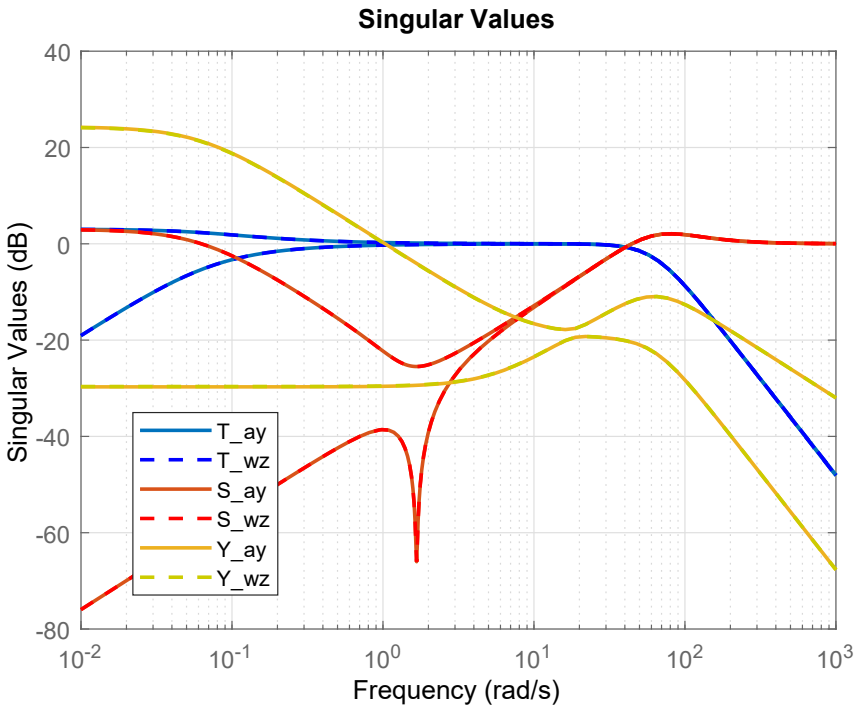

Figure 4.6: Singular value plots for yaw rate and lateral acceleration tracking for $\omega_1 = 0.01$ Hz and $\omega_2 = 10$ Hz.

seems to be the pole introduced by ω_1, where its time constant is $\tau = 1/(2\pi \times 0.01) \approx 16$ s. This results in a settling time of approximately 63 s, which is the cause of the slow response.

Increasing ω_1 by a factor of 10 reduces the settling time by a factor of 10, as seen in Figure 4.8. However, this comes at the cost of the frequency range that can track both output signals. This is an important design consideration which requires a compromise. This is especially a concern when the vehicle's steering wheel is brought back to zero. The tires could still be pointed together at a nonzero value, and take a long time to settle to zero.

These interactions can also be seen for the choice of tracking the yaw rate T_{ω_z}, appearing in red in Figure 4.7 and Figure 4.8

The singular value plots are updated with $\omega_1 = 0.1$ Hz shown in Figure 4.9. The frequency band where the singular values of T_0 are near zero dB decreases from $1 - 60$ rad s^{-1} to about $10 - 60$ rad s^{-1}. An interesting observation is that the actuator output to reference input transfer function for yaw rate (Y_{wz}) has a lower maximum

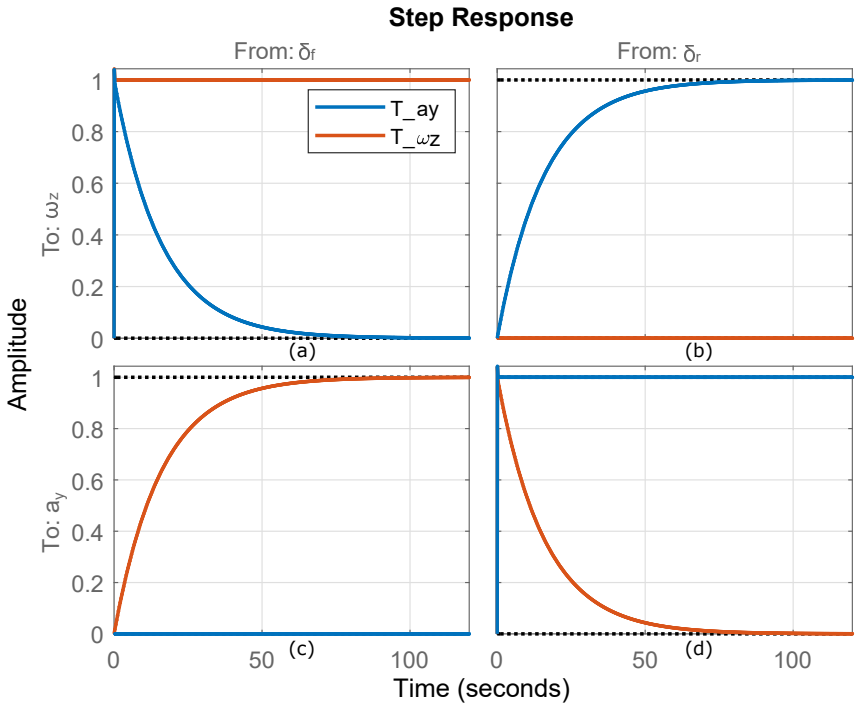

Figure 4.7: Step Response for $\omega_1 = 0.01$ Hz and $\omega_2 = 10$ Hz.

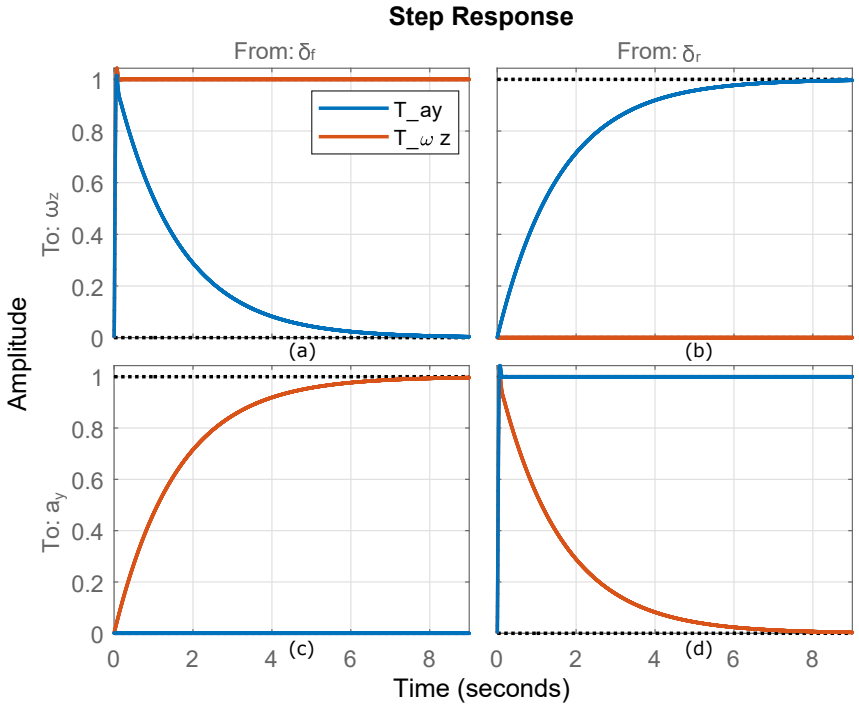

Figure 4.8: Step response $\omega_1 = 0.1$ Hz and $\omega_2 = 10$ Hz.

singular value. This indicates that tracking the yaw rate at low frequencies requires less actuator effort.

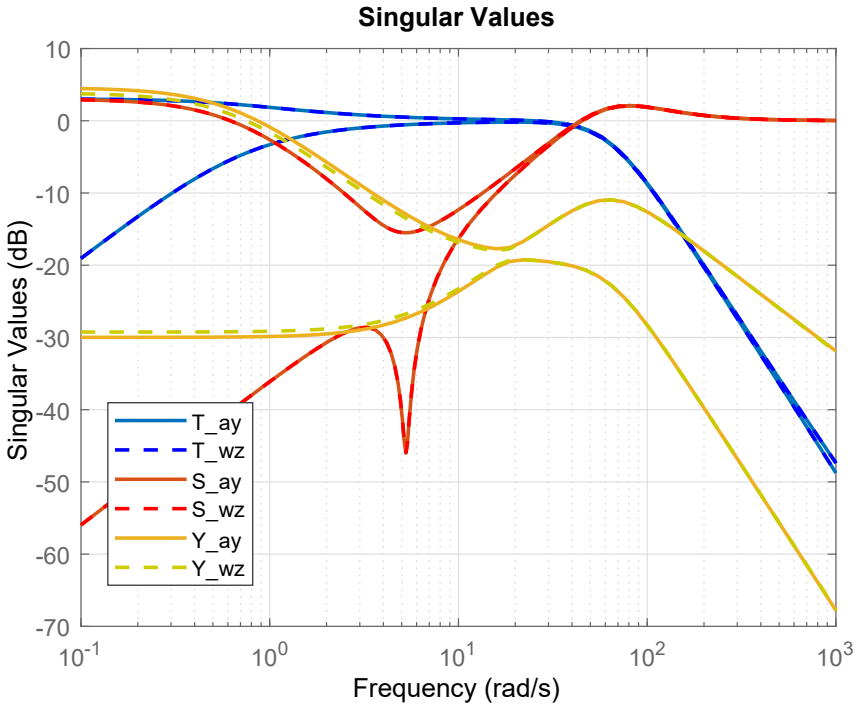

Figure 4.9: Singular value plots for yaw rate and lateral acceleration tracking for $\omega_1 = 0.1$ Hz and $\omega_2 = 10$ Hz.

In order to further illustrate the tradeoffs, an exponential chirp signal is used as an input to some of the transfer functions. The reference input spans $0.01 - 2$ Hz. The control system considered continues to be the system where the lateral acceleration is tracked at steady state. The first plot, Figure 4.10, shows how T_{ay} responds when a chirp signal is used as the reference lateral acceleration while the reference yaw rate is zero. Both signals track the lateral acceleration well because they both have a bandwidth of 10 Hz. However, they differ in the yaw rate where the signal with the larger ω_1 value (in red) deviates more at low frequencies. The signal with the smaller ω_1 value (in blue) shows better frequency matching but with an offset problem at higher frequencies.

This offset from zero is much clearer when the actuators are examined. Figure 4.11 shows that for the signal with the smaller ω_1 value the front and rear wheels are offset from zero, and very slowly return to zero. For example, if the frequency was kept at 2 Hz and the simulation was left to continue, the front and rear wheels would eventually come

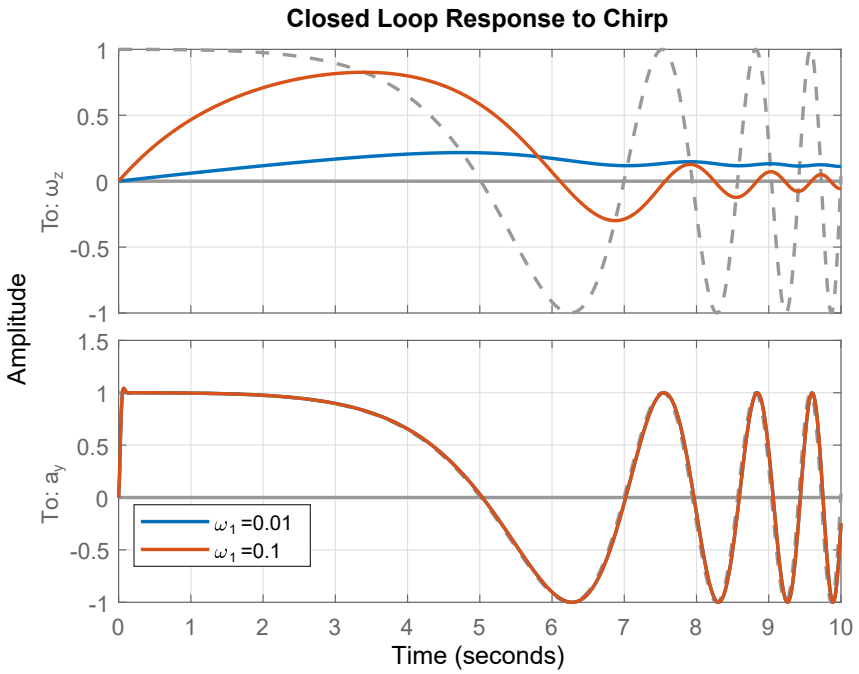

Figure 4.10: Closed loop response to an exponential chirp spanning 0.01 - 2 Hz.

back to oscillate about zero in approximately 63 s, the time constant from the dominant pole.

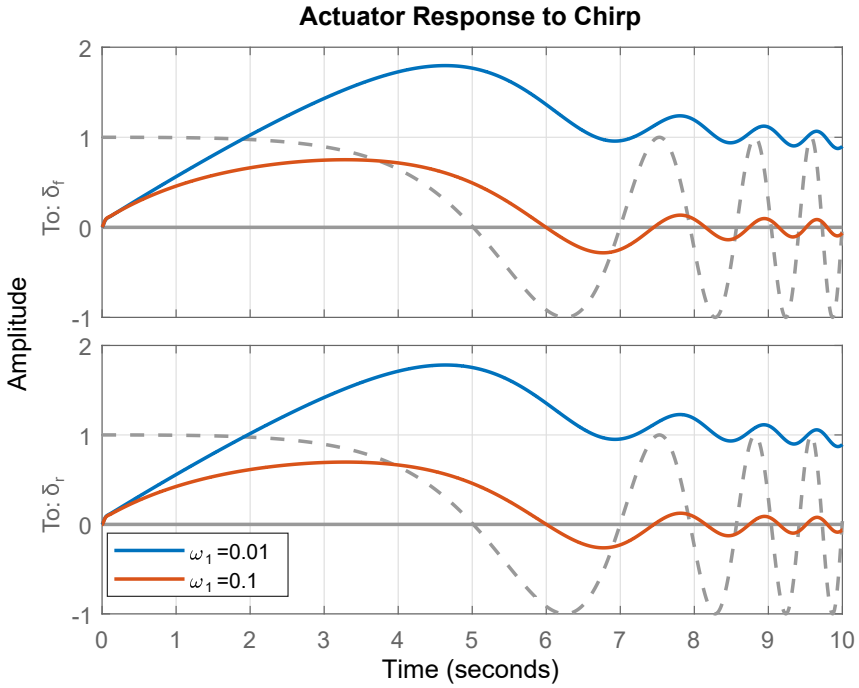

Figure 4.11: Actuator response to an exponential chirp spanning 0.01 - 2 Hz.

4.3.5 Controller Design Considering the Model Reference

The design of the model reference has an impact on the final tracking. In general, at steady state a vehicle cannot track an arbitrary yaw rate and an arbitrary lateral acceleration. Taking the steady state of the lateral acceleration yields

$$a_y(s \to 0) = v_{x0}\omega_z \tag{4.43}$$

which tells us that the steady state lateral acceleration is the product of the yaw rate and forward velocity. Therefore, decoupling is not possible at steady state which is what is enforced in the controller design.

However, if the model reference is based on a vehicle which also has this steady state coupling between signals, then a special result happens. Let the steady state of a model reference have the signals:

$$r_0 = \begin{bmatrix} w_{zref0} \\ a_{yref0} \end{bmatrix} \tag{4.44}$$

where $a_{yref0} = v_{x0} w_{zref0}$

When the signal passes through the closed loop transfer function $\hat{T}_{a_y}$ where the plant and controller are not scaled, the following is generated:

$$y = T_{a_y}\big|_{s\to 0}\, r_0 \tag{4.45}$$

$$= \begin{bmatrix} 0 & 1/v_{x0} \\ 0 & 1 \end{bmatrix} \begin{bmatrix} w_{zref0} \\ a_{yref0} \end{bmatrix} \tag{4.46}$$

$$= \begin{bmatrix} 1/v_{x0} \\ 1 \end{bmatrix} a_{yref0} \tag{4.47}$$

$$= \begin{bmatrix} w_{zref0} \\ a_{yref0} \end{bmatrix} \tag{4.48}$$

Notice that the yaw rate and lateral acceleration of the output is equal to the reference. It appears as though that both signals track. However, only the yaw rate is being tracked. The coupling design has the consequence of producing the correct lateral acceleration in a sort of feedforward output. Therefore, using this coupled controller design, we can get

the desired reference of both signals, however only one of the signals is truly being tracked through feedback.

4.4 Simulation Results

The selected simulations demonstrate how the real vehicle's dynamic properties change with the choice in virtual wheelbase. In order to show the advantages of the proposed control, the simulations will include a conventional RWS implementation. Conventional RWS uses a lookup table which outputs a ratio of rear-wheel steer angle to front-wheel steer angle. This ratio is adjusted according to the forward speed of the vehicle. The conventional system is labeled as "Conv" in the plots. In addition, the nominal vehicle is included which contains no RWS algorithms. This is labeled as "Nom" in the plots.

The control system is applied to a vehicle model from CarSim, a high fidelity vehicle simulation software. This will be the plant G_p depicted in Figure 4.3. The yaw rate and the lateral acceleration outputs from CarSim are integrated into Matlab/Simulink for use in the the MIMO controller. The vehicle used for the simulations is a D-class Sedan, which is considered a mid-size vehicle or compact executive car. Vehicles that fit this size are the Audi A4, BMW 3 Series, Cadillac CTS, and Mercedes-Benz C-Class. Some approximate parameters of the vehicle are provided in Table 4.2. The cornering coefficients were found by curve fitting the data from CarSim which use 215/55 R17 tires.

Table 4.2: Approximate parameters of the D-Class Sedan.

Description	Symbol	Value	Unit
Distance From C.G. to Front	a	1.14	m
Distance From C.G. to Rear	b	1.64	m
Total Mass of Vehicle	m	1530	kg
Moment of Inertia of Vehicle	J_z	2732	$\mathrm{kg\,m^2}$
Front Cornering Coefficient	C_f	2×68,348	$\mathrm{N\,rad^{-1}}$
Rear Cornering Coefficient	C_r	2×48,578	$\mathrm{N\,rad^{-1}}$

4.4.1 Open Loop Test with Fixed Wheelbase Length

The simulations presented in this section use the proposed system with the wheelbase length fixed at two lengths. The first is a length three times longer than the nominal wheelbase and can be thought of as a limousine. This is labeled as "Long" in the plots. The second is shortened to half the length of the nominal. This is labeled as "Short" in the plots.

The first simulation set uses a sinusoidal input at the steering wheel after half a second. An amplitude of 30° and a frequency of 0.5 Hz is used for a constant forward speed of 48 km h^{-1}.

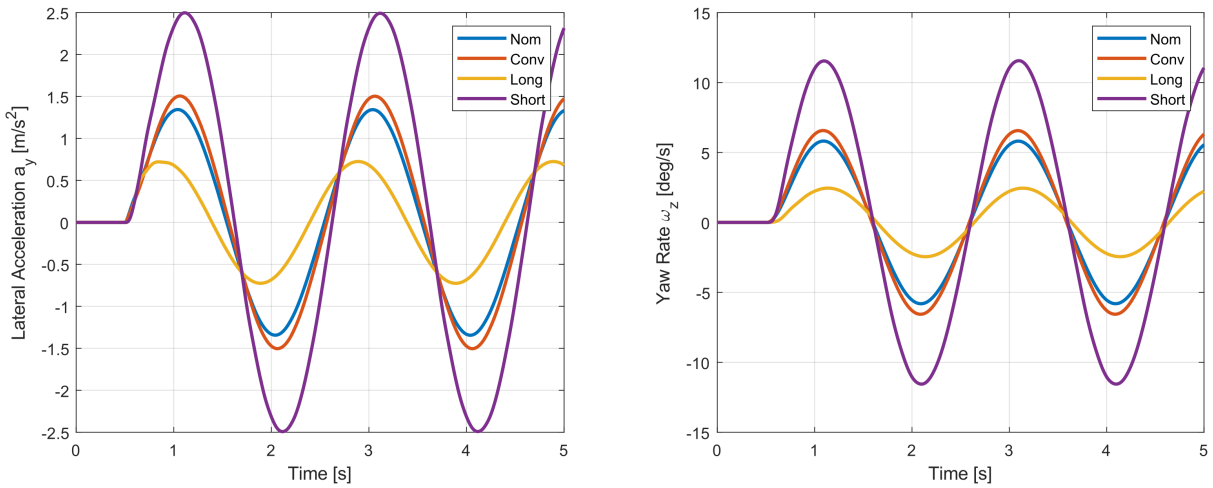

Figure 4.12: Lateral acceleration and yaw rate response to a sinusoidal input at 48 km h^{-1}.

The results in Figure 4.12 shows that when the wheel base is made longer, the yaw rate and lateral acceleration are reduced in amplitude. This is expected as the moment of inertia is made larger, making the vehicle less agile and harder to turn. This could hypothetically be used during straight line driving, where the handling and ride could feel more stable and smooth. On the other hand, shortening the wheelbase made the vehicle more agile, with a larger amplitude in the lateral acceleration and yaw rate. This choice would conceivably be better on winding roads which need a faster response and improved handling. If used in straight line driving, the short wheelbase could make the car feel fidgety evidenced by the high amplitude motion outputs.

The steer angles of the tires are shown in Figure 4.13. The front tire angles for each

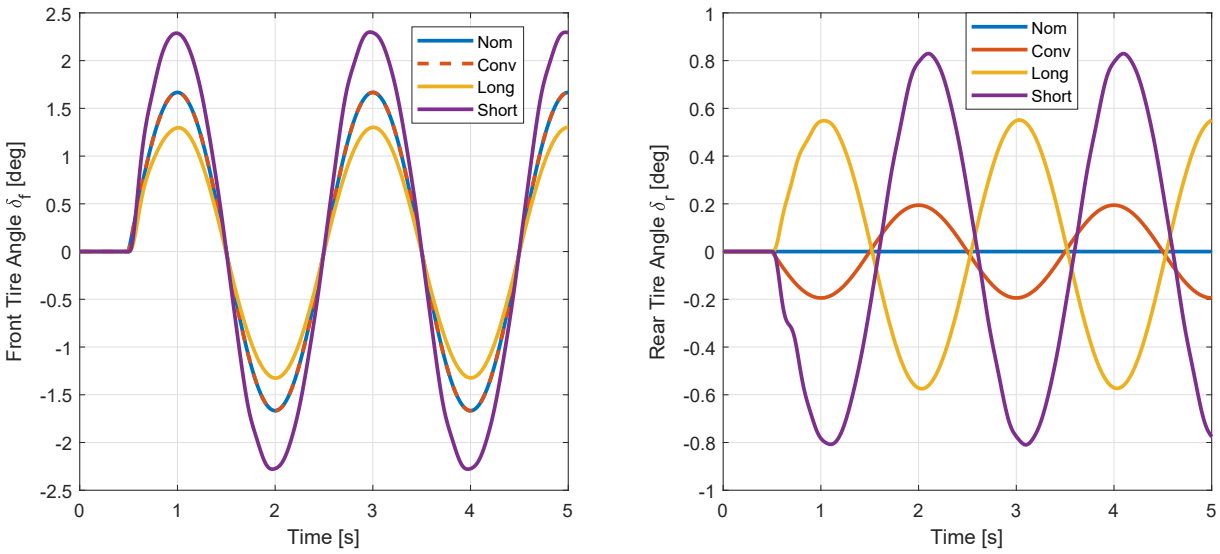

Figure 4.13: Front and rear tire angles for a sinusoidal input at 48 km h^{-1}.

set up are the same phase but differ in amplitude. The short wheelbase reference uses the largest amount of front tire steer. However, the plots of the rear tire angles show the largest differences between the systems. The longer wheelbase has the rear tire angle in phase with the front. The shorter wheelbase is out of phase with the front. This matches the 'virtual wheelbase' explanation of rear-wheel steering, and the results match expectations. The tire angle magnitudes are all reasonable. Finally, the conventional algorithm uses out of phase steering. This is because the crossover point from out-of-phase steering to in-phase steering is set to be at 60 km h^{-1}. An important concept to note is that the rear tires do not have perfectly aligning zero-crossover points. Although in-phase steering and out-of-phase steering can be seen, the rear tires are not steered according to the front tires for the virtual wheelbase system. They are responding in the manner necessary to track the yaw rate and lateral acceleration that the model reference demands. This is an important distinction between the proposed algorithm and the conventional RWS.

The second simulation set also uses a sinusoidal input. An amplitude of 15° and a frequency of 0.2 Hz is used for a constant forward speed of 95 km h^{-1}. These simulations demonstrate the conventional RWS set up steering in-phase with the front for comparison with the proposed algorithm.

The results in Figure 4.14 and Figure 4.15 shows similar trends to the first simulation

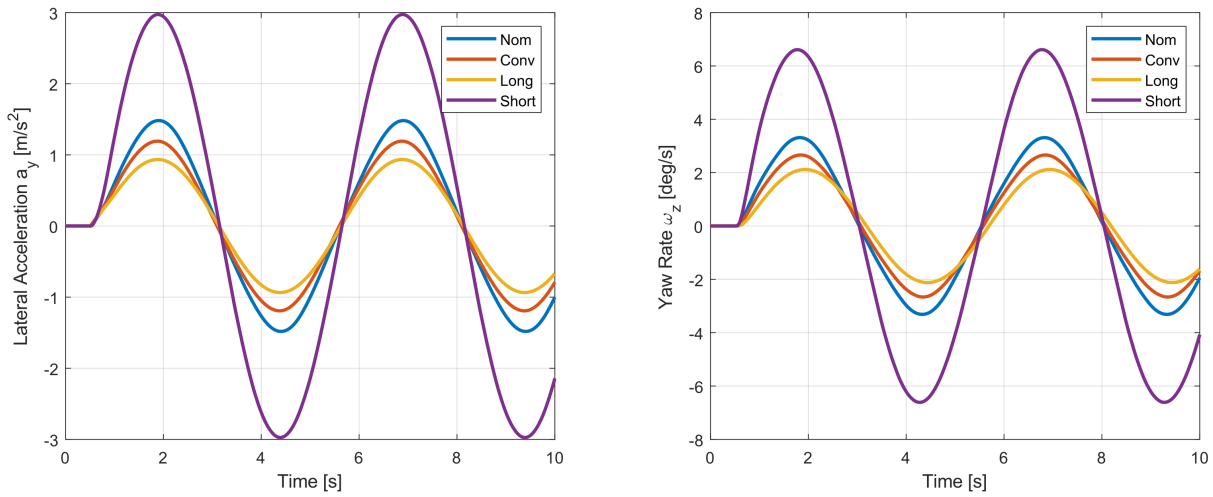

Figure 4.14: Lateral acceleration and yaw rate response to a sinusoidal input at 95 km h^{-1}.

set at 48 km h^{-1}. The long wheelbase model reference and the conventional system behave similarly with their tire angles, as expected.

Some of the driving cases discussed requires a driver to close the loop between the steering input and the path. The next sections demonstrate the systems with a driver model.

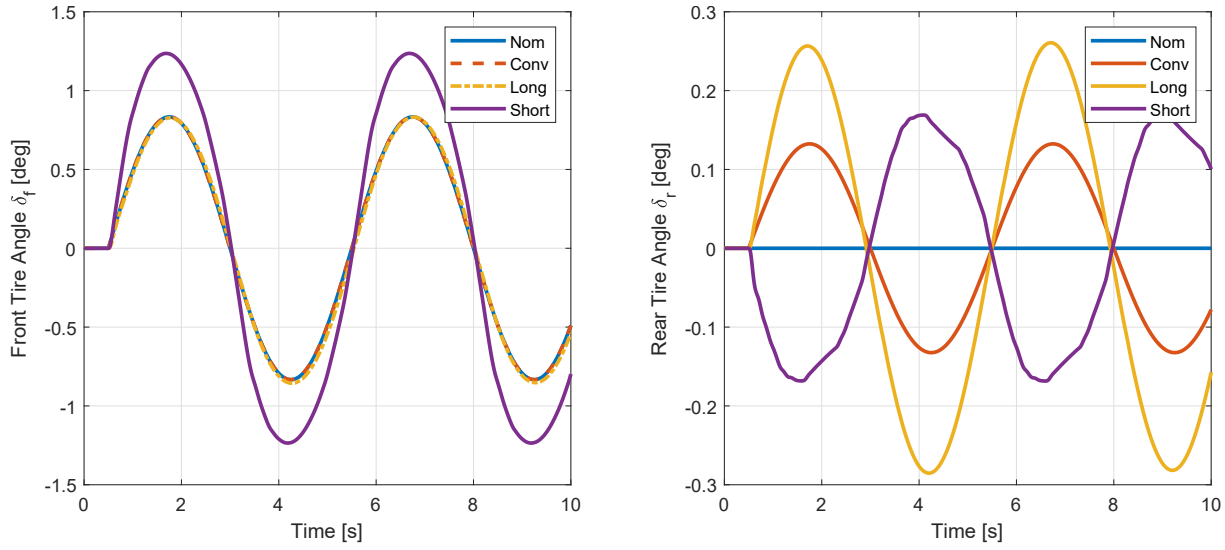

Figure 4.15: Front and rear tire angles for a sinusoidal input at 95 km h^{-1}.

4.4.2 Closed-Loop Test with Fixed Wheelbase Length

The simulations in this section integrate a driver model from CarSim to follow a predetermined path. The driver model steering wheel decision is now exported from CarSim for use in the Matlab/Simulink environment. The driver model steering wheel input is appropriately transformed to a tire angle and used as the input to the model reference.

A lane change is simulated at 95 $\mathrm{km\,h^{-1}}$. The path is a line that moves laterally over a longitudinal distance of 75 m. The driver model inputs in the CarSim vehicle are shown in Figure 4.16. As expected from the open-loop simulations, for the long wheelbase reference to turn enough, the steering wheel will have to be greater than the other systems. Conversely, the short wheelbase reference needs to steer less.

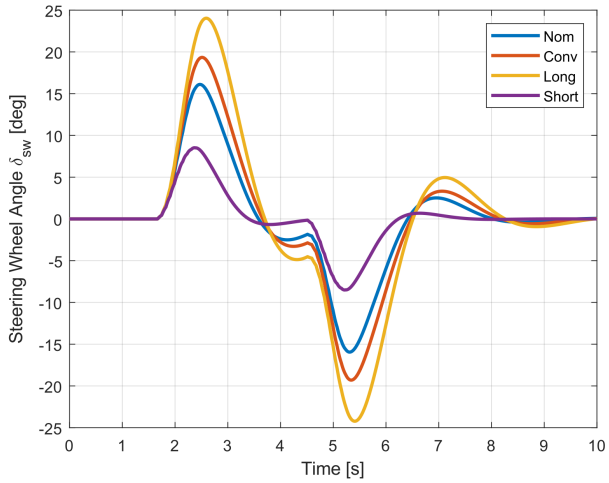

Figure 4.16: Steering wheel angle of a lane change at 95 $\mathrm{km\,h^{-1}}$.

Figure 4.17 shows that both the lateral acceleration and yaw rates of the longer wheelbase reference are lower in amplitude, and respond slightly slower. The conventional system does trend in the same manner, since the high speed uses in-phase steering. The shortened wheelbase vehicle responds the fastest.

Finally, the tire angles are shown in Figure 4.18. The tire angles are reasonable and not excessive.

The proposed algorithm still requires the wheelbase to be set. As discussed, having the vehicle feel longer during straight driving and shorter in curvy roads could have benefits

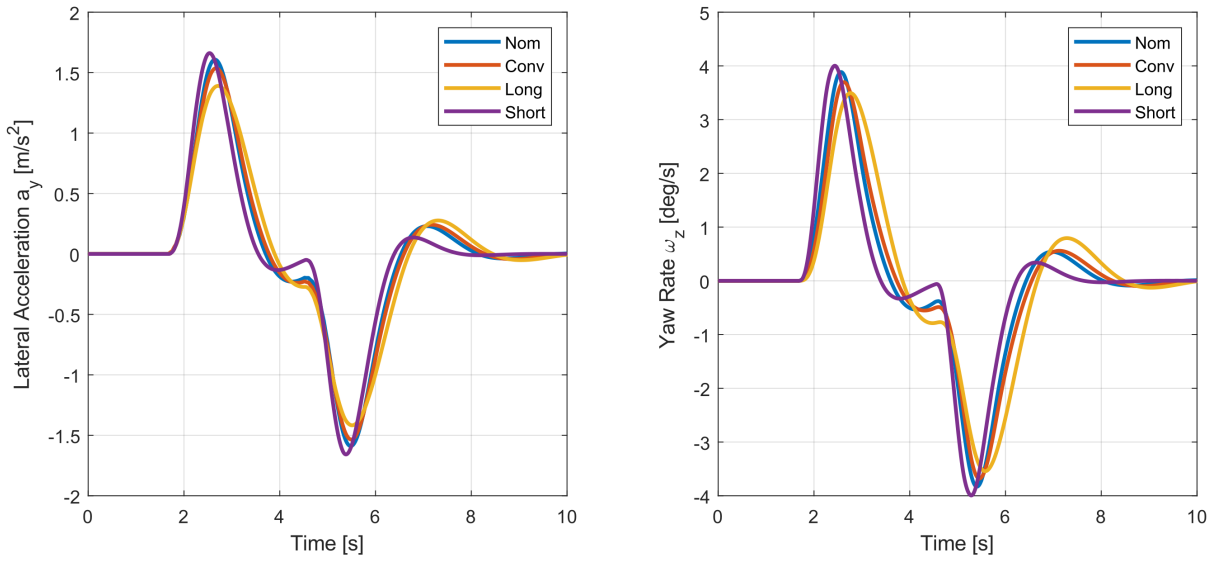

Figure 4.17: Lateral acceleration and yaw rate response of a lane change at 95 km h^{-1}.

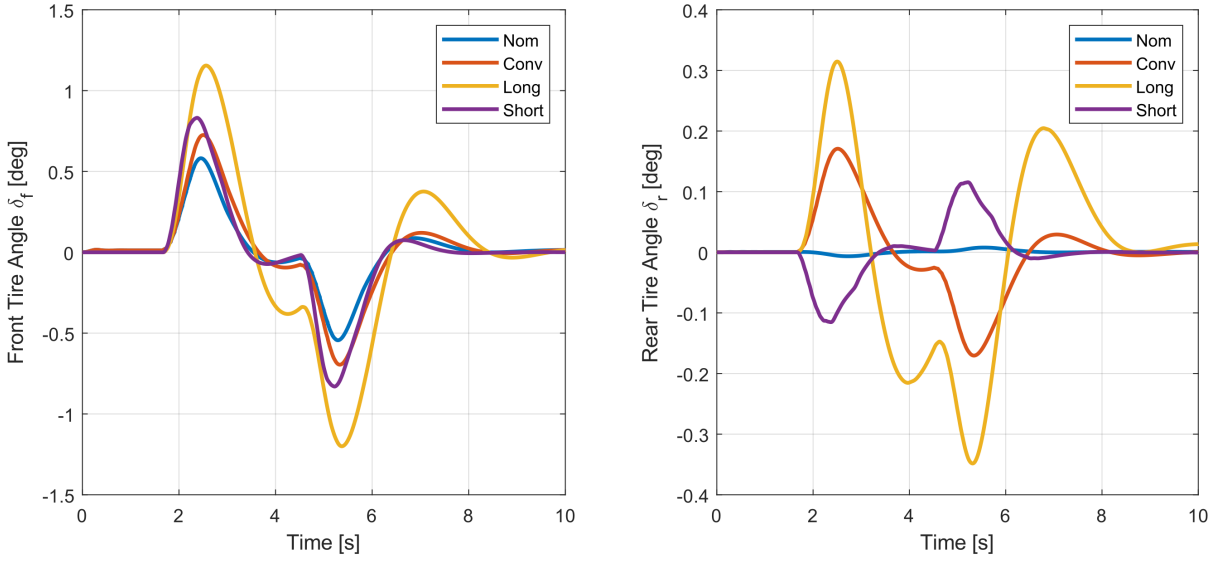

Figure 4.18: Front and rear tire angles of a lane change at 95 km h^{-1}.

for handling. As a preliminary study into this idea, a control law for the wheelbase length is proposed in the next section.

4.4.3 Closed-Loop Test with Dynamic Wheelbase

So far the simulations shown use a constant wheelbase where various lengths are compared. The vehicle will now track the yaw rate and lateral acceleration signals while the wheelbase of the model reference varies.

One idea of implementation is for an autonomous vehicle, where if a vehicle has knowledge of the path ahead the model reference can adjust in order to best negotiate the path. In traditional RWS control where only the forward velocity is fed back, the system has no knowledge of what the intentions of the driver are. A highway off ramp and a lane change are treated the same. However, knowledge of the curvature of the road is helpful in negotiating a turn because the vehicle properties can change to reflect the upcoming driving scenario. If a vehicle wants to simply change lanes on a straight stretch of highway, having the vehicle behave like it has a longer wheelbase could reduce the amount of yaw rate. The car would simply drift to the next lane without having to yaw the vehicle very much. If the vehicle is negotiating a series of winding curves, a shorter wheelbase would allow for more yaw rate and allow the vehicle to handle better.

In the following simulation, a course is negotiated by a driver model in CarSim which is made up of winding turns and curves. Therefore, a simple proposal is made. Assuming that the autonomous vehicle can generate the curvature of the road, the wheelbase will be a function of the curvature. When the path is straight, the wheelbase is long. When the curvature increases, the wheelbase should begin to shrink. Therefore, the following control law is proposed:

$$L = L_{max} - k|\rho| \tag{4.49}$$

where ρ is the curvature relative to the vehicle, k is some choice in slope with units of m^2, and L_{max} is the longest wheelbase desired while the road is at a straight path. When the path begins to curve, the wheelbase shrinks. The proposed control law linearly reduces

the wheelbase as the curvature increases. More complicated choices can be implemented as well. A saturation operator is added to limit the wheelbase so it does not become too small.

In the simulation, the driver model can also accelerate and decelerate, limited to a total acceleration of 5 $\mathrm{m\,s^{-2}}$. The vehicle's speed varies from $40 - 120$ $\mathrm{km\,h^{-1}}$ under these limitations. However, the model reference is based on a planar model with constant forward speed. In order to have more realistic lateral acceleration reference signals, the vehicle's actual speed is fed back to the model reference under the assumption that the vehicle's forward change in speed is not extreme. The controller developed in Section 4.3 is continued to be used.

The results show that the driver model successfully navigated the course with the varying wheelbase system. Figure 4.19 shows a snapshot of the lateral acceleration and yaw rate. Included for comparison are the conventional RWS system and the nominal vehicle without RWS. A location to note on the plot is at around 96 s, where the variable wheelbase has higher peaks in the signal outputs. This is due to the virtual wheelbase being long at that point in time. The driver model is attempting to stay on the generated path for the course, so it steers aggressively to follow the path. An idea for remedying this is using the curvature of the path ahead of the vehicle instead of the instantaneous path at the vehicle. Regardless, the signals show smoother movement in the motion outputs.

Figure 4.20 shows the actuation of the front and rear tires. The rear tires do not exceed 5° in the snapshot of the simulation, which is reasonable.

Figure 4.21 demonstrates the steering wheel motion for navigating the course. The larger steering angles of the variable wheelbase system coincide with a longer wheelbase, shown in Figure 4.22. Figure 4.22 shows the curvature and reference wheelbase chosen by Equation 4.49. The wheelbase change uses a smoothing filter in order to avoid abrupt changes. The wheelbase control proposal is not sophisticated by any means, but accomplishes the goal of demonstrating this proof of concept.

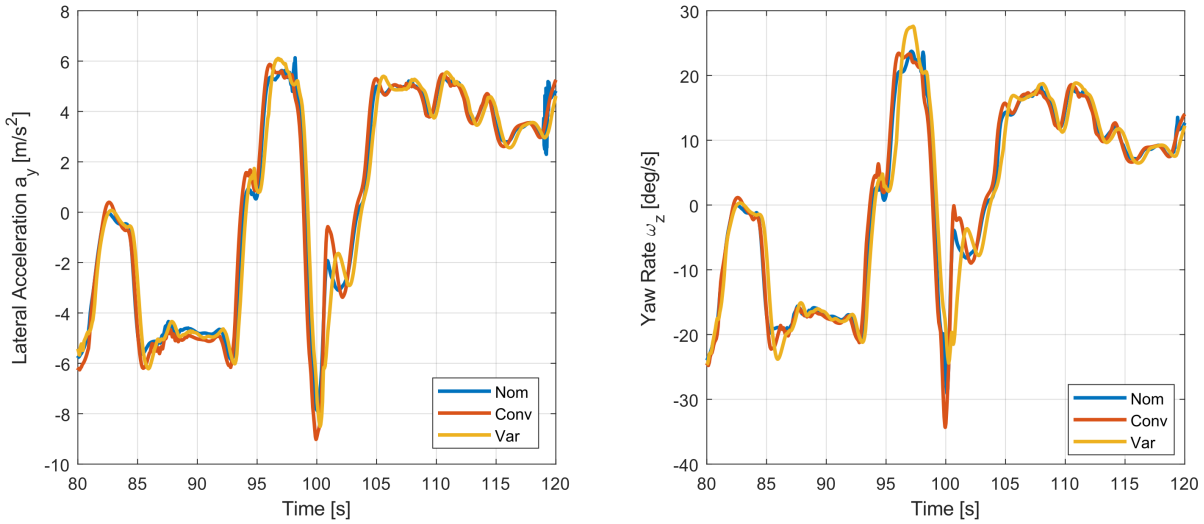

Figure 4.19: Yaw rate and lateral acceleration signals on a course in CarSim.

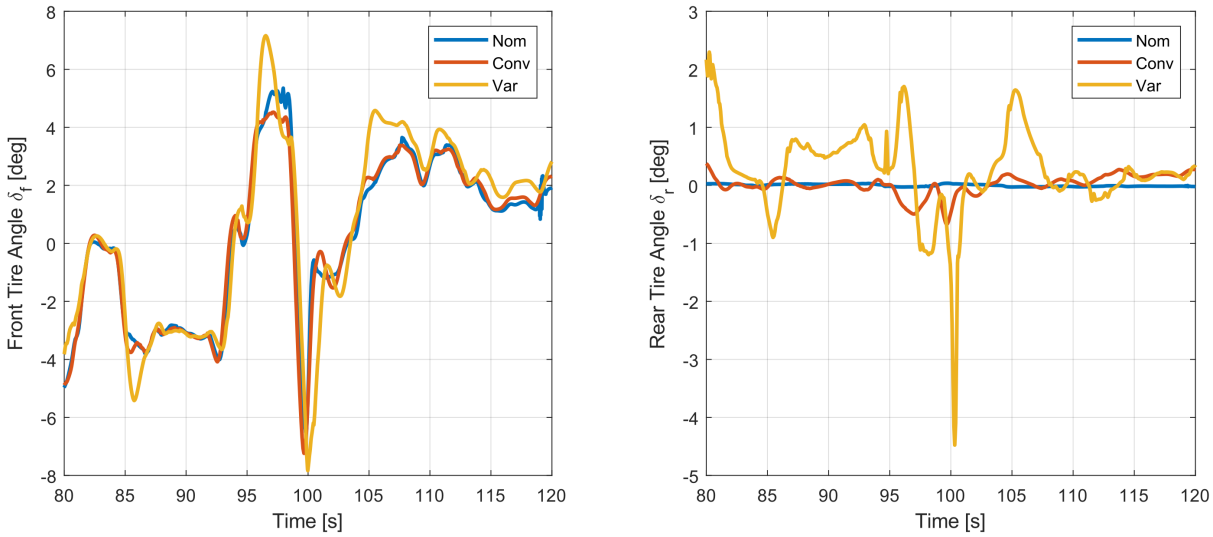

Figure 4.20: Front and rear tire angles of the vehicle on a course in CarSim.

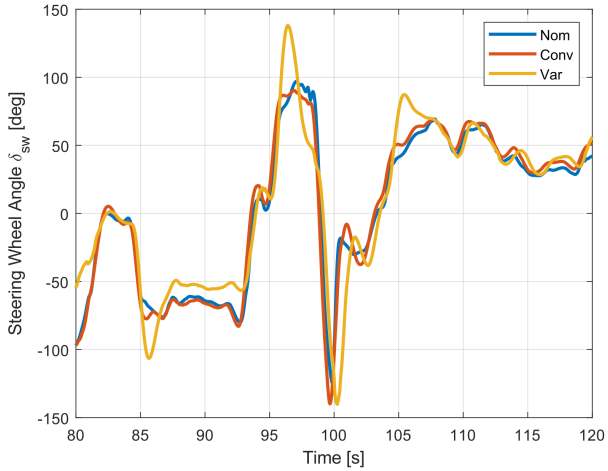

Figure 4.21: Steering wheel angle on a course in CarSim.

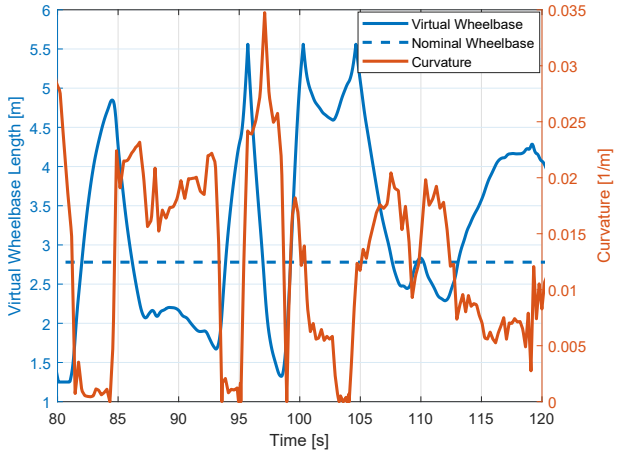

Figure 4.22: Model reference wheelbase and curvature of the road on a course in CarSim.

4.5 Conclusion

To conclude, a novel proposal for controlling the front and rear wheels has been described and demonstrated. The system described allows a vehicle with active front and rear wheels to handle like a long limousine, or a small nimble car. The model reference is set up such that the only parameter needed to change is the wheelbase length, which is intuitive to control. In the open-loop simulations, it was demonstrated that the longer wheelbase outputs less yaw rate and lateral acceleration, as expected with a real vehicle comparison. A shorter wheelbase was just the opposite.

Further research can investigate adding fidelity to the model reference. For maneu-

vering at higher lateral accelerations, the model reference needs tire forces that can saturate in order to avoid unrealistic lateral acceleration references, which can destabilize the system. In addition, the two degree-of-freedom system can be extended to a three degree-of-freedom system, allowing for longitudinal acceleration which was not done in this dissertation. This would also be helpful for extreme handling situations. Additionally, passenger comfort and handling needs to be properly investigated though quality evaluations. This can be done through virtual simulators.

The use of feedback in the system indicates that there can be robustness to disturbances, such as wind gusts. Further research can investigate the robustness of the control system due to uncertainties of the vehicle parameters, sensor noise, and disturbances.

Furthermore, a simple control law is proposed and used to control the wheelbase. A proof of concept shows successful tracking of reference signals by the controller while the wheelbase changes dynamically during simulation. Further research can investigate a more sophisticated choice in controlling the wheelbase of the model reference.

Chapter 5

Stability with Rear-Wheel Steering

When stability is discussed with respect to RWS, the connotation is improving the stability of the driver-vehicle system during straight-line driving. When conventional RWS is applied, the vehicle's stability does not change. This can be easily seen in Equation 2.4 and Equation 2.5. The poles of the vehicle model are unaffected with this open-loop control. If conventional rear wheel steering was applied to a vehicle with parameters that make it oversteer and was operating above its critical speed, the vehicle would still be unstable.

This chapter investigates designing a controller and using only RWS to stabilize a vehicle that is inherently unstable. It also investigates this SISO control system on a vehicle in split-μ conditions.

5.1 Oversteering Vehicle Condition

Oversteering in a vehicle is due to two main issues. The first is the overall parameter set of the vehicle, which can be derived from a linear bicycle model. The other is due to a combination of normal force variation, tire properties, and steering inputs which can be referred to as induced oversteering. In order to design an oversteering vehicle, the former cause is considered. The characteristic equation of a linear bicycle model is as follows:

$$\Delta = s^2 + \left[\frac{C_{yf} + C_{yr}}{mv_{x0}} + \frac{a^2C_{yf} + b^2C_{yr}}{J_z v_{x0}}\right]s + \frac{(a+b)^2 C_{yf}C_{yr}}{mJ_z v_{x0}^2} + \frac{bC_{yr} - aC_{yf}}{J_z} \tag{5.1}$$

When the last term of the polynomial becomes negative, the vehicle becomes unstable.

The term $(bC_{yr} - aC_{yf})$ determines if the linear vehicle is oversteer, understeer, or neutral steer. Although v_{x0} is constant in the bicycle model, its variation determines the point in which an oversteer vehicle goes unstable, which is at the critical speed v_{xcrit}. Its relationship is shown below.

$$v_{xcrit}^2 = -\frac{(a+b)^2 C_{yf} C_{yr}}{m(bC_{yr} - aC_{yf})} \tag{5.2}$$

This section investigates stabilizing an oversteering vehicle that is operating beyond its critical speed. To have a reasonably realistic case, the rear tire cornering coefficient C_{yr} is lowered until a reasonable critical speed is reached. Other parameters can also be manipulated to create an oversteering vehicle, such as the center of gravity location. However for this study, the oversteering condition is attributed to a bad set of tires in the rear of the vehicle.

A relationship can be developed to calculate the necessary rear cornering coefficient for a desired critical speed. This is seen below in Equation 5.3, where OS stands for oversteer.

$$C_{yrOS} = \frac{maC_{yf} v_{xcrit}^2}{mbv_{xcrit}^2 + (a+b)^2 C_{yf}} \tag{5.3}$$

The procedure for designing a test condition would be to select an operating condition, choose a critical speed that is below the operating condition, then calculate the rear-tire cornering-coefficient.

The parameters used are the D-class sedan from Table 4.2. The operating speed selected is $v_{x0} = 100\ \mathrm{km\,h^{-1}}$ while the critical speed is $v_{xcrit} = 80\ \mathrm{km\,h^{-1}}$. This results in a rear cornering coefficient C_{yrOS} which is almost 50% lower than the nominal.

5.1.1 Controller Design

The RWS controller uses the rear wheels to keep the yaw rate at some value set by a reference model. It is derived considering the transfer function of the unstable vehicle

design. The transfer function from the rear wheels to the yaw rate is as follows:

$$\frac{\omega_z}{\delta_r} = -\frac{\frac{bC_{yr}}{J_z}\left[s + \frac{(1+\frac{a}{b})C_{yf}}{mv_{x0}}\right]}{\Delta} \tag{5.4}$$

where C_{yrOS} is used in place of C_{yr}.

5.1.1.1 Stabilizing Controller

Using Youla parameterization [84], a framework for a stabilizing controller is created. The system has one pole in the right-half plane. The plant can be expressed generically as the following:

$$G_{us}(s) = \frac{\omega_z}{\delta_r} = k_G \frac{(s+z)}{(s+p)(s-p_u)} \tag{5.5}$$

where p_u is the unstable pole. The subscript on the plant, "us," stands for unstable. When designing the Youla (or Q parameterization) transfer function, Y, a zero at the same location is introduced. Therefore, the design of Y begins with the inverse of $G_{us}(s)$, as follows:

$$Y'(s) = G_{us}^{-1} = \frac{1}{k_G}\frac{(s+p)(s-p_u)}{(s+z)} \tag{5.6}$$

In the design of the closed loop transfer function, where $T(s) = G(s)Y(s)$, the unstable pole requires an interpolation condition. $T(s = p_u) = 1$ needs to be satisfied in order to ensure no unstable pole-zero cancellation in the open loop $L(s)$. In addition, tracking is desired. Therefore, the design requires two conditions to be met:

- $T(s = p_u) = 1$
- $T(s = 0) = 1$

In order to meet these conditions, Y requires sufficient poles and zeros. This results in the following framework:

$$Y(s) = Y' k_Y \frac{s+\beta}{s^2 + 2\zeta\omega_n s + \omega_n^2} \tag{5.7}$$

Using Equation 5.7 and the plant transfer function to generate $T(s)$, the two conditions

are enforced. Solving for k_y and β leads to the following:

$$k_Y = p + 2\zeta\omega_n \tag{5.8}$$

$$\beta = \frac{\omega_n^2}{p + 2\zeta\omega_n} \tag{5.9}$$

Using β to satisfy this condition is helpful because it is more intuitive to tune the poles of the system rather than the zero. Therefore, the poles have two parameters remaining for the engineer to tune, ζ and ω_n. The generated controller will lead to a stable system with zero steady state error. The final control has the form of

$$K(s) = \frac{(p + 2\zeta\omega_n)}{k_G} \frac{(s + p_1)}{(s + z)} \frac{\left(s + \frac{\omega_n^2}{p+2\zeta\omega_n}\right)}{s} \tag{5.10}$$

The controller features pole-zero cancellation of the stable poles and zeroes from the plant, along with cancellation of the plant's gain. An additional zero and an integrator are now introduced. The Nyquist plot of the system displays a single counter-clockwise encirclement of the point -1, indicating the closed-loop system is stable. The bode plot in Figure 5.1 shows the closed loop $T(s)$, sensitivity $S(s)$, and Youla transfer function $Y(s)$.

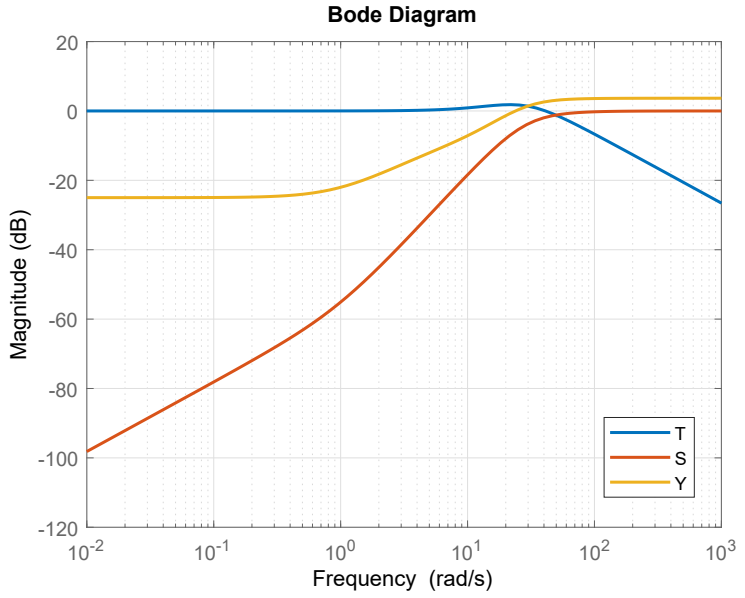

Figure 5.1: Bode plots of the control system.

As an example the figure uses $\zeta = 1$ and $\omega_n = 4.5 * 2\pi$. Depending on the definition of the bandwidth (definition can be based on $S(s)$ or $T(s)$), the bandwidth is somewhere between 5 Hz and 10 Hz.

The controller derived leads to a Nyquist plot shown in Figure 5.2 where there is a single counter-clockwise encirclement of the point -1. Because of the configuration of this particular system, the system requires a minimum gain to be stable.

5.1.1.2 Controller based on Nominal Vehicle

Here, a controller is designed around the stable vehicle where C_{yr} is the nominal value. The procedure is simplified since there are no interpolation conditions to be met. The controller can be designed using the following Y function.

$$Y(s) = G^{-1}(s)\frac{\omega_n^2}{s^2 + 2\zeta\omega_n s + \omega_n^2} \tag{5.11}$$

where $G(s)$ is the nominal, stable plant with the nominal rear cornering coefficient. This leads to a controller of the following form:

$$K(s) = G^{-1}(s)\frac{\omega_n^2}{s(s + 2\zeta\omega_n)} \tag{5.12}$$

The controller is tuned with the same parameters as before, where $\omega_n = 4.5$ Hz and $\zeta = 1$. The closed loop transfer function reveals that this tuning gives it a bandwidth of about 3 Hz. This controller is then applied to the unstable plant. The Nyquist plot is shown in Figure 5.2. The results show that there is a counter-clockwise encirclement of -1, indicating that the system is stabilized with the controller based on the stable vehicle.

This shows that the design of a controller around the nominal stable vehicle is capable of stabilizing the unstable vehicle for the conditions given.

5.1.2 Reference Generator

The reference generator considered is the yaw dynamics of a stable vehicle with only front-wheel steering. The transfer function from the front steer angle to the yaw rate is as follows:

$$\frac{\omega_z}{\delta_f} = \frac{\frac{aC_{yf}}{J_z}\left[s + \frac{(1 + \frac{b}{a})C_{yr}}{mv_{x0}}\right]}{\Delta} \tag{5.13}$$

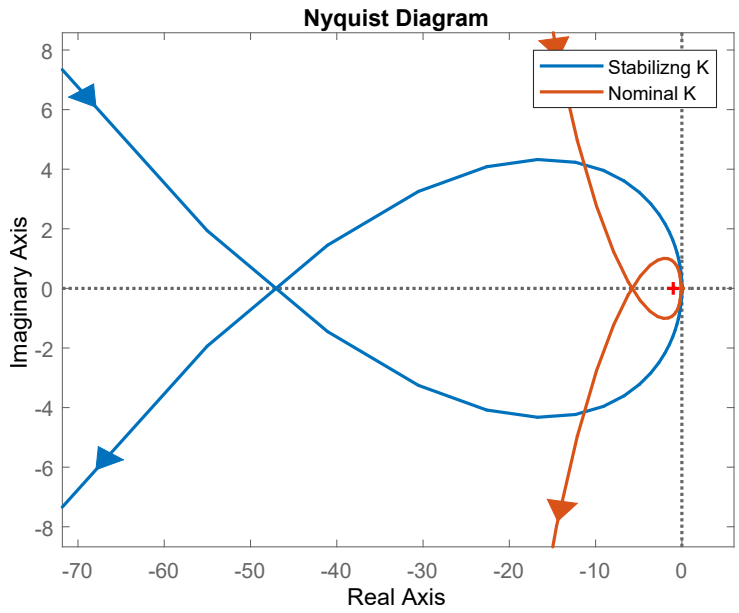

Figure 5.2: Nyquist plot for two different controller designs.

5.1.3 Simulation

The simulation uses the parameters in Table 4.2. The plant is the simplified planar model described in Section 3.2. The additional parameters necessary are the C.G. height and the track for the normal force variation, which are $h = 0.5$ m and $2c = 1.5$ m, respectively.

In order to make it oversteer, the rear tire cornering coefficient is lowered using the procedure described earlier. The operating speed and critical speed are the same values used previously, where $v_{x0} = 100\ \mathrm{km\,h^{-1}}$ and $v_{xcrit} = 80\ \mathrm{km\,h^{-1}}$.

The reference will simply have the nominal rear cornering coefficient, outputting a stable yaw rate to track. The stabilizing controller is used for the simulation.

The input is a filtered step steer where the final value is 1.5°. A first order filter with a settling time of $T_s = 0.2$ s is used.

Some results for the uncontrolled vehicle are shown in Figure 5.3 and Figure 5.4. The slip angles become substantially large for all tires and the driver loses steering ability.

Results for when the controller stabilizes the system is shown in Figure 5.5 and Figure 5.6.

The controller is not only successful in stabilizing the vehicle, but it tracks the yaw

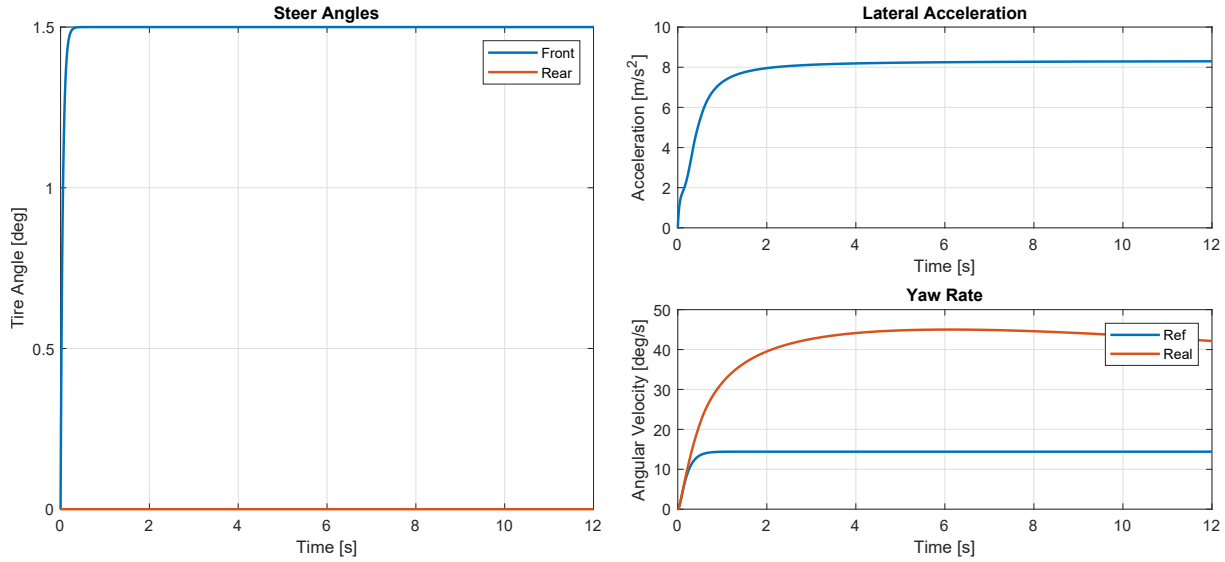

Figure 5.3: Steer angles and vehicle signals when uncontrolled.

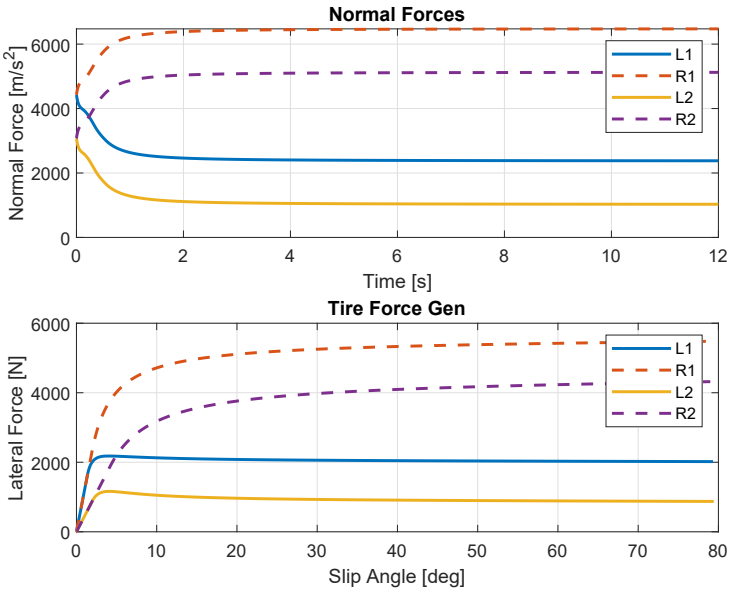

Figure 5.4: Tire response when uncontrolled.

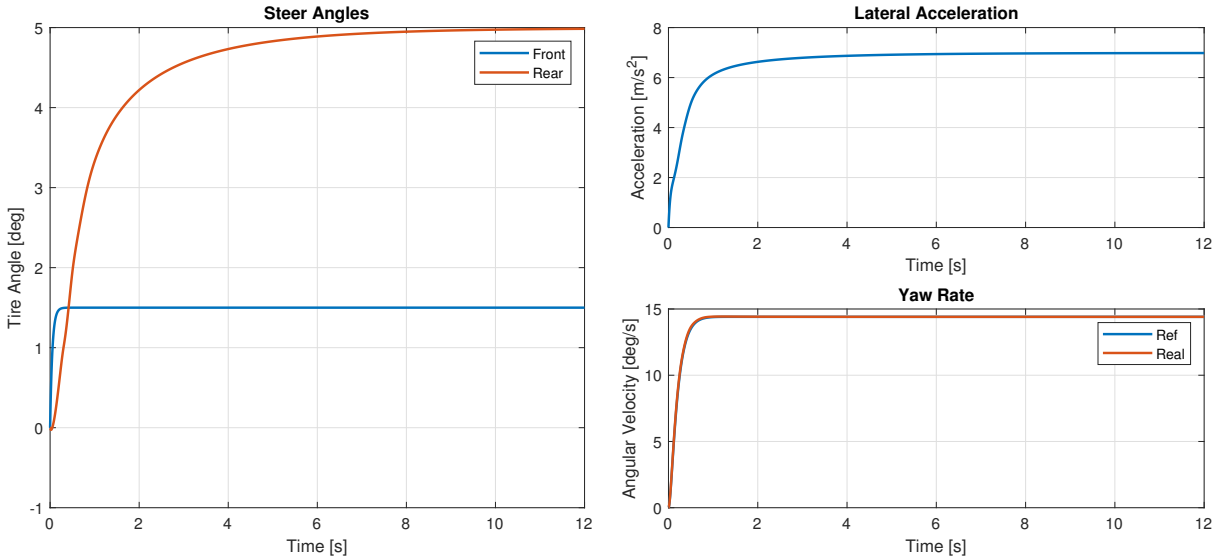

Figure 5.5: Steer angles and vehicle signals when stabilized.

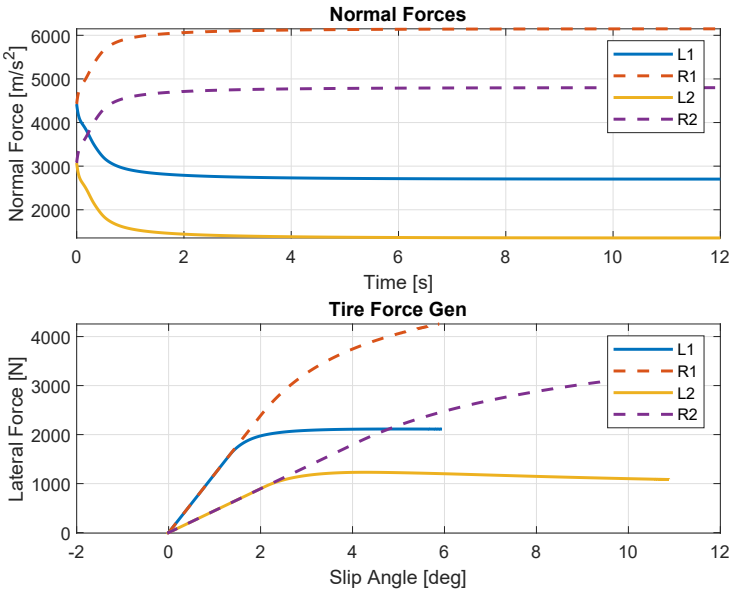

Figure 5.6: Tire response when stabilized.

rate signal as well. In order to stabilize the vehicle, the rear wheels had to steer more than the front wheels. This is concerning because it seems possible to hit the actuator limits which are typically in the range of about $5 - 10°$. At the moment the model reference is a bicycle model with linear tires which will make the controller go unstable if the real tire forces go past their saturation limits.

The results also show the slip angles exceeded 10°, as seen in Figure 5.6. The inside tires reach saturation due to the load transfer to the outside tires. However, the outside tires are capable of providing enough tire force to keep the vehicle under control.

The model reference parameters were not tuned for a specific purpose other than provide a stable signal to follow. Increasing the front steering by a degree results in a vehicle that is unstable. The research shows that stabilizing an oversteer vehicle while it exceeds its critical speed is possible.

The next step is to have some braking ability on a split-μ road.

5.2 Split-μ

The split-μ condition is an environment where the tires on one side of a vehicle experience different grip capabilities than the other side. Examples where this can manifest could be due to a patch of ice that one side travels over, or part of the vehicle travels on the road while the other part of the vehicle travels on the unpaved shoulder. The left and right experience different friction values, μ.

The problem with split-μ is when the driver brakes or accelerates the vehicle. However for this section, only braking is considered. Because of the different friction coefficients, the low friction side generates less of a braking force than the high friction side. This results in a yaw moment which turns the vehicle, even if the steering is held straight. Without ABS, the low friction wheels may lock up. ABS can help maximize the peak braking force and prevent wheel lock up at each wheel, but there will still be a braking force imbalance causing a yaw moment. Using the brakes only still requires driver steering intervention to correct the turning of the vehicle.

Commercial ABS and ESC products may already contain logic to make driver steering

intervention easier [85, 63]. These systems create a yaw moment buildup delay to make the vehicle yaw buildup slower, giving more time to correct for the driver. This is done by slowing the braking build up on the high friction side. Corrective steering is necessary to maximize the braking ability of the vehicle. Otherwise in order to prevent the yaw moment, both sides of the vehicle would need equal braking forces. However, this leaves precious braking potential which can slow the vehicle even faster in an emergency.

Therefore it would be worthwhile to determine if RWS could stabilize the vehicle. The driver's intentions would be to keep the vehicle going straight when the brakes are applied. This situation is explored here.

5.2.1 Modeling

The split-μ condition requires additional degrees of freedom in the vehicle model. Therefore, the higher fidelity model described in Section 3.2 is used. The model requires additional parameters, which are listed in Table 5.1

Table 5.1: Additional parameters of the D-Class Sedan.

Description	Symbol	Value	Unit
Half Track Width	c	0.775	m
Height of C.G.	h	0.500	m
Front Long. Coefficient	C_{xf}	116,335	N/[-]
Rear Long. Coefficient	C_{xr}	82,244	N/[-]
Spin Inertia of Tire	J_w	0.9	$\mathrm{kg\,m^2}$
Effective Radius	r_e	0.325	m

Additional conditional statements are added to the model to make sure the wheels do not reverse, since a direct torque is applied on the wheels. This will keep the wheels "locked" when the braking torque exceeds the longitudinal forces on the wheel. The logic implemented can be found in Appendix A.

In addition, a simple ABS logic is used which directly uses the slips. The slips are not easily available. However, for comparison purposes and simplicity, the slips are assumed available. The ABS logic uses a relay block for each corner of the vehicle. When the high

threshold slip value is crossed, the relay turns off the braking for its respective wheel. The slip value chosen is -0.25. Peak forces for dry asphalt typically occur at around slip values of $0.15 - 0.2$. The relay turns the braking torque back on once it reaches a slip value of -0.05.

In order to make the brake switching more realistic, a low pass filter is added to simulate the braking dynamics, including the fluid properties of the system. Conventional ABS and traction control has an average operational frequency of $3 - 10$ Hz [86]. Documentation from CarSim states that the cycling frequency is typically around 10 Hz. This is affected by its settings in fluid dynamics in addition to the wheel inertia and tire longitudinal relaxation length, Therefore, to be conservative, a low pass filter with a cutoff frequency of 5 Hz is used. This is applied to each wheel's braking torque after the relay block.

The braking distribution of the vehicle typically skews heavier on the front and lighter in the rear since the vehicle pitches forward during braking. This shifts the normal forces to the front allowing the front to apply more brake forces. Therefore, a distribution of $70 - 30$ is used for the braking torques at the front and rear.

5.2.2 Control Robustness to Forward Speed

The stabilizing controller from the previous section is capable of tracking the yaw rate and can be applied on a stable vehicle. A concern is whether it would be effective on a vehicle that is slowing. A simple check would be to see if the controller would have reasonable margins at various speeds of a bicycle model plant. The operating range considered is $v_{x0} \in [10\ 120]$ $\mathrm{km\,h^{-1}}$. Matlab's Robust Control Toolbox allows uncertain parameters to be defined in order to create an uncertain plant. Creating a feedback loop, the worst case gains can be found for the uncertainty range. Figure 5.7 shows the sensitivity function when the forward velocity is changed. The worst case gain for the sensitivity function is found to be within a magnitude of 1.002, which is practically negligible. The worst case gain for the closed-loop function is found to be within a magnitude of 1.1122, or 0.92 dB.

The frequency response seems to be unaffected by changing the forward speed.

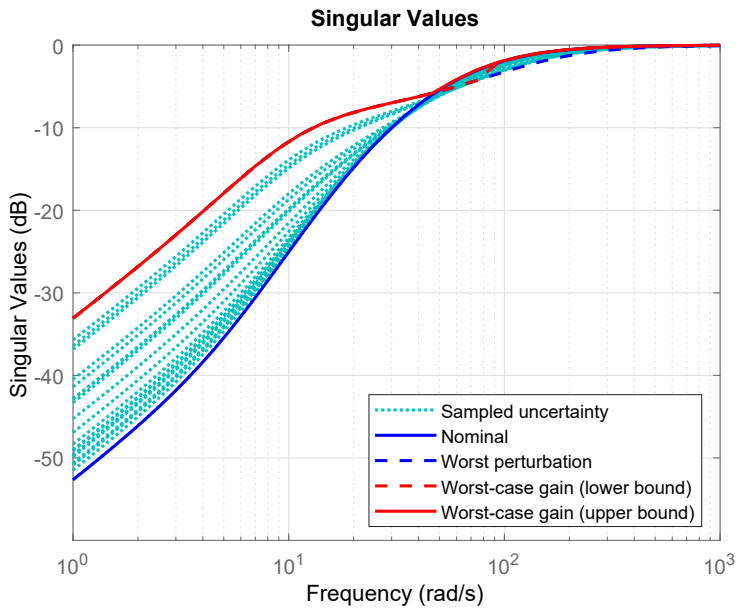

Figure 5.7: Sensitivity Function with uncertain parameter v_{x0}

This linear approach to control robustness does not study the controller interaction with changing normal forces or loss of lateral force ability due to saturation of the tire forces due to low friction on one side of the vehicle.

5.2.3 Simulation

The simulation begins at a forward speed of 100 kph, where the brakes are applied through a filtered step with a time constant of $\tau = \frac{1}{2\pi \times 10}$. Enough braking torque is applied to lock the wheels and activate ABS on the low friction side. The front wheels of the vehicle are kept straight. The vehicle travels on a split-μ surface where the left has a friction coefficient of 0.85 while the right has a coefficient of 0.2.

The first two simulations (not shown) were done without RWS. One simulation had ABS on while the other did not. Both generated large yaw rates and spun out.

The next two simulations do use RWS, where the rear wheels are actively controlled. Again, one simulation had ABS on while the other did not. Since the steering was kept at zero, the reference yaw rate value is kept at zero for all time. RWS attempts to keep the yaw rate at zero, and is successful as seen in Figure 5.8.

The system with ABS is observed to behave in an oscillatory manner due to the quick

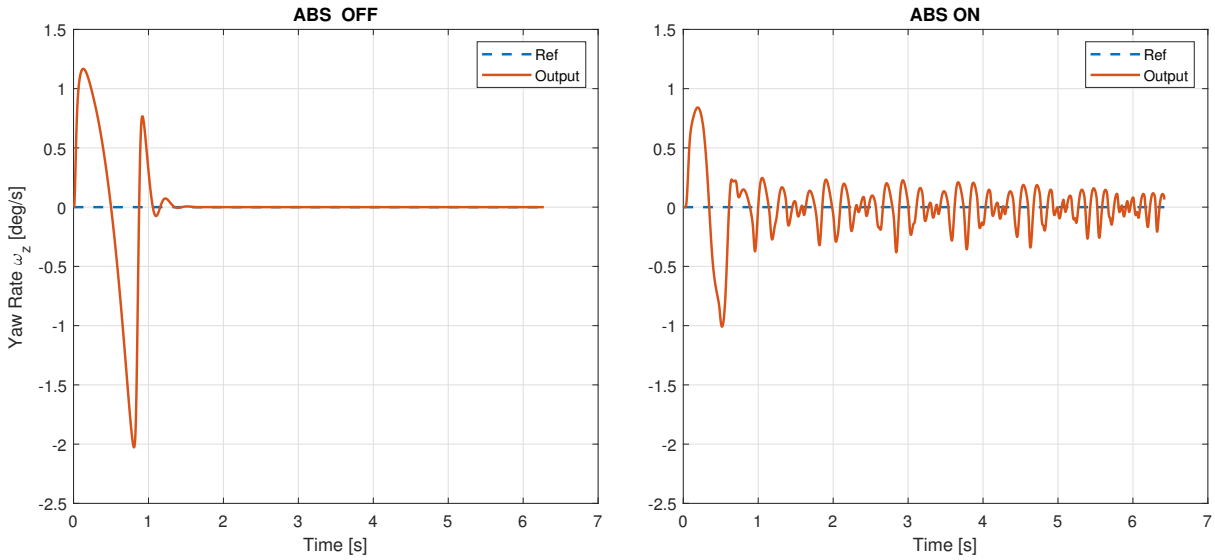

Figure 5.8: Yaw rate response with RWS on split-μ.

changes in braking torque. This is also seen in the lateral acceleration plot in Figure 5.9. However, this oscillation is less than a tenth of a G of acceleration and could be considered a necessary consequence from RWS and ABS both being on.

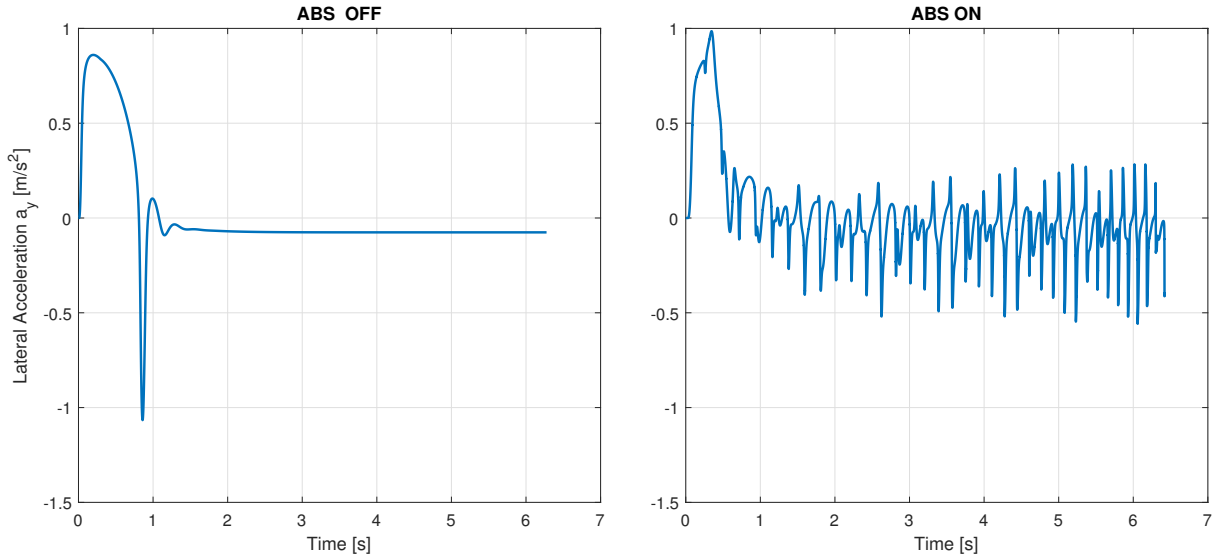

Figure 5.9: Lateral Acceleration response with RWS on split-μ.

Figure 5.10 and Figure 5.11 show the individual wheel responses as the ABS modulates. It can be seen that the wheels for ABS off lock up resulting in zero speeds, due to the left side of the vehicle having a low friction value.

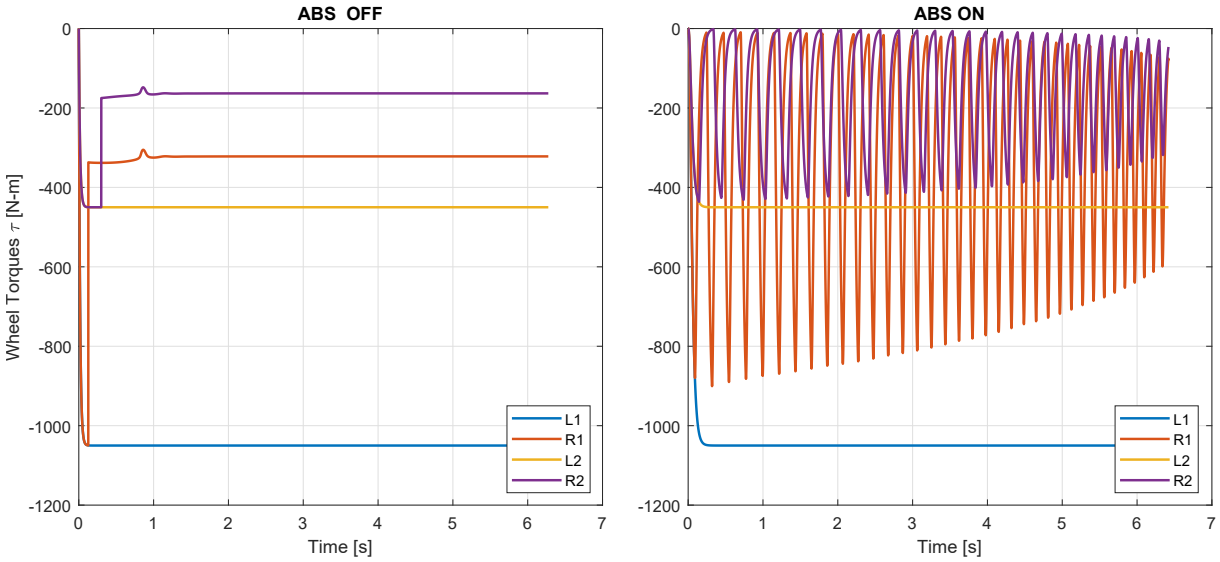

Figure 5.10: Torque response with RWS on split-μ.

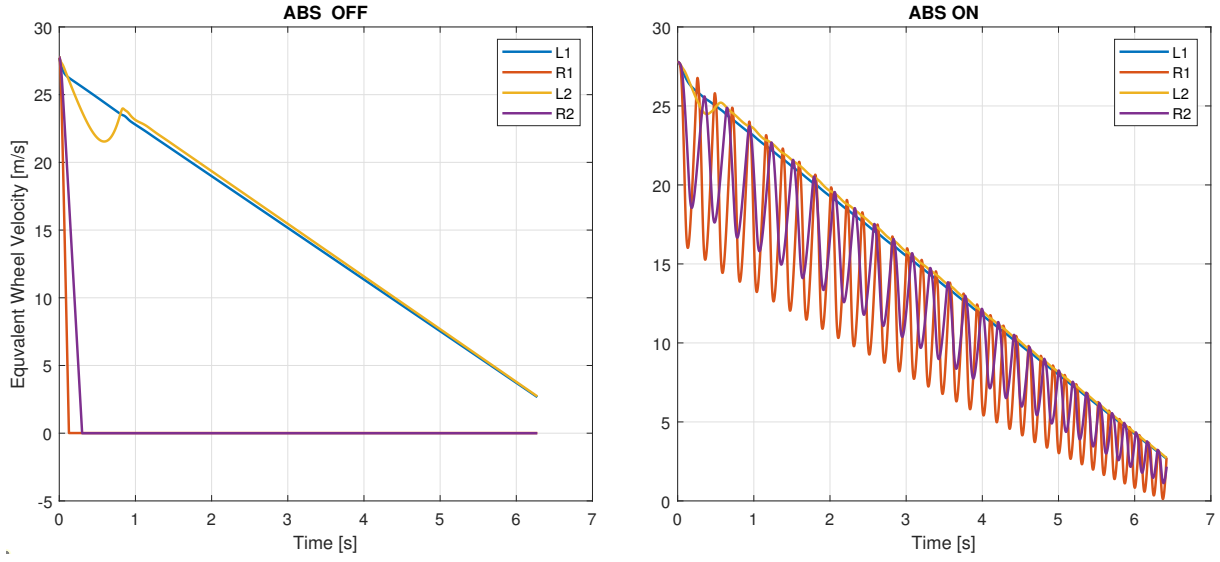

Figure 5.11: Wheel Speed response with RWS on split-μ.

Figure 5.12 shows the tire angles of the vehicle. The front wheels are held straight while the rear stabilize the vehicle. Because of the coupling between the lateral and longitudinal forces, the rear tire angles are constantly changing while the ABS is working. However, oscillation is small. The tire angles also do not exceed 10° when ABS is on, but does when it is off.

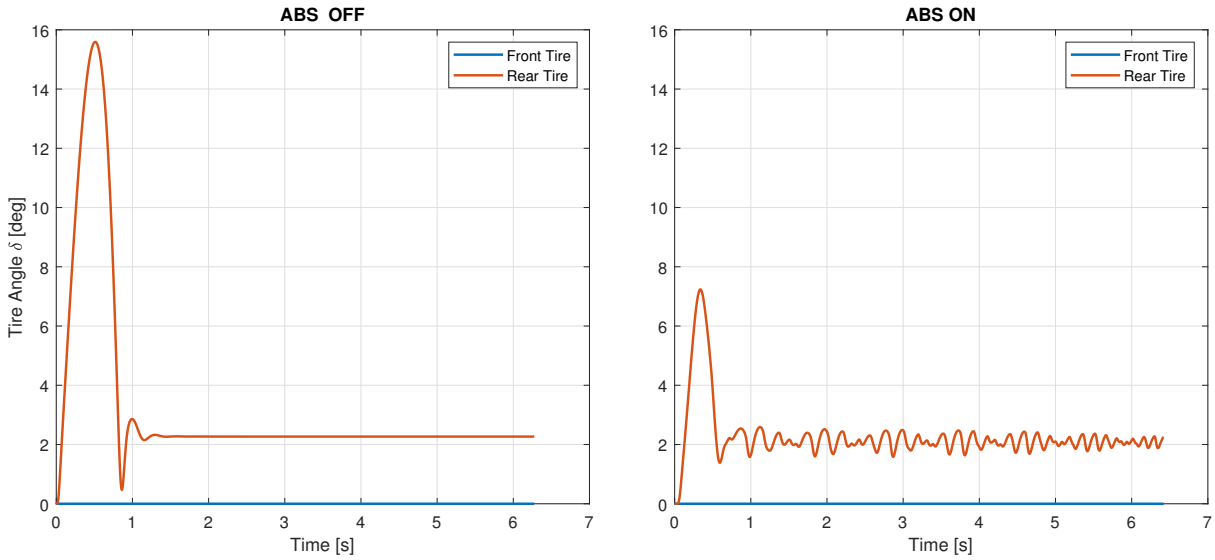

Figure 5.12: Tire angles with RWS on split-μ.

Because of the braking, the vehicle pitches forward and causes a normal force variation. Since this simulation assumes an algebraic relationship, the vehicle does not really pitch forward, but does have the normal force effects. This can be seen in Figure 5.13, where the front normal forces increase while the rear decrease. The rear does lose grip capabilities due to the normal force variation. However, it still has enough normal force to correct the yaw rate of the vehicle.

Finally, Figure 5.14 and Figure 5.15 show the force vs slip curves of each wheel. Its clear that without ABS, the longitudinal tire forces of the right side settle on a final value with a slip of zero. This causes the lateral forces of the right side to have near zero capability. The high friction left side has enough tire grip to make up for the loss. With ABS on, lateral tire forces are possible on the right side. Therefore, the left side does not need as large slip angles.

In conclusion, RWS is capable of correcting the yaw rate of a vehicle on a split-μ

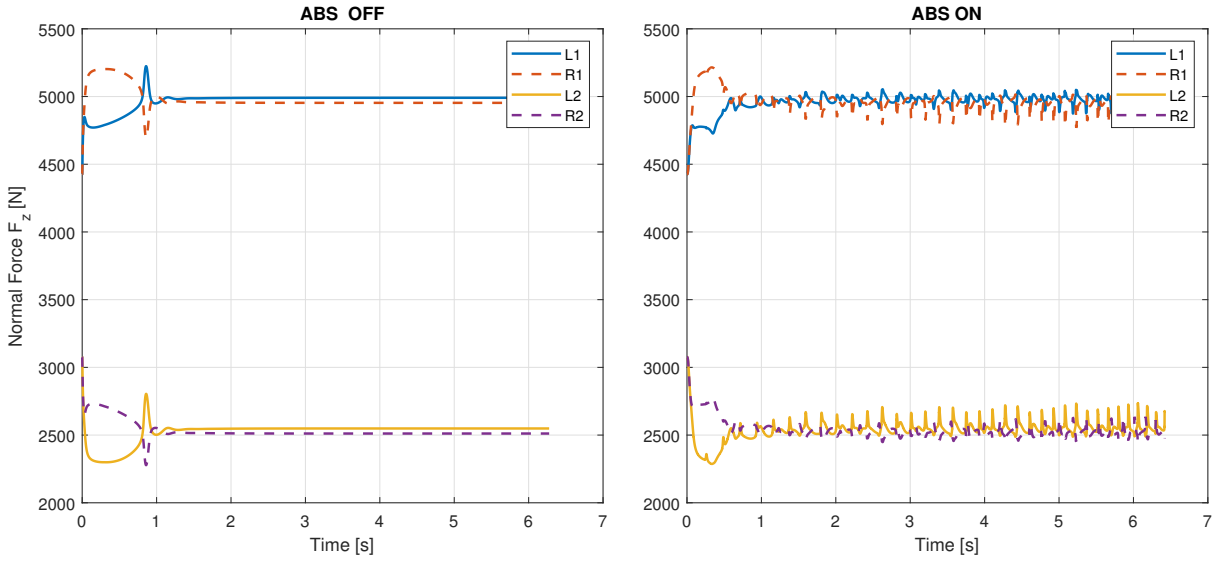

Figure 5.13: Normal Forces with RWS on split-μ.

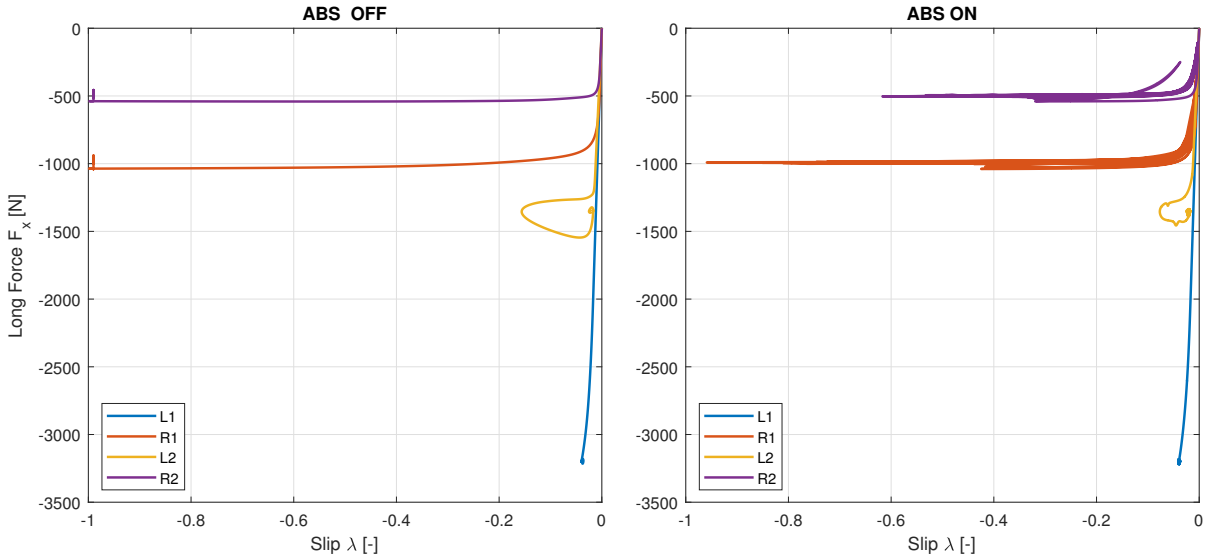

Figure 5.14: Longitudinal force vs slip with RWS on split-μ.

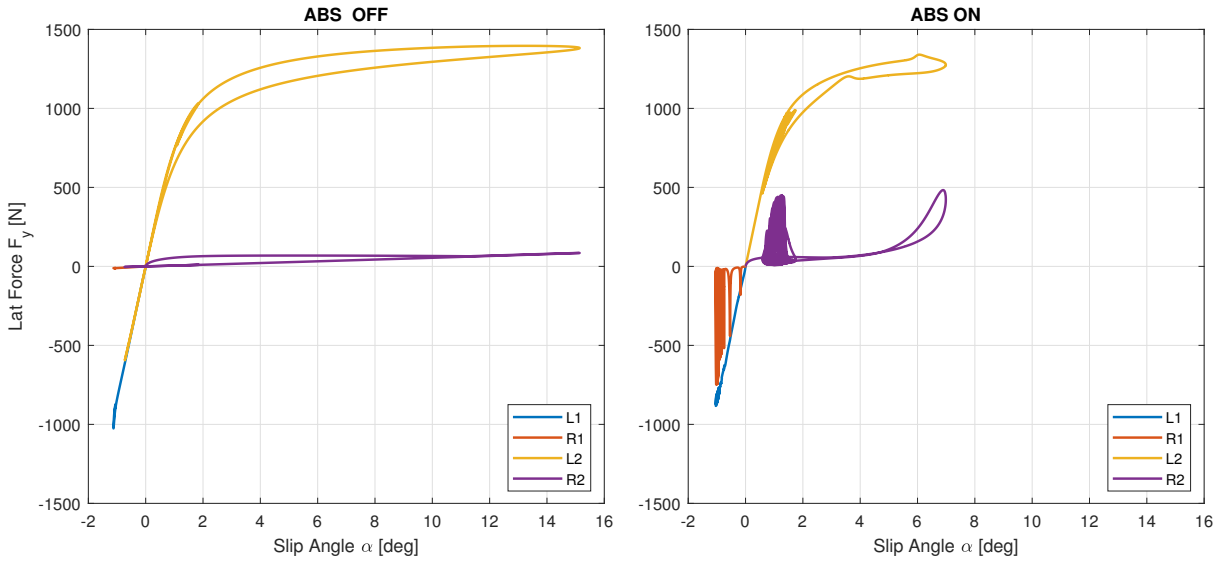

Figure 5.15: Lateral force vs slip angle with RWS on split-μ.

environment. It is also capable of working better with ABS on. However, the ABS causes the RWS to keep responding to the the quick oscillation that occur, which may be disconcerting.

5.3 Randomized Split-μ

In order to push the study further, a test condition is proposed where the split-μ condition is randomized. While the vehicle travels, it will randomly hit a patch of low-μ friction on either side of the vehicle. The randomizer does not allow both tires to have low friction, but it does allow both to have high friction. The seed of the randomizer is kept constant so that each run hits the same sequence of high and low friction patches. Every 12 ft(3.6m), the friction can randomly change. The simulations are run on the specific environment shown in Figure 5.16. This was selected because the system with RWS turned off is not unstable. Increasing the patch length leads to a spin out, while the system with RWS can still operate.

It can be seen that after the front tire hits the patch, the rear hits the patch after the vehicle travels the length of its wheelbase. Since the low friction patches are distance dependent, the vehicle spends less time on each patch at the beginning of the simulation as it has a higher speed.

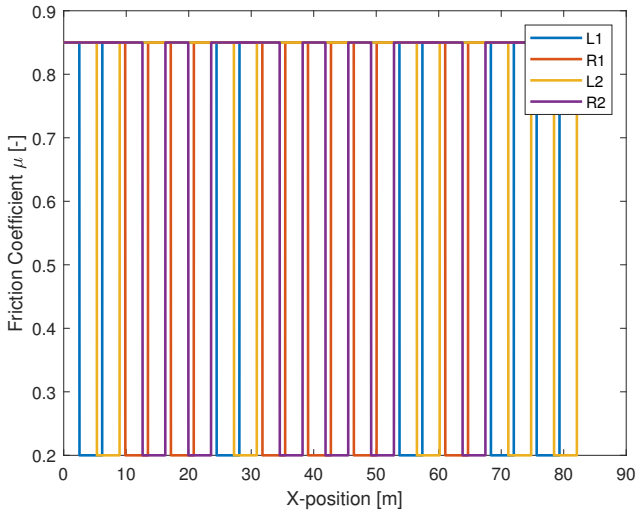

Figure 5.16: Friction patches.

When simulated without ABS, the wheels on both sides of the vehicle lock up. Therefore, the simulations in this section use ABS. Two cases are compared, one with RWS on and one with it off.

The same stabilizing controller is used as before, and the vehicle begins from a speed

of 100 km h^{-1} with the same braking behavior applied. The steering wheel is kept at zero for the duration of the test.

Figure 5.17 shows the yaw rate response. Without RWS, the system generates large yaw rates. When the patches of low friction are made longer, the vehicle eventually goes unstable. However with RWS turned on, the rear wheels keep the yaw rate close to zero, within 4° s^{-1}.

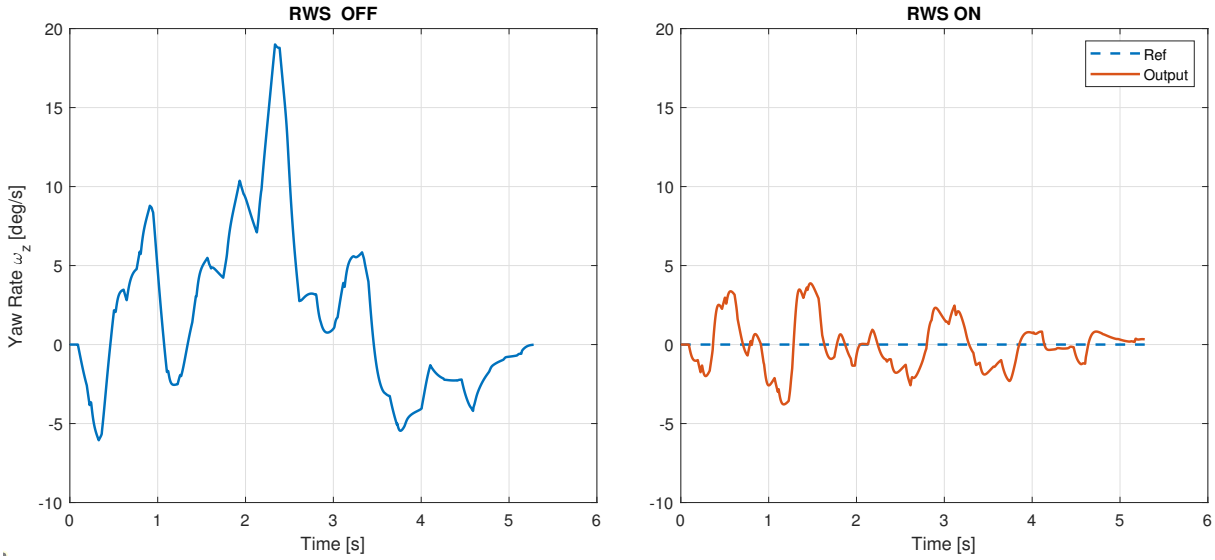

Figure 5.17: Yaw rate response with ABS on random patches of split-μ.

The system without RWS is observed to generate large yaw rates and, as a consequence, large lateral accelerations as seen Figure 5.18. RWS keeps the lateral acceleration relatively small.

Figure 5.19 and Figure 5.20 show the wheel responses and torques. The ABS performs nearly identically regardless of whether RWS is on or off.

The tire angles shown in Figure 5.21 shows RWS working within 3° to keep the yaw rate near zero, which is a reasonable range for the actuator.

Figure 5.22 shows the normal forces. With RWS, the normal forces are similar to the simulations in the previous section. However without RWS, the system generates large yaw rates and lateral accelerations. This translates to normal force variations laterally, as observed in the plot.

The normal force variation also shows up in the force-slip plots in Figure 5.23 and

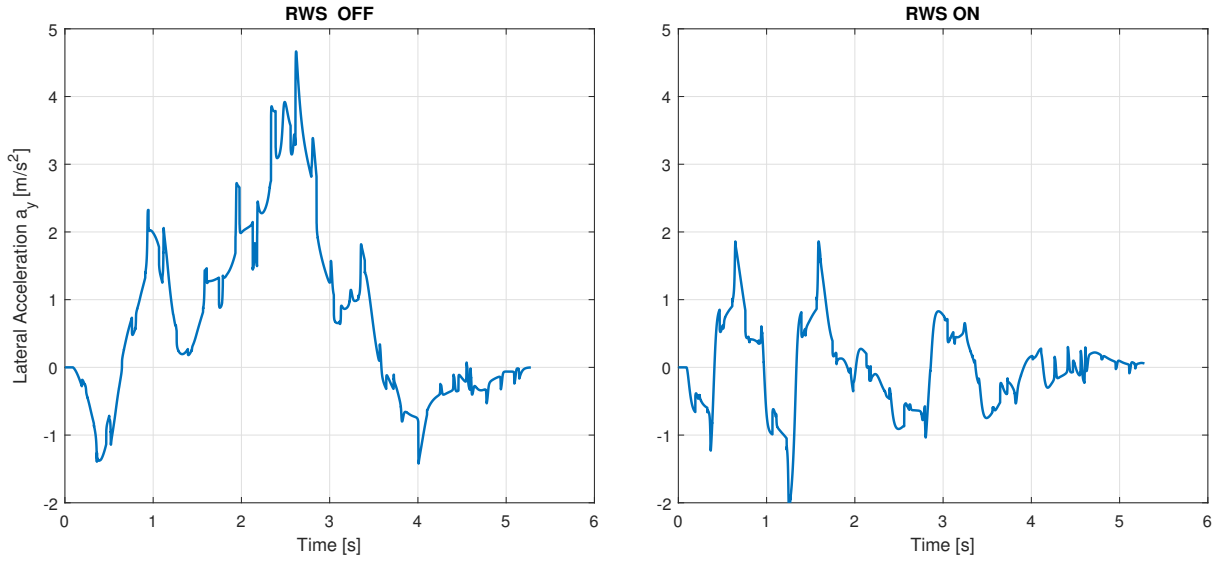

Figure 5.18: Lateral Acceleration response with ABS on random patches of split-μ.

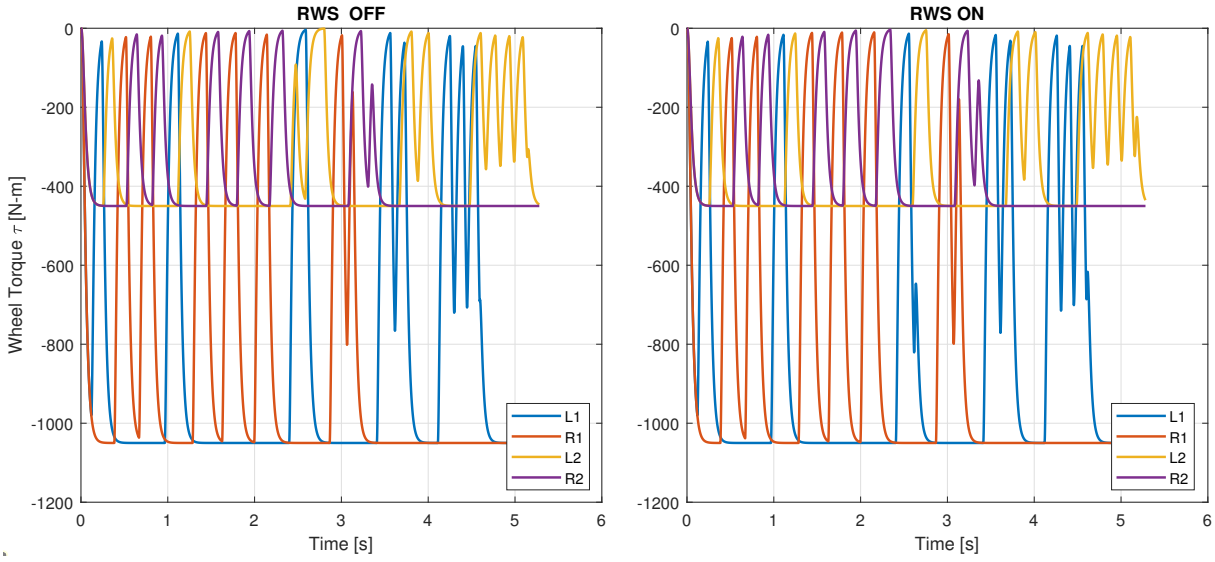

Figure 5.19: Torque response with ABS on random patches of split-μ.

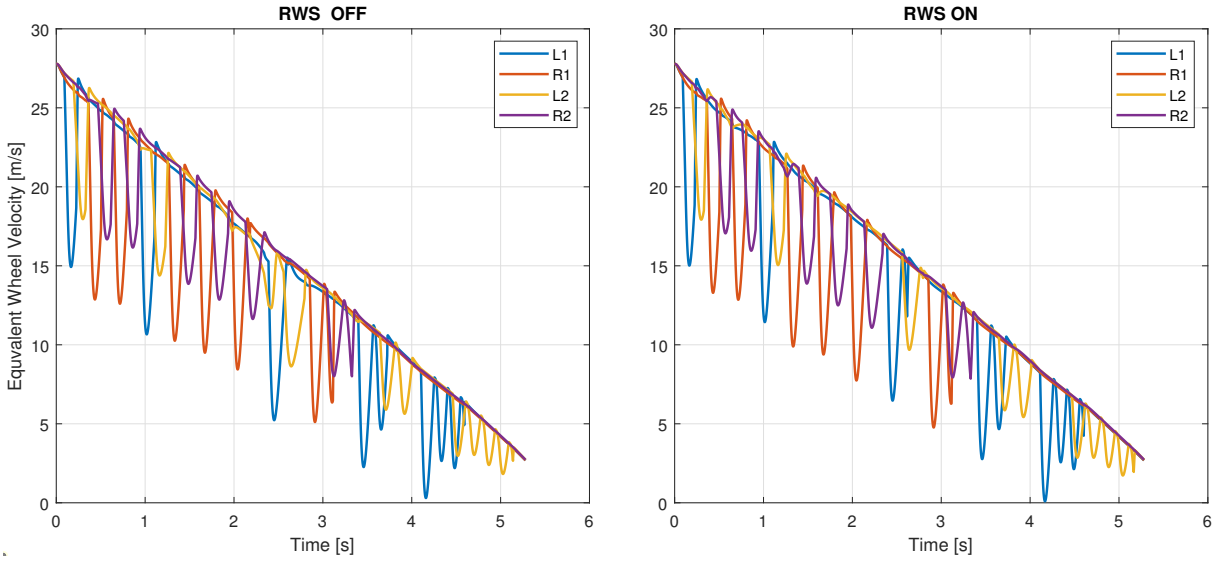

Figure 5.20: Wheel Speed response with ABS on random patches of split-μ.

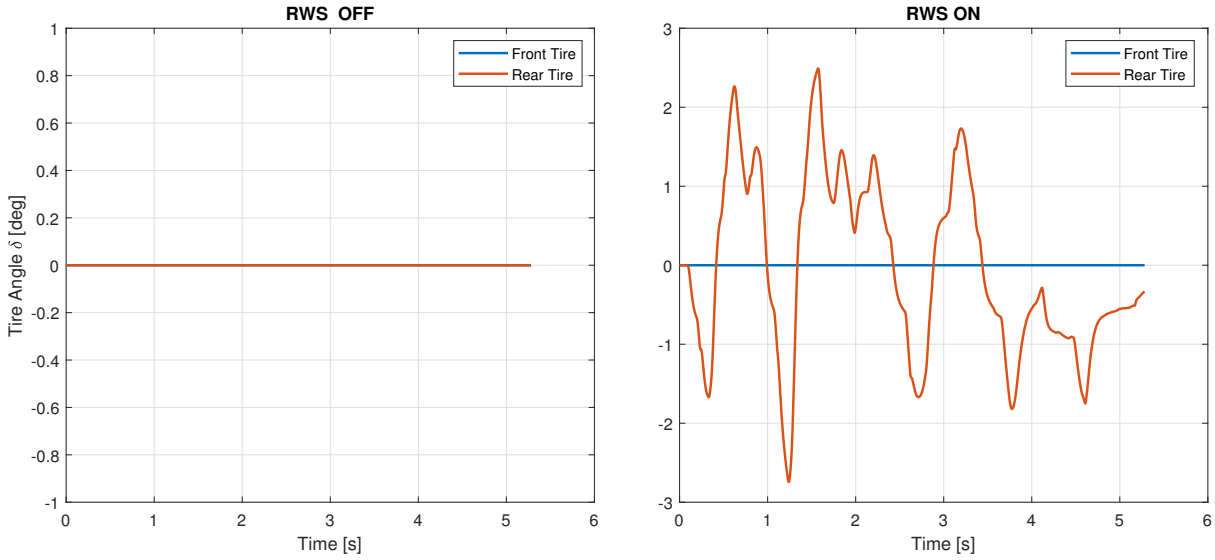

Figure 5.21: Tire angles with ABS on random patches of split-μ.

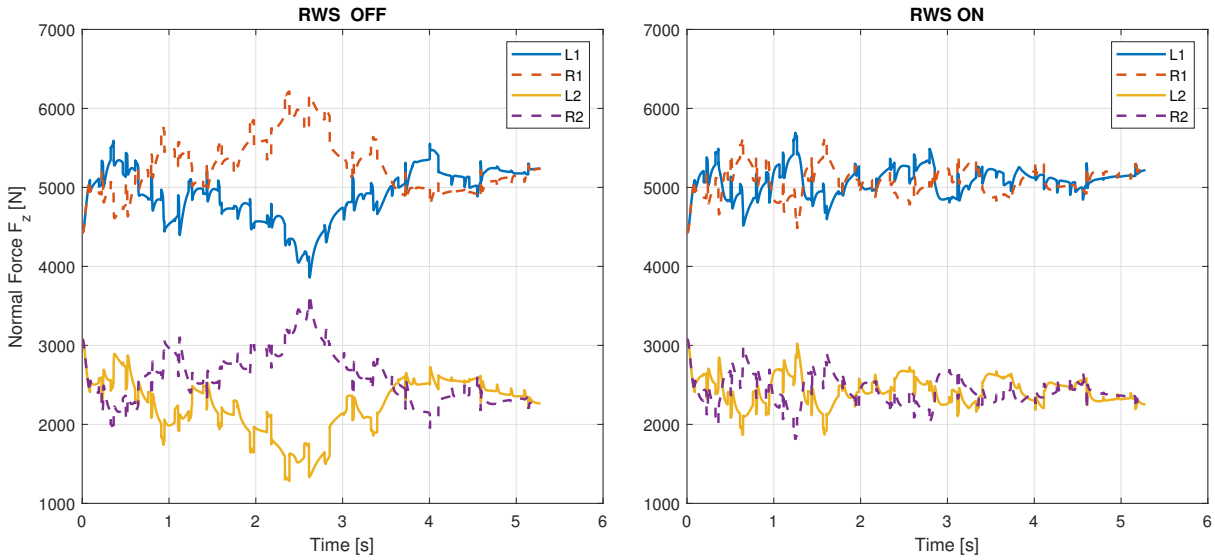

Figure 5.22: Normal Forces with ABS on random patches of split-μ.

Figure 5.24. Without RWS, there are large variations in how much lateral forces each tire can make. With RWS on, the system is more predicable in the forces it can generate.

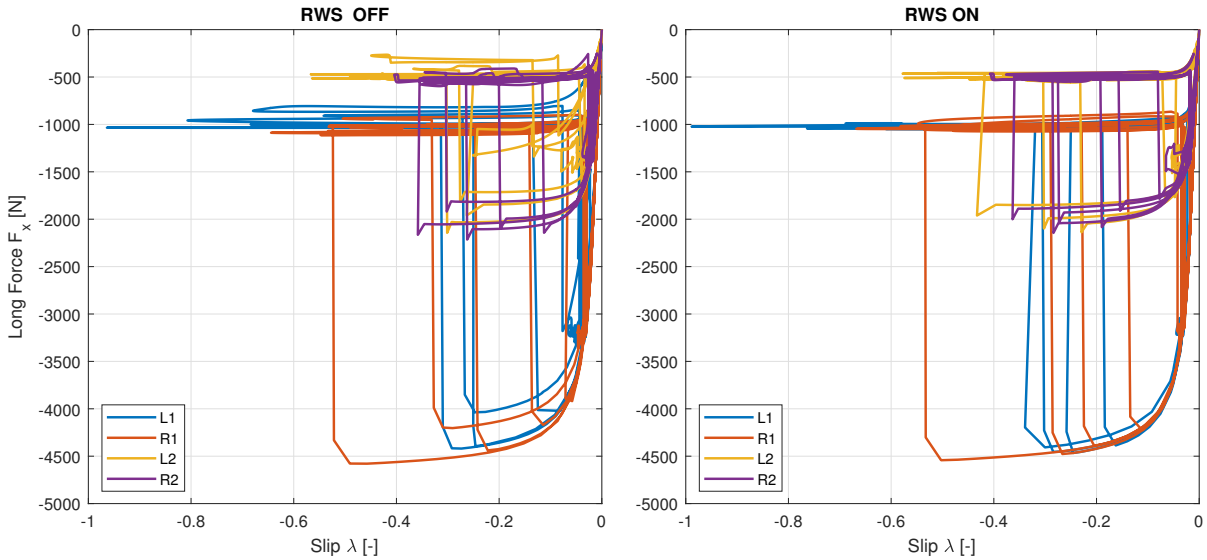

Figure 5.23: Longitudinal force vs slip with ABS on random patches of split-μ.

5.4 Conclusion

To conclude, it is shown that RWS has the capability to stabilize the vehicle in a variety of situations. The two main environments are the application of a stabilizing controller

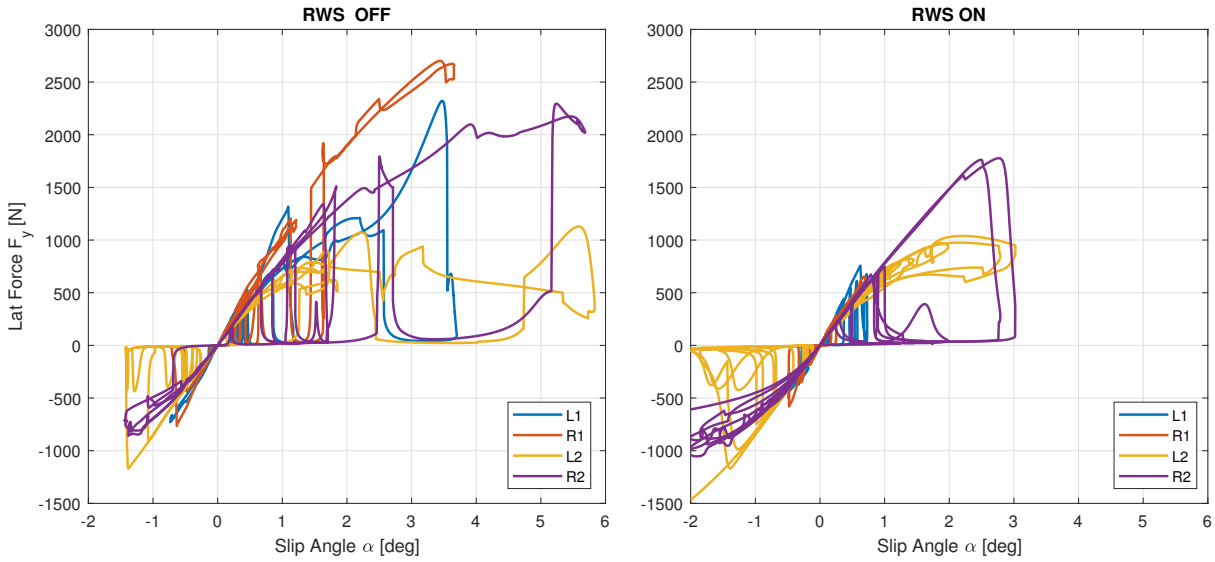

Figure 5.24: Lateral force vs slip angle with ABS on random patches of split-μ.

on an inherently unstable vehicle, and to help support a driver in split-μ condition. The system is shown to keep the intent of the driver and thus drive straight. Additionally, the same controller with the same tuning is applied in all of the simulations showing how robust it can perform to changes in the rear tire coefficient and the forward speed. It can also work with ABS on.

Chapter 6

Integrating RWS with ESC

Having explored RWS for stability in the previous chapter, a reasonable next step is to compare it to a standard in stabilization. The de-facto stabilization method for vehicles is electronic stability control (ESC), which strategically uses the brakes to apply a yaw moment on the vehicle in order to correct its motion. A review of ESC can be found in Section 2.3.

The literature discusses the range of operation best suited for each actuation method. RWS is typically placed in the low to medium handling range, while the use of the brakes is best at the extreme handling conditions. One paper [66] has looked at comparing RWS and ESC. The purpose of the work presented here is to explore improvements to stabilization by incorporating RWS in conventional ESC. Its feasibility is explored.

6.1 Model

The test procedure used to validate the systems is a handling test that causes an uncontrolled vehicle to spin out. The maneuver takes the vehicle to the limits of handling. With such an extreme handling test, many modes and different parts of the vehicle may be excited or affected. Therefore, a high fidelity modeling software is used. The vehicle model used is a class-D sedan from CarSim.

6.2 NHTSA Procedures

In order to compare results of the different actuation methods, a test procedure that is simple to reproduce and challenges the stability of the vehicle is necessary. The procedure used here is the FMVSS126 ESC certification test, which is used to verify that a vehicle's ESC system meets a standard set by the National Highway Traffic Safety Administration and the U.S. federal government. This is an open-loop test that does not require a driver or driver model, just an input to the steering wheel.

Given that the steering has compliance, the steering rack has nonlinearities and other modeling considerations, the NHTSA guidelines are followed in order to generate the correct lateral acceleration for the tests. The procedure for this is a slowly increasing steer (SIS) maneuver, which is used to determine the steering wheel angle labeled as $\delta_{0.3g}$. $\delta_{0.3g}$ is the angle that produces a lateral acceleration of 0.3 g at 50 mph.

$\delta_{0.3g}$ is then used for calculating the steering input for the maneuver in the test, which is a sine with dwell maneuver at 50 mph. The sine wave input is at a frequency of 0.7 Hz, and the dwell lasts 500 ms. The shape of the input is shown in Figure 6.1. The steering amplitude is incremented by $0.5*\delta_{0.3g}$ up to a maximum of $6.5*\delta_{0.3g}$ or 270°, whichever is greater.

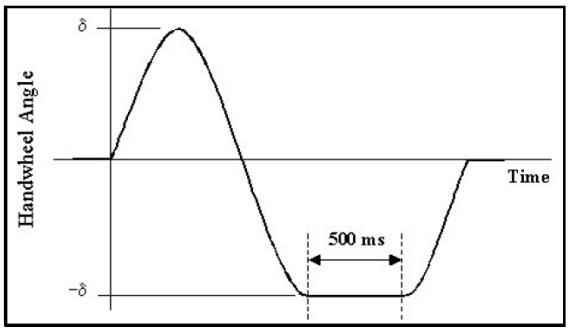

Figure 6.1: Steering input for the define sine with dwell test.

There are some metrics used to assess a vehicle's lateral stability and responsiveness criterion. Two important metrics are the yaw rate threshold and lateral displacement. The yaw rate threshold is the ratio between a yaw rate at some moment in time and a peak yaw rate. The peak yaw rate value used for the threshold is defined as the first local

yaw rate peak produced by the reversal of the steering wheel. The two important points in time defined for the test are 1.0 and 1.75 seconds after the completion of the sine with dwell tests. Satisfaction of yaw rate thresholds is defined as follows:

$$\frac{\dot{\Psi}_{(t_0+1.00)}}{\dot{\Psi}_{Peak}} \times 100 \leq 35\%$$
$$\frac{\dot{\Psi}_{(t_0+1.75)}}{\dot{\Psi}_{Peak}} \times 100 \leq 20\%$$

The responsiveness criterion measures the ability of a vehicle to respond to the driver's inputs during an ESC intervention. The criterion is defined as the lateral displacement of the C.G. with respect to the straight line before the steering input. It is satisfied if the following is true

$$\int_{t_0}^{t_0+1.07} \int_{t_0}^{t_0+1.07} A_{y_{c.g.}}(t) dt' dt \geq 1.83m$$

for a vehicle less than 3,500 lbs. Otherwise, the lateral displacement minimum is 1.22 m. The double integral of the lateral acceleration signal is not the true displacement, but an approximation. The reason for using this metric instead of the true displacement is that the alternative would require using G.P.S. measurements which adds costs and time to the test. The short integration time has good agreement with tests using G.P.S. information.

These metrics and criteria are examined on the sine with dwell test with the highest steering amplitude input allowed. Other details are also looked at such as whether the tire lifts off the ground. These are also monitored during the simulations.

6.3 ESC design

The description of a conventional ESC control algorithm for oversteering vehicles is as follows. When the rear of the vehicle begins to slide out, the system detects the heading is changing faster than appropriate for a driver's intended path (high yaw rate). It momentarily applies the outside front brake to apply a corrective yaw moment. This is demonstrated in Figure 6.2

A practical implementation is presented in [66] which uses equations by Robert Bosch GmbH for development of the ESC. The desired yaw rate of the driver based on the

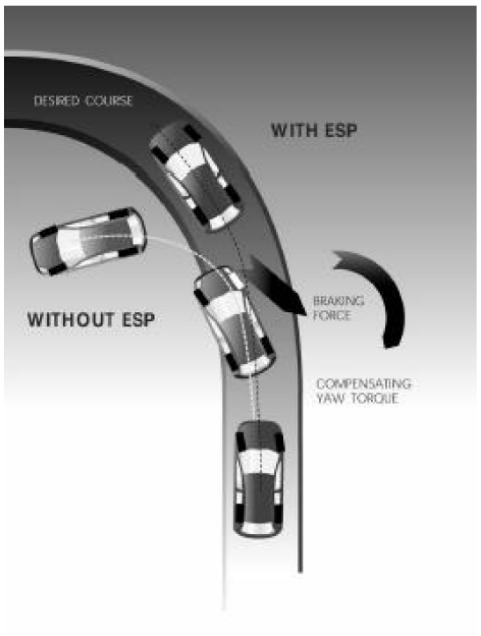

Figure 6.2: Oversteering example from [62].

steering input is defined as

$$\dot{\Psi}_{des} = \delta_f \frac{v_{x0}}{L(1 + Ku_0^2)} \tag{6.1}$$

$$K = \frac{m}{L^2}\left(\frac{b}{C_f} - \frac{a}{C_r}\right) \tag{6.2}$$

where the desired yaw rate speed needs to be limited base on the road friction.

$$|\dot{\Psi}_{des}| \leq \frac{\mu_y g}{v_{x0}} \tag{6.3}$$

Using the same steady-state bicycle model equations, the desired body slip is

$$\beta_{des} = \delta_f \frac{b}{L(1 + Kv_{x0}^2)}\left(1 - \frac{mav_{x0}^2}{bLC_r}\right)$$

An empirical formula is used to ensure that the slip angle does not exceed the friction limits. This is as follows:

$$|\beta_{des}| \leq \arctan(0.02 * \mu_y * g)$$

The control system used here is a proportional controller which uses a combination of

the states to produce the braking torque. This is defined as

$$C_{ESC} = K_{ESC,\dot{\Psi}}\ e_{\dot{\Psi}} + K_{ESC,\beta}\ e_{\beta}$$
$$e_{\dot{\Psi}} = \dot{\Psi}_{des} - \dot{\Psi}$$
$$e_{\beta} = \beta_{des} - \beta$$

Finally, a dead zone is defined in order to have the ESC turn on at appropriate times. The simplest is $|e_{\dot{\Psi}}| > D_{\dot{\Psi}}$, where it turns on when the yaw rate error exceeds the predefined choice $D_{\dot{\Psi}}$.

6.3.1 ESC Design Adapted From Literature

For the simulations presented here, only the yaw rate will be considered for the control logic. Therefore, only Equations 6.1, 6.3, and the dead zone are considered. The feedback will only use the yaw rate error and a proportional gain.

First, the model reference accesses the steering angle and forward velocity of the vehicle. The desired yaw rate is limited by the friction of the road which is assumed to be known. An example of this saturation can be found in Appendix A.

Without taking into account the limitations of the road, the yaw rate reference would request a yaw rate that is not possible. An easy fix to this would be to implement a saturation of the braking torque request, which would certainly exist in a real system. This would work well for a proportional controller in lieu of the yaw reference limiter. However, if a more advanced controller with dynamics was implemented, saturation of the actuator downstream could make the system unstable.

Next, the controller is defined with a dead band. An example can be found in Appendix A. For now, the system only corrects oversteering tendencies. Using counter-clock wise as positive, if the vehicle oversteers in a left hand turn, the yaw rate error would be a negative value. However if the vehicle oversteers in a right hand turn, the error would be positive value. This is taken into account by adding a negative sign to the braking torque in one of the conditions. In addition, the wheel torques are not allowed to be positive since only braking torques are used in this system.

6.3.1.1 Oversteer and Understeer Considerations

The NHTSA guidelines define ESC as a corrective measure for oversteering. Understeering correction is defined as part of ESC as well, but does not specify any understeering performance criteria because of the difficulty of implementing a repeatable test to exhibit this phenomenon. A separate algorithm that includes understeering is created separately for consideration and can be found in Appendix A. This uses the rear brakes for the understeering correction.

6.3.2 Model Reference

The conventional description of ESC in the literature uses an algebraic relationship between the steering wheel angle and the desired yaw rate. This works fine when ESC activates briefly when the deadband threshold of the yaw rate error is crossed. The brakes can be activated very quickly to engage and disengage. However, considering the dynamics of RWS and the vehicle, it is not useful to subject RWS to an algebraic model reference. RWS can be on at all times since it does not slow the vehicle like ESC. Attempting to activate RWS like ESC for a brief moment also is not useful, since it does not have the same bandwidth capabilities. The final consideration is that RWS's main secondary effect is on the lateral acceleration, unlike ESC which has a large effect on the longitudinal acceleration. An instantaneous change in lateral acceleration can be unsettling to the driver, just as ESC can be in the longitudinal direction.

Taking these thoughts into consideration, in order to implement both systems fairly, the model reference used is a dynamic bicycle car model which will saturate its outputs similar to the conventional ESC implementation. This outputs a reference yaw rate that the rear wheels attempt to track at all times when RWS is used. ESC activates only when it must: when the yaw rate error exceeds a threshold. This allows both systems to operate to their full capacity in their proper domain without stifling either system's ability. In this way, RWS acts to prevent activation of ESC until the deadband of the ESC is crossed. Since RWS is on at all times, it is attempting to correct for oversteering and understeering at all times. Depending on which version of ESC is being used, it will correct only oversteering or for oversteering and understeering.

6.4 RWS Controller Design

The same controller design approach is taken as discussed in Section 5.1.1. The only difference is that the nominal stable vehicle is considered rather than an unstable vehicle.

One important consideration in the design is the saturation of the RWS actuator. Preliminary testing done with both ESC and this controller design indicates that windup of the integral control component can be an issue. Therefore, some design choices are required. Literature surrounding anti-windup techniques and applications are almost exclusive to PID controllers. The integrator term of a PID in parallel form can be accessed directly such that the integrated error can be manipulated.

A Youla designed controller is created which has the same number of poles and zeros as a PID with an added low pass filter on the derivative term. Therefore, it is proposed to put the stabilizing controller in the PID form in order to use well established antiwindup techniques.

The PID can be described in the following form

$$K_{PID} = k_P + \frac{k_I}{s} + k_D \frac{s}{\frac{1}{N}s + 1} \tag{6.4}$$

$$= k_P + \frac{k_I}{s} + k_D \frac{Ns}{s + N} \tag{6.5}$$

$$= \frac{(k_P + k_D N)s^2 + (k_I + k_P N)s + k_I N}{s^2 + Ns} \tag{6.6}$$

The original stabilizing controller can be represented as follows:

$$K(s) = \frac{a_2 s^2 + a_1 s + a_0}{s^2 + b_1 s} \tag{6.7}$$

Setting Equation 6.6 equal to Equation 6.7, the PID terms can be derived as follows:

$$N = b_1$$
$$k_I = \frac{a_0}{N}$$
$$k_P = \frac{a_1 - k_I}{N}$$
$$k_D = \frac{a_2 - k_P}{N}$$

Matlab offers two antiwindup approaches based on the suggestions from [87]: back-calculation and clamping. Back-calculating uses the difference between the output of the controller before and after the saturation to feedback to the error signal going into the integrator term. This can be seen in Figure 6.3. This also uses a tuning gain for determining the rate at which the integral term resets. The suggested choice is usually either equal to the integrator term k_I or a combination of the integrator term and derivative term $\sqrt{k_I k_D}$.

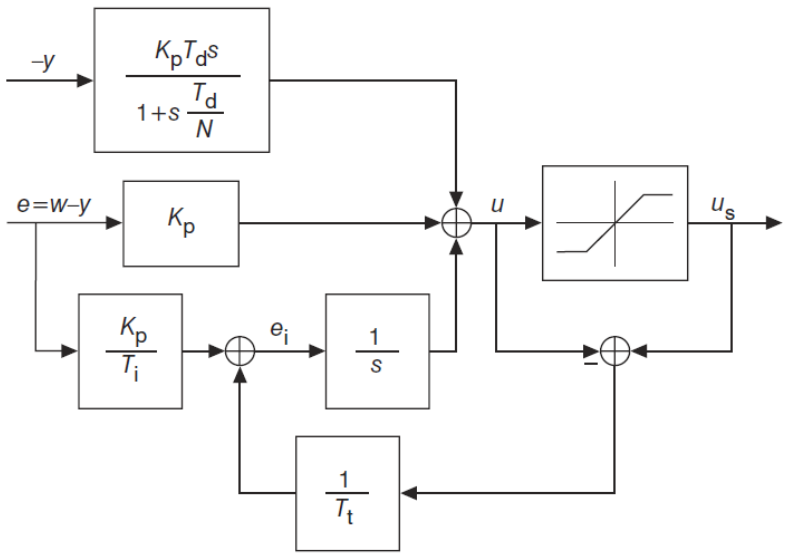

Figure 6.3: Back-calculation approach for antiwindup [87].

The second method, clamping (also known as conditional integration), uses logic to determine when it can increase the integral term or keep it constant. There are multiple methods of application, but Matlab evaluates whether the actuator is saturating ($u \neq u_s$) and if the error and controller output have the same sign ($e \times u > 0$). If both conditions are met, then the integration is stopped. For this particular implementation, the simulation halted due to zero-crossing detection. This is Simulink's technique to improve run time, but can cause some simulations to halt before completion. This is on by default and is turned off in this instance.

In addition, a controller without an integrator term is explored.

6.4.0.1 Proportional Controller

An alternative to the controller design using Youla is to forgo tracking. A proportional controller tuned appropriately to match the bandwidth of the previous controller is proposed. Since there is no tracking ability with just a proportional controller, the approach for the control design is to design the system with a bandwidth similar to the Youla derived controller. A prefilter is added before the control loop to increase the reference input and have near zero steady-state error. Without an integrator there should not be any windup concerns. Figure 6.4 shows the bode diagram of the closed-loop responses which results in the desired design. A step response shows the that although the tracking is removed, the prefilter makes up for the steady state error and gives a good response.

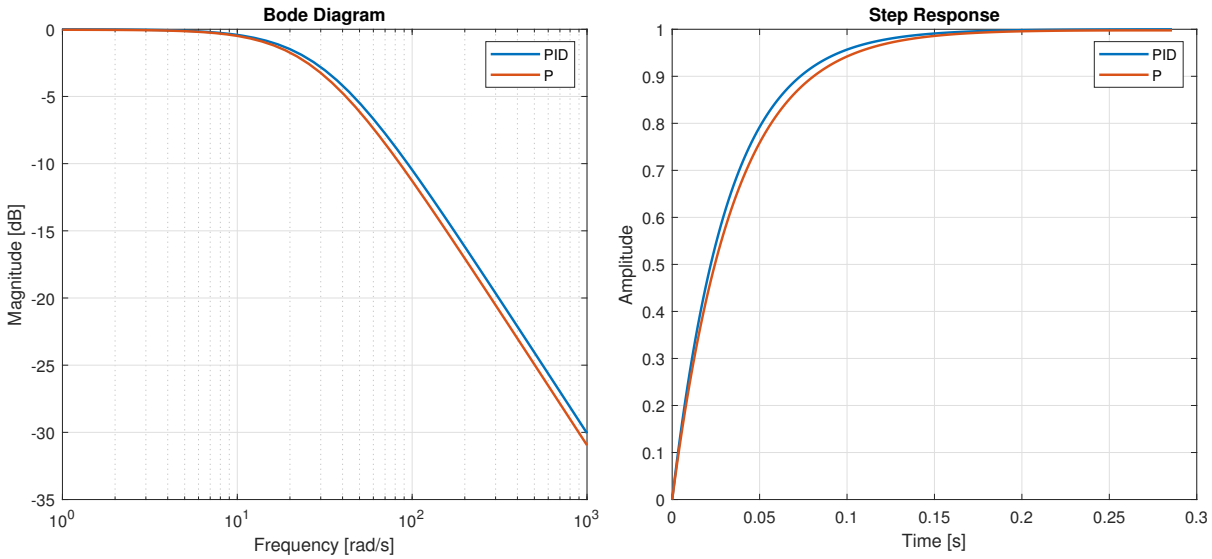

Figure 6.4: Closed loop transfer function and step response of PID and P controlled systems.

6.5 Simulation

The simulations are done at the maximum steering wheel input dictated by the NHTSA test guidelines, described in Section 6.2. The guidelines dictate that the sine with dwell maneuver be done at an initial velocity of 50 *mph* ($\approx 80\ \mathrm{km\,h^{-1}}$). The most important metric to monitor is how much the real vehicle deviates from the reference. This is done by comparing the RMS error of each run. The criterion described by the NHTSA are

monitored but not presented because all runs result in negligible error (less than 1%). The RMS is calculated using first 3 seconds of the simulation, since the yaw rate is at zero beyond three seconds. Another metric that needs explanation is the lowest normal force on any tire. The test guidelines require monitoring of the tires to make sure they do not leave the ground. The body slip is an important metric monitored in the literature when studying planar dynamics so this is included as well.

Four control architectures are used to compare the results. All of the architectures use ESC. The first is labeled "No RWS." This only uses ESC to correct the yaw rate of the vehicle. The second, "Conventional," uses the widely used method of controlling the rear wheels with ESC. The rear steers as a function of the front wheels through a lookup table. The lookup table accesses the front tire angle and forward speed to determine the rear steering.

"Antiwindup" is the PID controller designed with the clamp method of antiwindup in conjunction with ESC. Finally, the "Proportional" controller is the controller discussed in the previous section with ESC.

The first simulation is a vehicle without any active controls, shown in Figure 6.5. This results in the simulation ending early because the heading angle exceeds 90°. The yaw rate stays excessive after the first second of simulation, causing the vehicle to spin out. This demonstrates the difficulty of keeping the vehicle under control after the steering input crosses zero and reaches the dwell part of the test.

6.5.1 Oversteering Correction

The first test uses only the oversteering correction aspect of ESC for the brakes. The yaw rate, lateral acceleration, and rear wheel responses are shown in Figure 6.6 and Figure 6.7, respectively.

Important metrics for the response of the vehicle are shown in Table 6.1. The RMS error e_{RMS} is larger for a vehicle without RWS and only ESC. This is expected because there is a deadband that must be exceeded before ESC is activated. The system also ends with the lowest forward velocity, indicating that more braking was performed for yaw correction, thus slowing the vehicle.

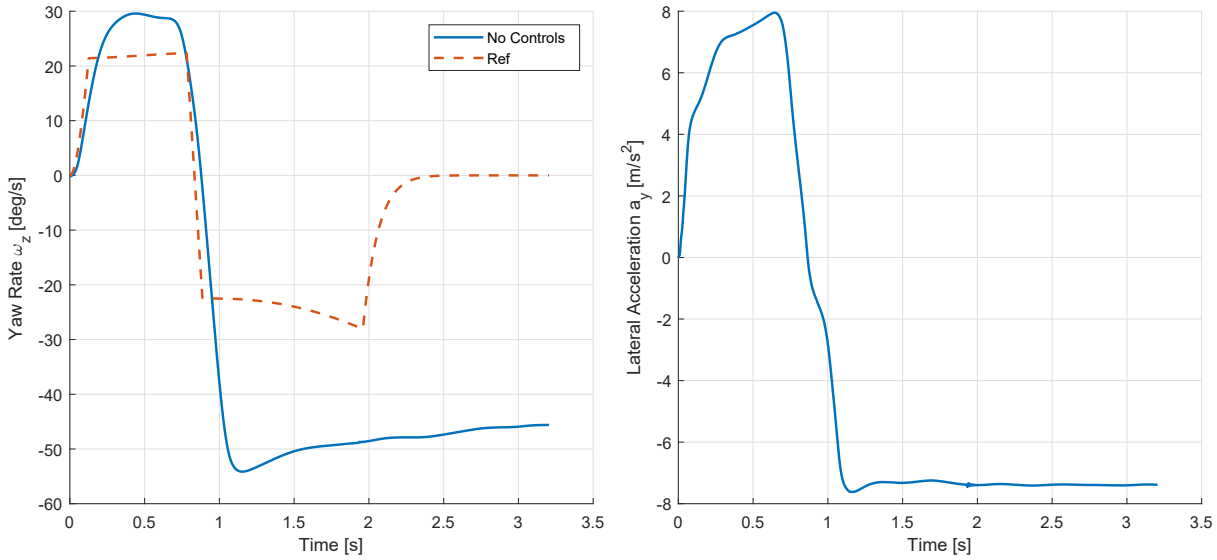

Figure 6.5: Yaw rate and lateral acceleration response for the uncontrolled vehicle (Initial $v_x = 50\ mph$).

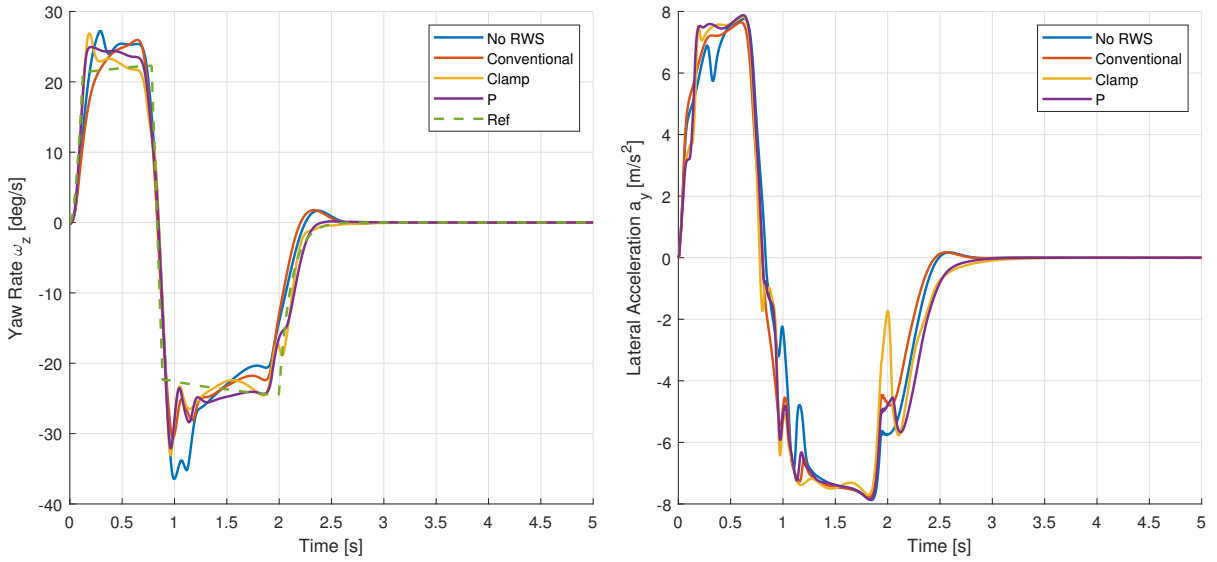

Figure 6.6: Yaw rate and lateral acceleration response with ESC oversteering correction only (Initial $v_x = 80\ \mathrm{km\,h^{-1}}$).

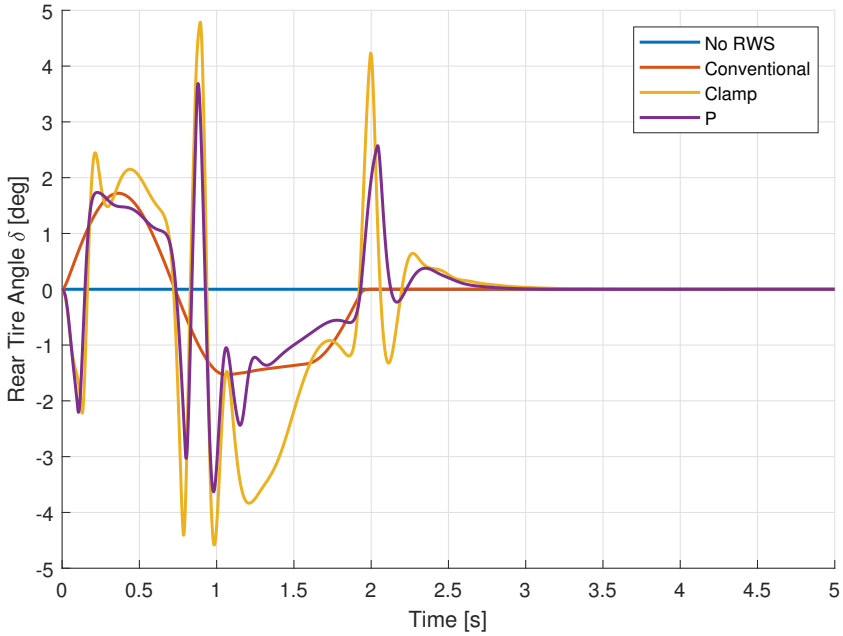

Figure 6.7: Rear tire angle response with ESC oversteering correction only (Initial $v_x = 80\ \mathrm{km\,h^{-1}}$).

Table 6.1: Vehicle metrics.

Control Type	$e_{RMS}[^\circ\,\mathrm{s}^{-1}]$	$v_{x-final}[\mathrm{km\,h}^{-1}]$	$N_{min}[\mathrm{N}]$	$\beta_{max}[^\circ]$
No RWS	4.56	64.8	780	4.37
Conventional	3.60	68.1	688	3.22
Antiwindup	2.82	66.0	237	3.72
Proportional	2.77	67.5	278	3.88

The best response appears to be done by the proportional controller, which has the lowest e_{RMS} and the highest final velocity. All of the vehicles do not lose ground contact with any of the tires. Finally, there are small variations in the maximum body slip angle β_{max}. These metrics can be important to the designer depending on the design criterion.

Table 6.2 show some important metrics with regards to the actuators. The maximum rear tire angle δ_{R-max} does not reach the saturation point of the actuator, which is set to 5 °. The antiwindup controller has the largest peak power of all the systems. However, the total energy used and dissipated by both the rear-wheel steering actuator and the brakes of the vehicle show that ESC is the most wasteful. The brakes dissipate energy at

Table 6.2: Actuator metrics.

Control Type	$\delta_{R-max}[^\circ]$	$P_{peak-RWS}$[W]	E_{Total}[kJ]
No RWS	N/A	N/A	19.4
Conventional	1.72	20.4	10.8
Antiwindup	4.79	487	13.0
Proportional	3.69	313	11.6

orders of magnitude larger than the steering actuator, indicating that any reduction in brake is welcomed.

The conventional RWS actuator combined with ESC uses the least amount of energy. The system is able to keep the error within the deadband selected for more time than the other systems. This is good, but this open-loop controller does not reduce the yaw rate error like the other controllers. The proportional controller does have a comparatively low energy use compared to the conventional system.

6.5.2 Oversteering and Understeering Correction

In this section,the oversteering and understeering correction aspect of ESC for the brakes are used. The yaw rate, lateral acceleration, and rear wheel responses are shown in Figure 6.8 and Figure 6.9, respectively.

Results show that the inclusion of understeering correction in the ESC algorithm made almost all of the metrics worse for each control system, even the RMS yaw rate error. The trend however is the same as the previous simulation set without understeering correction, as can be seen in Table 6.3. Any inclusion of RWS improves the yaw rate error, the final forward velocity, and the maximum body slip angle.

The minimum normal force that the vehicle experiences, F_{z-min}, becomes smaller with the addition of RWS. This makes sense given that RWS uses lateral forces in the rear to correct the yaw rate. Larger lateral forces gives larger lateral accelerations, which can give larger roll angles and less normal force at the extremes. This should be carefully monitored in order to not make the roll of the vehicle substantially worse.

The actuator metrics in Table 6.4 also show a consistent trend. Overall the addition of

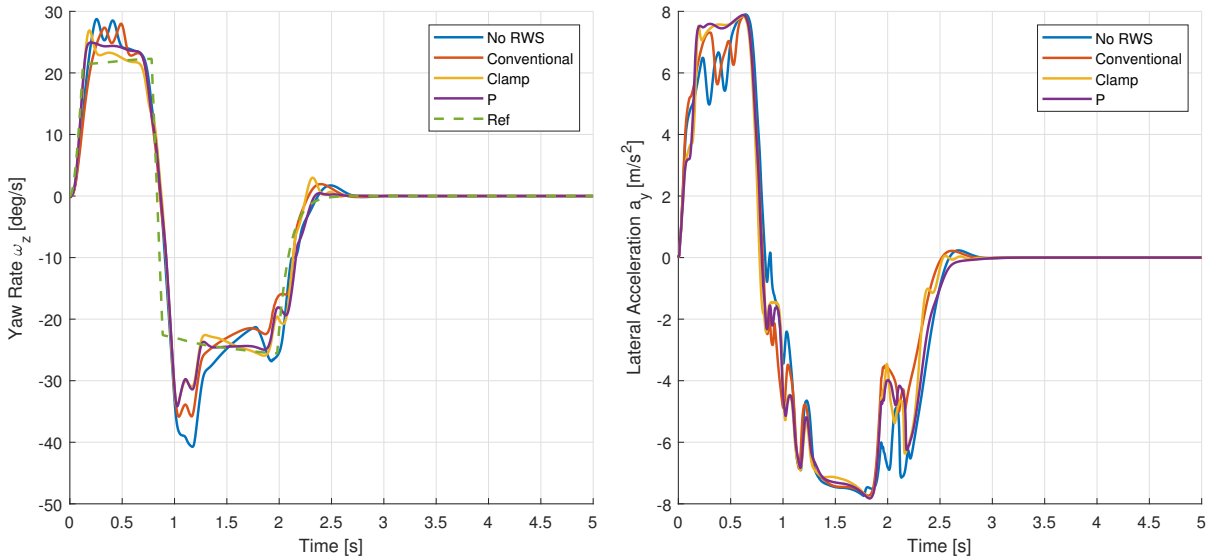

Figure 6.8: Yaw rate and lateral acceleration response with ESC oversteering and understeering correction (Initial $v_x = 80$ km h^{-1}).

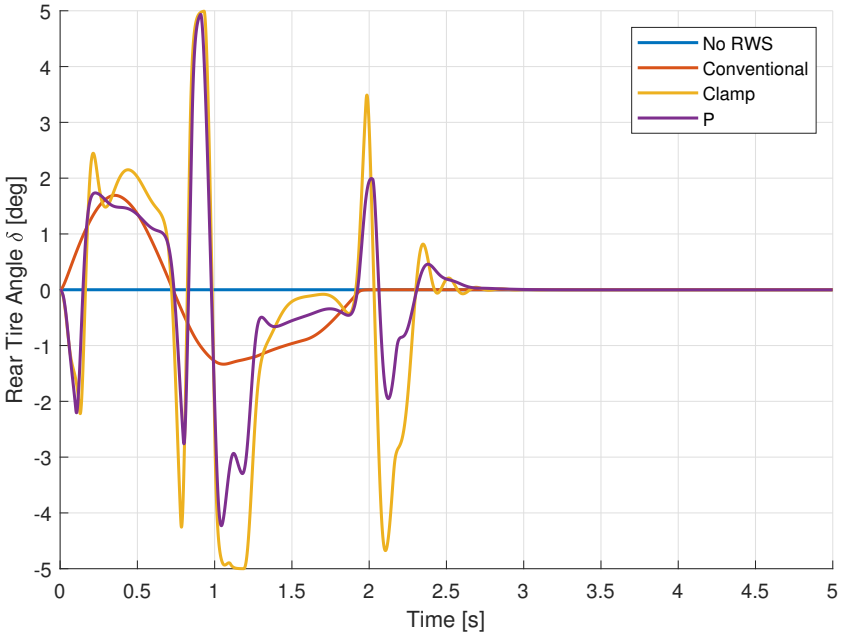

Figure 6.9: Rear tire angle response with ESC oversteering and understeering correction (Initial $v_x = 80$ km h^{-1}).

Table 6.3: Results from sine with dwell test.

Control Type	$e_{RMS}[^\circ\,\mathrm{s}^{-1}]$	$v_{x-final}[\mathrm{km\,h}^{-1}]$	$F_{z-min}[\mathrm{N}]$	$\beta_{max}[^\circ]$
No RWS	5.75	58.7	678	5.05
Conventional	5.00	61.0	531	4.39
Antiwindup	4.23	61.8	237	4.27
Proportional	4.20	62.1	278	4.42

Table 6.4: Actuation results from sine with dwell test.

Control Type	$\delta_{R-max}[^\circ]$	$P_{peak-RWS}[\mathrm{W}]$	$E_{Total}[\mathrm{kJ}]$
No RWS	N/A	N/A	51.8
Conventional	1.69	15.1	45.5
Antiwindup	5.0	297	35.9
Proportional	4.94	199	33.5

RWS to ESC improves many metrics of vehicle performance. The proportional controller has the best results overall.

Further investigation into the differences between having or not having understeering correction can be seen in Figures 6.10 and 6.11. The first plot shows the rear tire angle and the instances that the brakes come on. The second plot shows the yaw rate error and where the deadband threshold is crossed.

The biggest jump in error occurs right after the first peak of the sine wave input at around 0.8 seconds. Both systems behave identically before that time, but the rear braking is activated on the left side to correct for understeer. This causes the error to increase significantly, causing longer usage of the oversteering correction on the right front side. Right after that, the understeering correction comes on again. The understeering correction seems to make the performance worse and when coupled with RWS, causes the actuator to work a little harder.

The same type of plots are created for both ESC cases where RWS is not used, shown in Figure 6.12 and Figure 6.13. These highlight the differences in brake usage when RWS

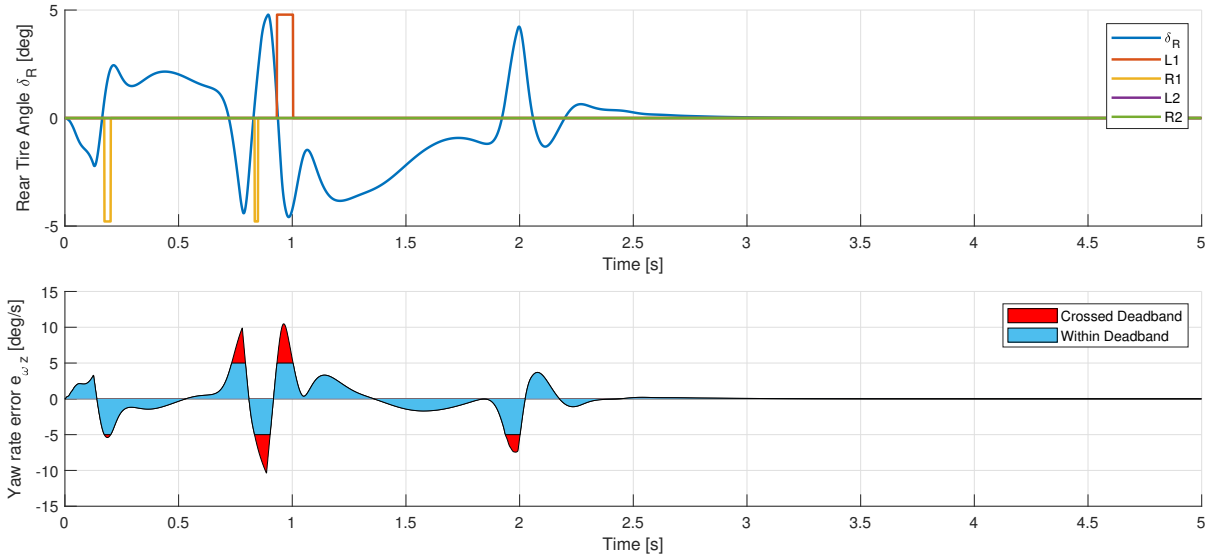

Figure 6.10: RWS and clamp PID controller with oversteering correction from ESC (Initial $v_x = 80$ km h^{-1}).

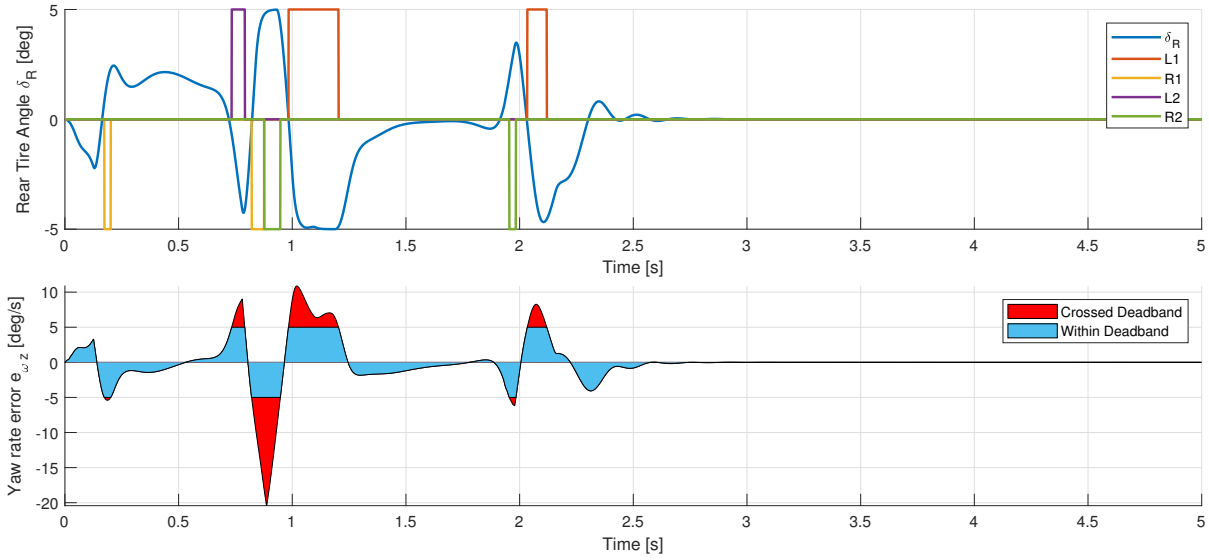

Figure 6.11: RWS and clamp PID controller with oversteering and understeering correction from ESC (Initial $v_x = 80$ km h^{-1}).

is not used. An important takeaway when comparing with and without RWS is that RWS does not cause ESC to activate any more than if the system did not have RWS at all. All activations of ESC with RWS equipped happen where the vehicle without RWS would activate anyway. This is important to note because it indicates that RWS does not cause any noticeable detriment to the system that ESC would have to fix. In fact the plots make it clear that RWS causes much less brake activation from ESC.

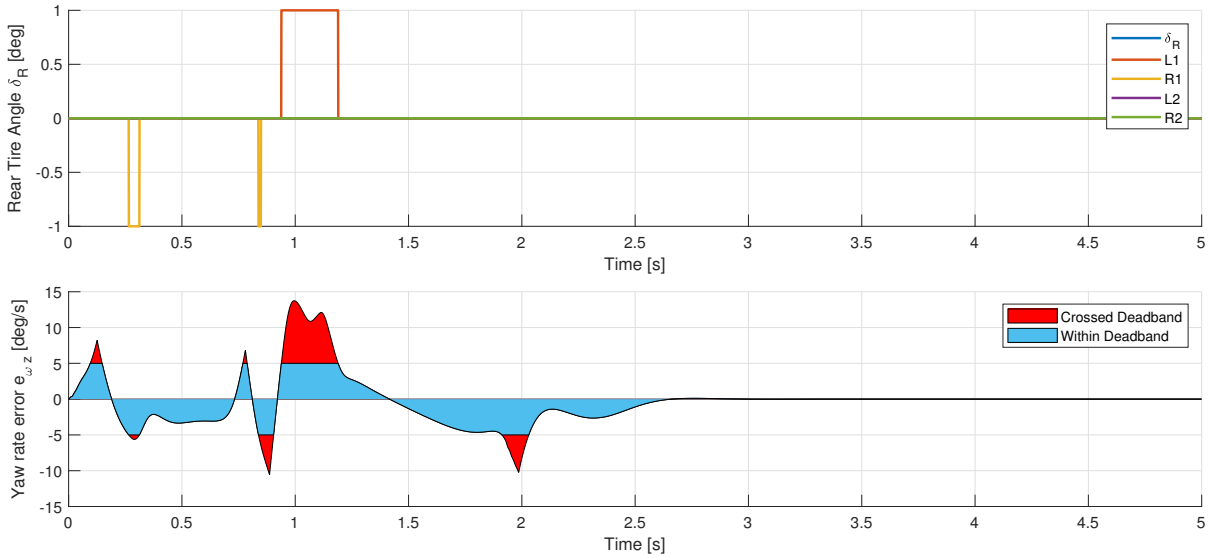

Figure 6.12: Oversteering correction from ESC only (Initial $v_x = 80$ km h^{-1}).

6.6 Conclusion

Integration of RWS and ESC was explored. RWS could be viewed in this work as a preventative measure such that ESC does not have to work as hard. In addition, the integration saves substantial energy that would be dissipated by the brakes. A simple ESC algorithm was used for brake actuation, correcting for oversteering and understeering. The brakes are equipped ABS to ensure the vehicle does not lose traction.

Many metrics were chosen to compare different combinations of RWS and ESC. In all instances, the addition of RWS improved performance in this testing procedure. However, when braking was implemented to correct for understeering, this made all of the metrics substantially worse. The results show that allowing understeering correction to be done by only RWS improves performance in the current set up and testing procedure. Since

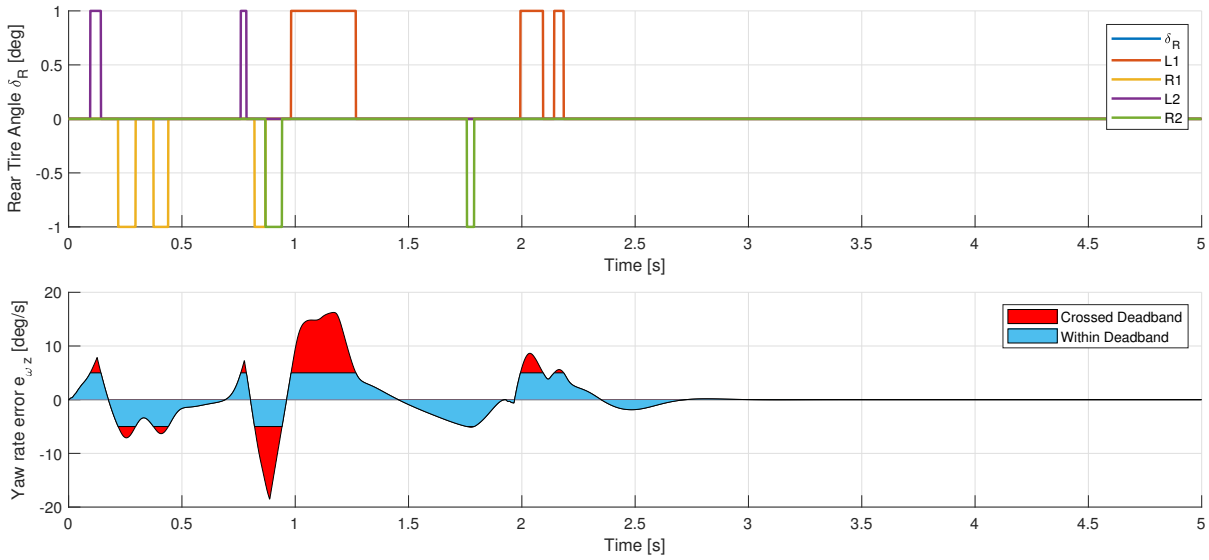

Figure 6.13: Oversteering and understeering correction from ESC only (Initial v_x = 80 km h^{-1}).

understeering correction would be done with the rear wheel brakes when using ESC, this would have interactions with RWS.

The work presented here was concerned with the response to an open-loop test scenario. However, an important metric that was not explored was the steering load, or the amount of work the driver has to put in to control the vehicle. Future work would investigate closed-loop testing with a driver model to determine if this makes steering the vehicle easier or harder for the driver since the driver still has direct control over the front wheels.

Chapter 7

Conclusion

This work sought out more benefits for RWS. Beyond conventional RWS, adding active front steering allows decoupling of yaw and lateral motions in the vehicle. This allows an arbitrary design of a vehicle to be controlled arbitrarily. This could be a vehicle with a large moment of inertia controlled as if it had a smaller moment of inertia. Or a vehicle to change its handling properties during driving, as proposed in this dissertation. An idea was also proposed for how to change the handling of the vehicle. If the curvature of the road was an input to the vehicle, the model reference could change to reflect this information. In straight line driving, changing lanes may not require excessive yaw motion, so making the vehicle behave as if it had a longer vehicle could be beneficial. In winding roads, the vehicle would need more yaw motion in order to navigate corners. Therefore, making the vehicle behave as if it were shorter would make changing its heading angle easier. Improvement in handling or comfort can be done depending on what is desired. A simple change in the model reference that is intuitive simplifies the design.

One of the most important benefits is safety. This is explored with tests using an unstable vehicle, testing a vehicle on a split-μ road, and finally a test that induces loss of control to a vehicle without ESC. In the case of an unstable vehicle, an oversteering vehicle is explored. This can happen from a change in the location of the center of mass or, in the example in the dissertation, changes in the cornering coefficient of the vehicle.

Split-μ is a specific test case where one side of the vehicle has different traction ability compared to the other side. ABS is used for gaining the maximum traction possible.

This however leads to yaw stability issues where a yaw moment is acting on the vehicle. The yaw correction can be done by the driver, but this dissertation uses RWS for the correction.

Finally, induced oversteering is explored where the open loop test, a sine with dwell input to the steering wheel, is used. Using this standard test, it was shown that RWS can add to the overall stability of the vehicle by aiding conventional ESC. Many metrics were improved, such as lowering the yaw rate error, body slip angle and the final forward speed. The brakes were used less which can translate to a savings in energy. This is useful if the goal was to turn hard without losing stability while keeping the forward speed, such as in a racing vehicle. If the goal was to keep the vehicle from an imminent crash however, it may be better to slow the vehicle.

Appendix A

Code Snippets

A.1 Brakes

Applying a direct torque on the wheels to simulate the brakes needs additional logic. Otherwise, in a condition where the wheels are locking up, the torque will eventually reverse the wheel velocity instead of keeping them at zero. To prevent the wheels from reversing, the logic below is implemented.

```
% Prevent the torque from reversing the wheels
if pwL1/Jw < lam          % Wheel speed almost zero
    if TL1 - FxL1*Reff  > 0  % If the torques allow rolling
        dpwL1 = TL1 - FxL1*Reff;
    else                              % Don't reverse
        dpwL1 = 0;
    end
else
    dpwL1 = TL1 - FxL1*Reff;
end
```

In addition, the tire model slip calculation needs some logic added. The Dugoff tire model will divide by zero otherwise. Therefore, the following is also implemented:

```
% Prevent slips greater than 1
if pwL1/Jw < lam
    SL1 = -0.99;
else
    SL1 = (pwL1/Jw*Reff - uL)/(uL);
end
```

A.2 ESC

The yaw rate reference needs to be saturated when a model assuming linear tires is used. For an algebraic relationship between the steering and yaw reference is used, the saturation looks like the following:

```
yawDes = deltaf*u0/(L*(1+K*u0^2));
yawMax = mu*g/u0;
if abs(yawDes) >= yawMax
    yawDes = sign(yawDes)*yawMax;
end
```

The next code snippet is logic for which brake to activate when only oversteering is corrected. *Dyaw* here represents the dead zone amount.

```
if abs(eyaw) > Dyaw      % Dead zone
    if yaw > 0           % Which side to brake
        % brake right side
        TR1 = Kesc*eyaw;
        if TR1>0
            TR1 = 0;
        end
        TL1 = 0;
    else
```

```
        % brake left side
        TL1 = -Kesc*eyaw;
        if TL1>0
            TL1 = 0;
        end
        TR1 = 0;
    end
else
    TL1 = 0;
    TR1 = 0;
end
```

Finally, when oversteering and understeering is corrected, the appropriate brake needs to be activated. A basic algorithm used in literature is as follows:

```
if abs(eyaw) > Dyaw      % Dead zone
    if yaw > 0           % Turning Left
        if eyaw<0        % Oversteering
            % Brake front right side
            TR1 = -Kesc*abs(eyaw);
            if TR1>0
                TR1 = 0;
            end
            TL1 = 0;
            TL2 = 0;
            TR2 = 0;
        else             % Understeering
            % Brake rear left side
            TL2 = -Kesc*abs(eyaw);
            if TL2>0
```

```
                TL2 = 0;
            end
            TL1 = 0;
            TR1 = 0;
            TR2 = 0;
        end
    else                % Turning Right
        if eyaw>0       % Oversteering
            % brake left side
            TL1 = -Kesc*abs(eyaw);
            if TL1>0
                TL1 = 0;
            end
            TR1 = 0;
            TL2 = 0;
            TR2 = 0;
        else            % Understeering
            % Brake rear right side
            TR2 = -Kesc*abs(eyaw);
            if TR2>0
                TR2 = 0;
            end
            TL1 = 0;
            TR1 = 0;
            TL2 = 0;
        end
    end
else
    TL1 = 0;
```

```
    TR1 = 0;
    TL2 = 0;
    TR2 = 0;
end
```

List of Symbols

Symbol	Description	Unit
C_x	Longitudinal slip stiffness of the wheel	$\mathrm{N}/[-]$
C_y	Cornering stiffness of the wheel	$\mathrm{N\,rad^{-1}}$
E	Energy	J
F_x	Force in the longitudinal direction	N
F_y	Force in the lateral direction	N
F_z	Force in the vertical direction (Normal Force)	N
G	Plant model	
J_z	Moment of inertia of the vehicle in the z-direction	$\mathrm{kg\,m^2}$
K	Controller	
L_o	Output loop transfer function	
P	Power	W
S_o	Output sensitivity function	
T_o	Output complimentary sensitivity function or closed-loop transfer function	
U	Unitary matrix related to the output singular vectors	
V	Unitary matrix related to the input singular vectors	
X	X-position of C.G. of the vehicle	m
Y_o	Output Youla function or actuator sensitivity function	
Y	Y-position of C.G. of the vehicle	m
Σ	Matrix of signular values	
α	Slip angle of wheel	rad

Symbol	Description	Unit
β	Body slip angle	rad
δ_{sw}	Steering wheel angle	rad
δ	Tire angle	rad
κ	Longitudinal slip of the wheel	[−]
μ	Friction coefficient of the road.	
ω_z	Yaw rate of the vehicle	$\mathrm{rad\,s^{-1}}$
ω	Rotational speed of the wheel	$\mathrm{rad\,s^{-1}}$
ϕ	Pitch angle of the vehicle	rad
ψ	Heading angle of the vehicle	rad
ρ	Curvature of the road	$\mathrm{m^{-1}}$
σ	Singular value	
τ	Torque on wheel	N m
θ	Roll angle of the vehicle	rad
a_x	Longitudinal acceleration of the vehicle	$\mathrm{m\,s^{-2}}$
a_y	Lateral acceleration of the vehicle	$\mathrm{m\,s^{-2}}$
a	Distance from the C.G. to the front axle	m
b	Distance from the C.G. to the rear axle	m
c	Half track distance	m
e	Error between reference and measured	
m	Total mass of vehicle	kg
r_e	Effective rolling radius of the wheel	m
r	Reference input	
s	Laplace operator	
u	Plant inputs	
v_x	Forward velocity of the vehicle	$\mathrm{m\,s^{-1}}$
v_y	Lateral velocity of the vehicle	$\mathrm{m\,s^{-1}}$
v_{tx}	Velocity component of the tire in the x-direction	$\mathrm{m\,s^{-1}}$

Symbol	Description	Unit
v_{ty}	Velocity component of the tire in the y-direction	$\mathrm{m\,s^{-1}}$
y	Plant outputs	

List of Abbreviations

2WS Two-wheel steering - Use of only the wheels of the front axle to steer a vehicle. Virtually all passenger vehicles use this method to steer. Interchangeable with FWS.

4WS Four-wheel steering - The ability to steer the wheels of the rear axle. Interchangeable with RWS and AWS.

ABS Anti-lock braking system - A lower level control system that prevents the wheel from locking up by varying the braking torque quickly.

AKC Active kinematics control - A RWS implementation made by ZF Friedrichshafen AG.

AWS All-wheel steering - The ability to steer the wheels of the rear axle. Interchangeable with RWS and 4WS.

ESC Electronic stability control - A method of stabilizing the vehicle by activating the brakes at specific corners of the vehicle. Also known by its proprietary names such as electronic stability program (ESP).

FWS Front-wheel steering - Use of only the wheels of the front axle to steer a vehicle. Virtually all passenger vehicles use this method to steer. Interchangeable with 2WS.

HICAS High-capacity actively-controlled steering - A RWS implementation made by Nissan.

RGA Relative gain array - A method for determening the best input-output pairings for a MIMO system.

RWS Rear-wheel steering - The ability to steer the wheels of the rear axle. Interchangeable with 4WS and AWS.

SIS Slowly increasing steer - A maneuver used to determine the steering wheel angle which creates 0.3 g of lateral acceleration at 50 mph. Used for the ESC sine with dwell test.

Bibliography

[1] C. P. Gilmore. "What's News". Imports. In: *Popular Science* 228.2 (Feb. 1986), p. 59.

[2] *The 'Denburg-Wagen'*. Daimler Global Media Site. URL: https://media.daimler.com/marsMediaSite/ko/en/9272027 (visited on 02/28/2019).

[3] *Other vehicles with off-road capability*. Daimler Global Media Site. URL: https://media.daimler.com/marsMediaSite/ko/en/%209272220 (visited on 02/28/2019).

[4] *The Mercedes-Benz G5*. Daimler Global Media Site. URL: https://media.daimler.com/marsMediaSite/ko/en/9361305 (visited on 02/28/2019).

[5] Rodger Ward. "Can We Beat the British at the Brickyard?" In: *Popular Mechanics* 127.5 (May 1967), p. 234.

[6] *Steering Angle Sensing Four-Wheel Steering System (4WS)/1987*. Heritage of Challenges. Honda Motor Co. URL: https://global.honda/heritage/episodes/19874ws.html (visited on 10/22/2018).

[7] "Concept Car". What's New. In: *Popular Science* 224.4 (Apr. 1984), p. 90.

[8] Herbert Shuldiner. "4-Wheel Steering -here now for all-out performance". In: *Popular Science* 228.2 (Feb. 1986), pp. 60–65, 115.

[9] Bill Hartford. "Two sidewinders". Imports. In: *Popular Mechanics* 163.1 (Jan. 1986), p. 12.

[10] S. Parker. "Steering to the Four". Imports. In: *Popular Mechanics* 163.2 (Feb. 1986), p. 94.

[11] *Skyline 4-door Hardtop GTS Twin-cam 24V Turbo (1986 : KRR31)*. Heritage of Challenges. Nissan Motor Corporation. URL: https://www.nissan-global.com/EN/HERITAGE/skyline_4door.html (visited on 10/22/2018).

[12] Dan McCosh and Tom Wilkinson. "Honda vs. Mazda 4-Wheel-Steering Showdown". Imports. In: *Popular Science* 231.2 (Aug. 1987), pp. 50–53.

[13] Dan McCosh. “First Instrumented Test: 4-Wheel Steer vs 2-Wheel Steer”. Imports. In: *Popular Science* 232.3 (Mar. 1988), pp. 30–34.

[14] “Road test of the Honda Prelude Si 4WS”. In: *Consumer Reports* 53.4 (Apr. 1988), pp. 220–222.

[15] “Road tests of sports sedans”. In: *Consumer Reports* 53.8 (Aug. 1988), pp. 511–518.

[16] James G Cobb. “A Turning Point for Big Trucks”. In: *New York Times* (Feb. 3, 2002).

[17] Rich Ceppos. “Honda Prelude Si 4WS”. In: *Car and Driver* 33.2 (Aug. 1987), pp. 40–45.

[18] Peter Herold and Markus Wallbrecher. “All-Wheel Steering”. In: *Steering Handbook*. Ed. by Manfred Harrer and Peter Pfeffer. Switzerland: Springer International Publishing, 2017. Chap. 17, pp. 493–512.

[19] Richard L. Stepler. “Twin turbos”. Automotive Newsfront. In: *Popular Science* 236.3 (Mar. 1990), pp. 36–39.

[20] Dan McCosh. “All-wheel drive, all-wheel steer”. Automotive Newsfront. In: *Popular Science* 237.4 (Oct. 1990), pp. 36–38.

[21] Richard Truett. “GM to drop Quadrasteer option”. Automotive News. In: *Autoweek* (Feb. 16, 2005).

[22] Andrew Ganz. “Rear-wheel steering could radically change pickup trucks and SUVs”. In: *The Washington Post* (July 1, 2017).

[23] Bernd Heißing and Metin Ersoy. *Chassis Handbook: Fundamentals, Driving Dynamics, Components, Mechatronics, and Perspectives*. Germany: Wiesbaden: Vieweg + Teubner Verlag, 2011. Chap. 7, pp. 517–520.

[24] Csaba Csere. “The Notorious GT3 - Porsche Radicalizes the 911”. Reveal of the Month. In: *Car and Driver* 58.11 (May 2013), pp. 17–19.

[25] ZF Group. *Active Rear Axle Steering on the Road to Success*. Press Release. Oct. 2, 2017.

[26] *Discover 4Control with the new Mégane GT, a world first in its class*. Renault Sport. URL: https://www.renaultsport.com/Discover-4Control-with-the-New-Megane-GT-a-world-first-in-its-class.html (visited on 09/18/2015).

[27] Bogdan Thaddeus Fijalkowski. *Automotive mechatronics: operational and practical issues. Vol. 2: ...* International series on intelligent systems, control and automation: science and engineering 52. OCLC: 838487387. Dordrecht: Springer, 2011. 523 pp.

[28] J. Ackermann and W. Sienel. "Robust yaw damping of cars with front and rear wheel steering". In: *IEEE Transactions on Control Systems Technology* 1.1 (Mar. 1993), pp. 15–20.

[29] John C. Whitehead. *Four Wheel Steering: Maneuverability and High Speed Stabilization*. SAE Technical Paper 880642. Feb. 1, 1988.

[30] Yoshimi Furukawa et al. "A Review of Four-Wheel Steering Studies from the Viewpoint of Vehicle Dynamics and Control". In: *Vehicle System Dynamics* 18.1 (1989), pp. 151–186.

[31] L. Pascali, P. Gabrielli, and G. Caviasso. "Improving Vehicle Handling and Comfort Performance Using 4WS". In: SAE 2003 World Congress & Exhibition. Mar. 3, 2003, pp. 2003–01–0961.

[32] Thomas D. Gillespie. *Fundamentals of Vehicle Dynamics*. Pennsylvania, United States: SAE International, 1992.

[33] Sang-Ho LEE et al. "Four-Wheel Independent Steering (4WIS) System for Vehicle Handling Improvement by Active Rear Toe Control." In: *JSME International Journal Series C* 42.4 (1999), pp. 947–956.

[34] Sangho Lee, Hyun Sung, and Unkoo Lee. *The Development of Active Geometry Control Suspension (AGCS) System*. SAE Technical Paper. 2005.

[35] Tadahiko Takiguchi et al. *Improvement of Vehicle Dynamics by Vehlcle-Speed-Sensing Four-Wheel Steering System*. SAE Technical Paper 860624. 1986.

[36] Shoichi Sano, Yoshimi Furukawa, and Shuji Shiraishi. *Four Wheel Steering System with Rear Wheel Steer Angle Controlled as a Function of Steering Wheel Angle*. SAE Technical Paper 860625. 1986.

[37] Y. Furukawa and H. Nakaya. "Effects of steering response characteristics on control performance of the driver–vehicle system". In: *International Journal of Vehicle Design* 7.5 (Jan. 1, 1986), pp. 262–278.

[38] N. Irie and J. Kuroki. "4WS Technology and the Prospects for Improvement of Vehicle Dynamics". In: *Vehicle Electronics in the 90's: Proceedings of the International Congress on Transportation Electronics*. Vehicle Electronics in the 90's: Proceedings of the International Congress on Transportation Electronics. Oct. 1990, pp. 429–437.

[39] Yasuji Shibahata et al. *The Development of an Experimental Four-Wheel-Steering Vehicle*. SAE Technical Paper 860623. Feb. 24, 1986.

[40] Shoichi Sano et al. "Handling Characteristics Of Steer Angle Dependent Four Wheel Steering System". In: 22nd FISITA Congress. Sept. 1, 1988.

[41] Yukio Fukunaga et al. "Improved handling and stability using four-wheel steering". In: Proceedings of the 11th International Technical Conference on Experimental Safety Vehicles (ESV). Washington DC, May 12, 1987, pp. 415–425.

[42] Lance Bredthauer and David Lynch. "Use of Active Rear Steering to Achieve Desired Vehicle Transient Lateral Dynamics". In: WCX World Congress Experience. Apr. 3, 2018.

[43] Hiroki Sato et al. *Development of Four Wheel Steering System Using Yaw Rate Feedback Control*. SAE Technical Paper 911922. 1991.

[44] Kwanwoo Park, Eunhyek Joa, and Kyongsu Yi. "Rear-Wheel Steering Control for Enhanced Maneuverability of Vehicles". In: WCX SAE World Congress Experience. Apr. 2, 2019, pp. 2019–01–1238.

[45] Mahmoud Mohsen Abdelfatah. "Yaw Center Control of a Vehicle Using Rear Wheel Steering". In: *Advances in Dynamics of Vehicles on Roads and Tracks*. Ed. by Matthijs Klomp et al. Series Title: Lecture Notes in Mechanical Engineering. Cham: Springer International Publishing, 2020, pp. 1313–1321.

[46] Steffen Wagner et al. "Pivot point-based control for active rear-wheel steering in passenger vehicles". In: (2018), p. 24.

[47] Robert L. Kisslinger and Michael J. Wendl. *Survivable Flight Control System Interim Report No. 1, Studies, Analysis, and Approach, Supplement for Control Criteria Studies*. Technical Report AFFDL TR 71-20 Supplement 1. Air Force Flight Dynamics Laboratory: McDonnell Aircraft Company, May 1971.

[48] Ken Ito et al. "A New Way of Controlling a Four Wheel Steering Vehicle - An Approach of Model Following Control". In: vol. 23. Transactions of SICE (in Japanese), 1987, pp. 828–834.

[49] Young H. Cho and J. Kim. "Design of Optimal Four-Wheel Steering System". In: *Vehicle System Dynamics* 24.9 (Oct. 1995), pp. 661–682.

[50] Masao Nagai and Hiroaki Hashigaya. "Analysis of 4-Wheel-Steering Automobiles by a Virtual Model Following Control". In: *Transactions of JSME (in Japanese)*. Vol. 53. 1987, pp. 2584–2587.

[51] M. Nagai and M. Ohki. "Theoretical study on active four–wheel–steering system by virtual vehicle model following control". In: *International Journal of Vehicle Design* 10.1 (Jan. 1, 1989), pp. 16–33.

[52] J. Ackermann. "Robust car steering by yaw rate control". In: *29th IEEE Conference on Decision and Control*. 29th IEEE Conference on Decision and Control. Dec. 1990, 2033–2034 vol.4.

[53] M. Canale and L. Fagiano. "Stability control of 4WS vehicles using robust IMC techniques". In: *Vehicle System Dynamics* 46.11 (Nov. 2008), pp. 991–1011.

[54] Toshihiro Hiraoka, Osamu Nishihara, and Hiromitsu Kumamoto. "Model-Following Sliding Mode Control for Active Four-Wheel Steering Vehicle". In: *Review of Automotive Engineering* (2004), p. 10.

[55] H E B Russell and J C Gerdes. "Low friction emulation of lateral vehicle dynamics using four-wheel steer-by-wire". In: *2014 American Control Conference*. 2014, pp. 3924–3929.

[56] H E B Russell and J C Gerdes. "Design of Variable Vehicle Handling Characteristics Using Four-Wheel Steer-by-Wire". In: *IEEE Transactions on Control Systems Technology* 24.5 (2016), pp. 1529–1540.

[57] Allan Y. Lee. *Emulating the Lateral Dynamics of a Range of Vehicles Using a Four-Wheel-Steering Vehicle*. SAE Technical Paper 950304. 1995.

[58] Allan Y. Lee. *Matching Vehicle Responses Using the Model-Following Control Method*. SAE Technical Paper 970561. 1997.

[59] Mehmet Akar and Jens C. Kalkkuhl. "Lateral dynamics emulation via a four-wheel steering vehicle". In: *Vehicle System Dynamics* 46.9 (Sept. 2008), pp. 803–829.

[60] *Laboratory Test Procedure for FMVSS 126, Electronic Stability Control Systems*. TP-126-01. U.S. DEPARTMENT OF TRANSPORTATION, National Highway Traffic Safety Administration: Office of Vehicle Safety Compliance, Apr. 10, 2008.

[61] *Federal Motor Vehicle Safety Standards; Electronic Stability Control Systems; Controls and Displays*. 49 CFR Parts 571 and 585 [Docket No. NHTSA–200727662] RIN: 2127AJ77. Department of Transportation, National Highway Traffic Safety Administration, 2007.

[62] *Final Regulatory Impact Analysis, FMVSS No. 126 Electronic Stability Control Systems*. U.S. DEPARTMENT OF TRANSPORTATION, National Highway Traffic Safety Administration: Office of Regulatory Analysis, Evaluation, National Center for Statistics, and Analysis, Mar. 2007.

[63] AT van Zanten. *Bosch ESP Systems: 5 Years of Experience*. SAE Technical Paper 2000-01-1633. 2000.

[64] Kazuhiko Shimada and Yasuji Shibahata. *Comparison of Three Active Chassis Control Methods for Stabilizing Yaw Moments*. SAE Technical Paper 940870. SAE International, 1994.

[65] M. Canale and L. Fagiano. "Comparing rear wheel steering and rear active differential approaches to vehicle yaw control". In: *Vehicle System Dynamics* 48.5 (May 2010), pp. 529–546.

[66] C. I. Chatzikomis and K. N. Spentzas. "Comparison of a vehicle equipped with Electronic Stability Control (ESC) to a vehicle with Four Wheel Steering (4WS)". In: *Forschung im Ingenieurwesen* 78.1 (May 2014), pp. 13–25.

[67] Shinichiro Horiuchi, Kazuyuki Okada, and Shinya Nohtomi. "Effects of Integrated Control of Active Four Wheel Steering and Individual Wheel Torque on Vehicle Handling and Stability - A Comparison of Alternative Control Strategies -". In: *Vehicle System Dynamics* 33 (sup1 Jan. 1, 1999), pp. 680–691.

[68] Jeonghoon Song and Woo Seong Che. "Comparison between braking and steering yaw moment controllers considering ABS control aspects". In: *Mechatronics* 19.7 (Oct. 2009), pp. 1126–1133.

[69] Men Jinlai et al. "Comparisons of vehicle stability controls based on 4WS, Brake, Brake-FAS and IMC techniques". In: *Vehicle System Dynamics* 50.7 (July 2012), pp. 1053–1084.

[70] Seongjin Yim. "Comparison among Active Front, Front Independent, 4-Wheel and 4-Wheel Independent Steering Systems for Vehicle Stability Control". In: *Electronics* 9.5 (May 12, 2020), p. 798.

[71] Jaewon Nah and Seongjin Yim. "Optimization of control allocation with ESC, AFS, ARS and TVD in integrated chassis control". In: *Journal of Mechanical Science and Technology* 33.6 (June 2019), pp. 2941–2948.

[72] Seongjin Yim. "Coordinated control with electronic stability control and active steering devices". In: *Journal of Mechanical Science and Technology* 29.12 (Dec. 2015), pp. 5409–5416.

[73] Zhou Zhou et al. "Vehicle Stability Control through Optimized Coordination of Active Rear Steering and Differential Driving/Braking". In: *SAE International Journal of Passenger Cars - Mechanical Systems* 11.3 (2018), p. 10.

[74] Edward J. Bedner and Hsien H. Chen. *A Supervisory Control to Manage Brakes and Four-Wheel-Steer Systems*. SAE Technical Paper 2004-01-1059. 2004.

[75] Hans Pacejka. *Tire and Vehicle Dynamics*. 3rd. SAE International, 2012.

[76] Howard Dugoff, P. S. Fancher, and Leonard Segel. "An Analysis of Tire Traction Properties and Their Influence on Vehicle Dynamic Performance". In: International Automobile Safety Conference. Feb. 1, 1970, p. 700377.

[77] Robert Bosch GmbH. *Automotive Handbook*. 9th. Wiley, 2014.

[78] D.C. Karnopp, D.L. Margolis, and R.C. Rosenberg. *System Dynamics: Modeling, Simulation, and Control of Mechatronic Systems*. 5th. Wiley, 2012.

[79] Andrzej G Nalecz and Alan C Bindemann. *Handling Properties of Four Wheel Steering Vehicles*. SAE Technical Paper 890080. 1989, p. 20.

[80] Mechanical Simulation Corporation. *CarSim*. 2022. URL: `https://www.carsim.com/`.

[81] J. Loyola and D. Margolis. "Variable wheelbase reference for vehicle with active front and rear-wheel steering". In: *Vehicle System Dynamics* (May 2, 2021), pp. 1–17.

[82] Duane D. MacInnis, William E. Cliff, and Kurt W. Ising. "A Comparison of Moment of Inertia Estimation Techniques for Vehicle Dynamics Simulation". In: SAE International Congress and Exposition. Feb. 24, 1997, p. 970951.

[83] S. Skogestad and I. Postlethwaite. *Multivariable Feedback Control: Analysis and Design*. Wiley, 2005.

[84] Farhad Assadian and Kevin R. Mallon. *Robust Control: Youla Parameterization Approach*. John Wiley & Sons Ltd, 2022.

[85] Konrad Reif, ed. *Automotive mechatronics: automotive networking, driving stability systems, electronics*. 1st edition. Bosch professional automotive information. New York: Springer, 2014.

[86] Valentin Ivanov, Dzmitry Savitski, and Barys Shyrokau. "A Survey of Traction Control and Antilock Braking Systems of Full Electric Vehicles With Individually Controlled Electric Motors". In: *IEEE Transactions on Vehicular Technology* 64.9 (Sept. 2015), pp. 3878–3896.

[87] A. Visioli. "Modified anti-windup scheme for PID controllers". In: *IEE Proceedings - Control Theory and Applications* 150.1 (Jan. 1, 2003), pp. 49–54.